SOUTHERN CALIFORNIA
EDISON®
An EDISON INTERNATIONAL® Company

A. Edward Scherer
Manager of
Nuclear Regulatory Affairs

October 25, 2004

U. S. Nuclear Regulatory Commission
ATTN: Document Control Desk
Washington, DC 20555-0001

Subject: **Docket Nos. 50-361 and 50-362**
Additional Information Supporting Third Ten-Year Inservice Inspection (ISI) Interval Relief Requests ISI-3-11, Revision 1 and ISI-3-12 to Support Potential Pressurizer Heater Sleeve Repairs.
San Onofre Nuclear Generating Station, Units 2 and 3

Reference: Letter from A. E. Scherer (SCE) to the Document Control Desk (NRC) dated October 15, 2004; Subject: Docket Nos. 50-361 and 50-362, Third Ten-Year Inservice Inspection (ISI) Interval Relief Requests ISI-3-11, Revision 1 and ISI-3-12 to Support Potential Pressurizer Heater Sleeve Repairs, San Onofre Nuclear Generating Station, Units 2 and 3

Dear Sir or Madam,

As requested, this letter provides the Southern California Edison (SCE) Calculation M-DSC-402, "Pressurizer Heater Sleeve J-Groove Weld Flaw Eval-SONGS 2 & 3" to support the SCE Relief Requests ISI-3-11, Revision 1 and ISI-3-12, which were submitted to the NRC by the referenced October 15, 2004, letter.

Should you have any questions, please contact Mr. Jack Rainsberry, Manager, Plant Licensing at (949) 368-7420.

Sincerely,

cc: B. S. Mallett, Regional Administrator, NRC Region IV
B. M. Pham, NRC Project Manager, San Onofre Units 2 and 3
C. C. Osterholtz, NRC Senior Resident Inspector, San Onofre Units 2 and 3

P.O. Box 128
San Clemente, CA 92674-0128
949-368-7501
Fax 949-368-7575

A047

CALCULATION TITLE PAGE

ICCN NO/ PRELIM. CCN NO.	PAGE OF

Calc No. M-DSC-402 DCP/FIDCN/ FCN/ECP No. & Rev. N/A | CCN CONVERSION: CCN NO. CCN-

Subject: Pressurizer Heater Sleeve J-Groove Weld Flaw Eval -SONGS 2&3 Sheet 1 of 110

System Number/Primary Station System Designators 1201 /BBB SONGS Unit 2 & 3 Q-Class I

Tech. Spec./LCS Affecting? ◉ NO ○ YES Section No. _____ Equipment Tag No. S2(3)1201ME087

Site Programs/Procedure Impact? ◉ NO ○ YES, AR No. _____

10CFR50.59/72.48 REVIEW	CONTROLLED COMPUTER PROGRAM/DATABASE		
Is this calculation revision being issued solely to incorporate CCNs? ◉ NO ○ YES AR No. 030900690-2	☒ PROGRAM ☐ DATABASE According to SO123-XXIV-5.1	PROGRAM/ DATABASE NAME(S) BIGIF* ☐ ALSO, LISTED BELOW	VERSION/ RELEASE NO. (S)

RECORD OF ISSUES

REV. DISC	DESCRIPTION	TOTAL SHTS. LAST SHT	PREPARED (Print name/sign/date) Initial PQS Block - Requires PQS T3EN64	APPROVED (Signature/date) Initial PQS Block - Requires PQS T3EN64
0	INITIAL ISSUE	110	ORIG. PQS VER. BY: NABIL M. EL-AKKAD 09/30/04	FLS PQS VER. BY: 10/4/04
N-M DEO		110	IRE PQS VER. BY: JUN GAOR 9/30/04	OTHER PQS VER. BY: ___
			ORIG. PQS VER. BY: ___	FLS PQS VER. BY: ___
			IRE PQS VER. BY: ___	OTHER PQS VER. BY: ___
			ORIG. PQS VER. BY: ___	FLS PQS VER. BY: ___
			IRE PQS VER. BY: ___	OTHER PQS VER. BY: ___
			ORIG. PQS VER. BY: ___	FLS PQS VER. BY: ___
			IRE PQS VER. BY: ___	OTHER PQS VER. BY: ___

Space for RPE Stamp, Identify use of an alternate calc., and notes as applicable.

* THE BIGIF COMPUTER PROGRAM (REFERENCE 8) WAS USED BY APTECH TO PERFORM THE STRESS INTENSITY FACTOR AND THE FATIGUE CRACK GROWTH ANALYSES. THE ACCURACY OF THE BIGIF PROGRAM HAS BEEN VERIFIED FOR BOTH ANALYSIS TYPES.

POOR QUALITY DOCUMENT
BEST AVAILABLE COPY

SIGNED: N. El-A 10/12/04
DOCUMENT ORIGINATOR DATE

SITE FILE COPY

This calc. was prepared for the identified DCP/FCN/ISCO ECP. DCP/FCN/ECP completion and turnover acceptance to be verified by receipt of a memorandum directing DCN/ECN Conversion. Upon receipt, this calc. represents the as-built condition. Memo date. _____ by _____.

Site File Copy

CALCULATION CROSS-INDEX

ICCN NO./ PRELIM. CCN NO.	PAGE _____ OF _____
	CCN CONVERSION: CCN NO. CCN-

Calculation No. M-DSC-402 Sheet No. 2 of _____

Calc. rev. number and responsible FLS initials and date	INPUTS These interfacing calculations and/or documents provide input to the subject calculation and if revised may require revision of the subject calculation.		OUTPUTS Results and conclusions of the subject calculation are used in these interfacing calculations and/or documents.		Does the output interface calc/ document require change?	Identify output interface calc/document ECP, CCN, DCN, TCN/Rev., FIDCN, or tracking number.
	Calc / Document No.	Rev. No.	Calc / Document No.	Rev. No.	YES / NO	
RLP 10/4/04	SO23-919-3, PROJECT SPEC FOR PRZ ASSEMBLY SONGS UNITS 2 AND 3	8				
	M-DSC-356, EVAL OF MOD PRZ HEATER SLEEVES - SONGS UNITS 2 AND 3	1				
	DRWG NO. SO23-919-79, PRZ GENERAL ARRANGEMENT	0				
	DRWG NO. SO23-919-86, HEATER ARRANGEMENT AND ASSEMBLY	1				

SCE 26-424 REV. 4 7/01 [REFERENCE: SO123-XXIV-7.15]

CALCULATION COVER SHEET

Calculation No.: AES-C-5212-2
SCE No. M-DSC-402, Rev. 0

Title: Pressurizer Heater Sleeve J-Groove Weld Flaw Evaluation — SONGS Units 2 and 3

Client: Southern California Edison

Project No.: AES 03105212-1Q

APTECH Office: Sunnyvale

Sheet No. 3 of 110

☐ **Uncontrolled** ■ **Controlled**

Document Control No.: I-2

Purpose: The purpose of this calculation is to evaluate the half-sleeve weld repair for the removal of Alloy 600 heater sleeve. For this repair, any flaws present in the original J-groove weld or sleeve stub shall be acceptable for the remaining service period for the pressurizer. This calculation is based on a fracture mechanics analysis of the repair geometry and conservatively evaluates the significance of flaws that could remain after repair.

Assumptions: The analysis assumptions are described in Section 3.

Results: The results of this calculation are summarized in Section 2. The evaluation period covered by this calculation is a 40-year service life considering loading from the original design. The postulated conditions following weld repair, including hypothetical flaws that are assumed to remain, are acceptable to the safety margins of ASME Section XI under IWB-3600 guidelines.

Revision No.	Prepared By / Date	Checked By / Date	Verified By / Date	Approved By / Date	Revision Description
0	RCC / 9/17/04	MTC / 17 Sep 04	MTC / 17 Sep 04	RCC / 9/17/04	Initial Release

APTECH ENGINEERING SERVICES, INC.

QAN45
REV. 8/96

TABLE OF CONTENTS

Section	Title	Page
	CALCULATION TITLE PAGE	1
	CALCULATION CROSS-INDEX	2
	CALCULATION COVER SHEET	3
1.0	INTRODUCTION	6
2.0	SUMMARY OF RESULTS	9
2.1	Scope and Objectives	9
2.2	Sleeve J-Groove Evaluation Results	9
3.0	ANALYSIS ASSUMPTIONS	11
4.0	METHODOLOGY	12
4.1	Technical Approach	12
4.2	Flaw Acceptance Criteria	13
4.3	Calculation of Flaw Size Parameters	14
4.3.1	Calculation of End-of-Life Flaw Size (a_f)	14
4.3.2	Calculation of Minimum Critical Flaw Size (a_c) for Normal/Upset Conditions	14
4.3.3	Calculation of Minimum Initiating Flaw Size (a_i) for Accident Conditions	15
4.4	Calculation of Stress Intensity Factor	16
4.5	Fracture Toughness Criteria of Appendix K	16
4.6	Definition of Stresses in the J-Groove Region	18
5.0	DESIGN INPUT	23
5.1	Sleeve and Bottom Head Geometry	23
5.2	Design and Operating Conditions	23
5.3	Material Properties	24
5.3.1	Mechanical Strength	24
5.3.2	Fracture Toughness	25
5.3.3	Fatigue Crack Growth Rate for the PZR Bottom Head	26

Section	Title	Page
6.0	REFERENCES	37
7.0	NOMENCLATURE	39
8.0	CALCULATIONS	41
8.1	Heater Sleeve Penetration Stresses	41
8.2	Consideration of Weld Residual Stresses	42
8.2.1	Fracture Resistance	42
8.2.2	Fatigue Crack Growth Rate	43
8.3	Definition of Cycle Stresses	43
8.4	Evaluation of Postulated Flaws at the J-Groove Weld	44
8.4.1	Flaw Model	44
8.4.2	J-Groove Weld Stresses	45
8.4.3	Allowable Flaw Depth Evaluation	45
	8.4.3.1 Appendix A Evaluation	45
	8.4.3.2 Appendix K Evaluation	46
8.4.4	Fatigue Evaluation	47
8.5	Evaluation of Borated Water Corrosion	48
	APPENDIX A—SUMMARY OF HEATER SLEEVE CYCLIC STRESSES	54
	APPENDIX B—BIGIF COMPUTER OUTPUT FOR J-GROOVE FLAW EVALUATION (UPHILL SIDE)	82
	APPENDIX C—BIGIF COMPUTER OUTPUT FOR J-GROOVE FLAW EVALUATION (DOWNHILL SIDE)	96

1.0 INTRODUCTION

The pressurizer (PZR) bottom head contains multiple penetrations for instrumentation and heater rod nozzles and sleeves. A schematic illustration of the PZR bottom head is shown in Figure 1-1 (Ref. 1). The heater sleeve penetrations are the scope of this calculation.

There are a total of 30 heater sleeves. An illustration of a typical heater sleeve and attachment weld is shown in Figure 1-2 (Ref. 2). The heater sleeves were originally designed to American Society of Mechanical Engineers (ASME) Section III (Ref. 3). An ASME Section XI evaluation (Ref. 4) is performed on the J-groove attachment weld to establish the flaw tolerance of the weld detail, in particular the underlining carbon steel bottom head.

The purpose of this calculation is to evaluate the heater sleeve penetrations with regard to the half-sleeve repair option strategy that removes a portion of the original Alloy 600 sleeve. The assumed cause of flaws in heater sleeves is primary water stress corrosion cracking (PWSCC) due to high surface tensile residual stresses near the J-groove attachment weld. The objective of this calculation is to demonstrate that the half-sleeve repair will satisfy ASME Code Section XI requirements. Since the original nozzle geometry has been restored, ASME Section III Code requirements are satisfied for allowable stress limits and fatigue usage. Therefore, the remaining Code requirements to be evaluated are ASME Section XI acceptance criteria for flaws postulated to exist in the repair. Specifically, the postulated condition assumed to exist after repair is an axially oriented flaw in the corner region within the J-groove weld. This postulated flaw is to address the question of the fracture and flaw growth resistance of the low alloy carbon steel bottom head.

The evaluated conditions addressed in this calculation are pressure, mechanical loads, and design basis transients. The design cycles for a 40-year design life are imposed to justify long-term acceptance. The flaw evaluation procedures, material properties, and acceptance criteria of ASME Section XI, Appendix A and Appendix K, are used as guidance in completing the calculations (Ref. 4).

The half-sleeve repair will allow primary water to come in contact with the carbon steel head. Therefore, there is a potential for general corrosion or wastage to occur in the annulus between the sleeve and bore hole. This degradation mechanism has been previously evaluated and determined not to be significant for a 40-year service life subsequent to repair (Ref. 5). Therefore, borated water corrosion will not impact the margin requirements of ASME Section XI.

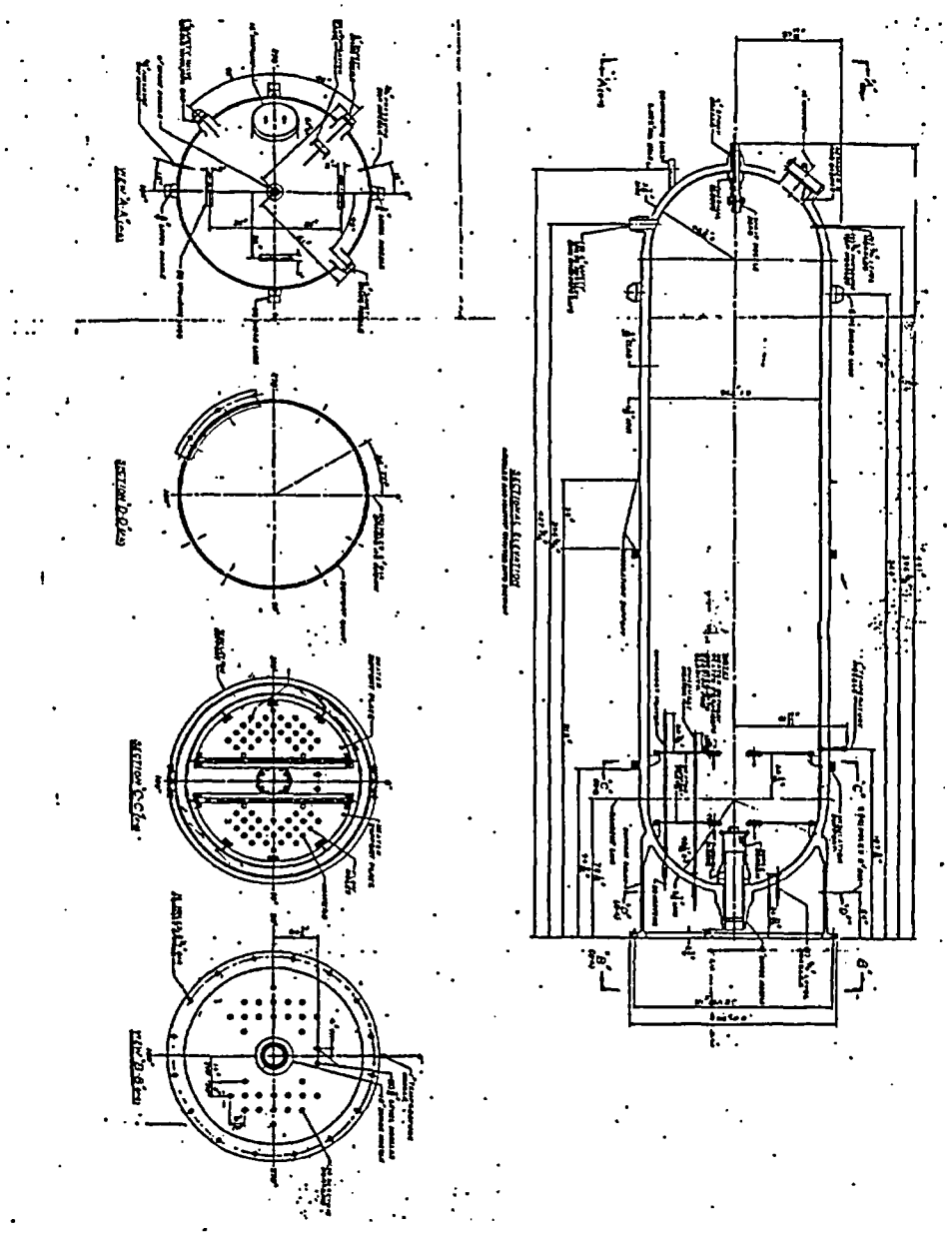

Figure 1-1 — Pressurizer Bottom Head Configuration.

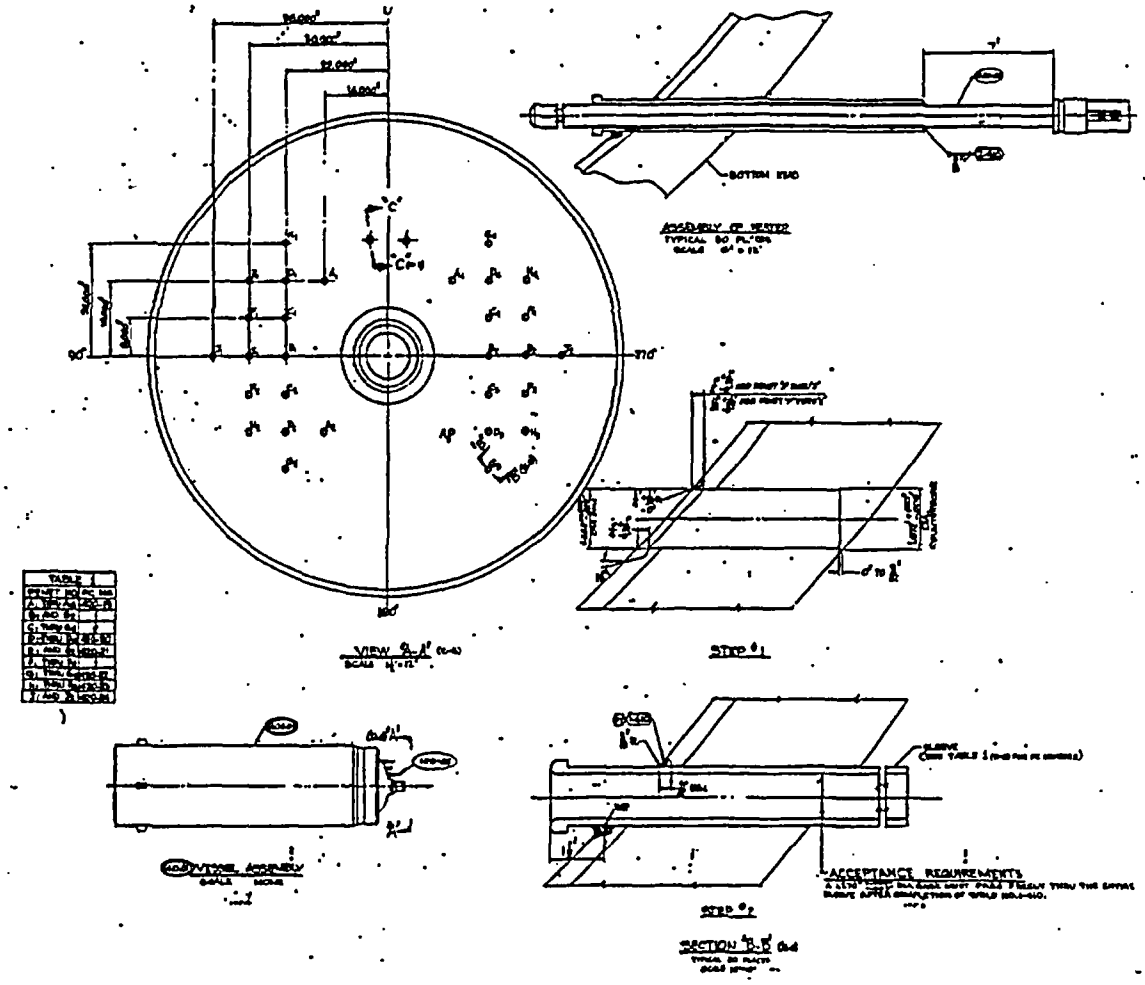

Figure 1-2 — Original J-Groove Weld Attachment Configuration.

2.0 SUMMARY OF RESULTS

2.1 Scope and Objectives

A fracture mechanics-based evaluation has been performed to justify the long-term acceptance of the weld repair option for heater sleeves in the PZR bottom head. This repair option involves the removal of a portion of the Alloy 600 sleeve and replace it with Alloy 690 sleeve. The Alloy 690 sleeve is attached to the bottom head at the outside surface by a J-groove weld forming a new pressure boundary for the sleeve. The original J-groove weld at the inside surface remains in service along with a portion of the original Alloy 600 sleeve.

The long-term acceptance of the PZR heater sleeve repair is subject to the acceptance of a postulated condition: the potential existence of axial cracks in the original J-groove attachment weld. The sleeves at the outer position were evaluated since they will be bounding in terms of service stress levels. The flaw evaluation rules and acceptance criteria of ASME Section XI were employed to establish the pressure boundary integrity and allowable service life for the PZR heater sleeve repair.

2.2 Sleeve J-Groove Evaluation Results

The flaw postulated to remain in the J-groove attachment weld was conservatively evaluated. The computed stresses for the outer heater sleeves were used to envelop the service conditions for all heater sleeve penetrations subject to repair. A large 1.0-inch depth corner crack, penetrating completely through the sleeve wall and J-groove weld and into the low alloy steel head was conservatively assumed to bound the size of any flaw remaining in the Alloy 600 material. The postulated flaw is illustrated in Figures 4-1 and 8-1. This postulated flaw depth is approximately 25% of the bottom head wall thickness

Fracture mechanics and fatigue crack growth (FCG) analyses following the procedures of ASME Section XI, Appendix A, were completed to determine the allowable flaw depths and service life. The calculations for this evaluation are given in Section 8.4. It is assumed that the flaw is surface-connected so that the alloy steel head is exposed to the reactor water. The FCG behavior in a reactor water environment was conservatively assumed. However, pressure loading acting on the crack face was neglected, given the conservative size of the initial flaw assumed in the analysis. In terms of the allowable flaw depth, the limiting flaw location between the uphill and downhill weld locations is the uphill side.

The allowable flaw depth is computed to be 1.45 inches for the uphill side of the penetration. The acceptance criterion is based on maintaining a minimum safety factor of $10^{1/2}$ on load for normal and upset loading conditions and $2^{1/2}$ on load for emergency and faulted conditions, whichever is limiting. For the completed evaluation, the limiting service condition is the cooldown transient with flooding for which the smallest allowable flaw depth is calculated (i.e., a_{allow} = 1.42 inches).

An ASME Section XI Appendix K toughness evaluation procedure and acceptance criteria was also performed to verify the input parameters and assumptions used for determining allowable flaw depth by Appendix A procedures. The Appendix K procedures are directly applicable given the service temperature (i.e., upper shelf condition) and postulated flaw depth assumptions used in this analysis. The results from the Appendix K evaluation confirm that the allowable flaw depths from Appendix A are conservative.

The maximum flaw growth for the postulated initial flaw (a_o = 1.0 inches) for a 40-year design life is computed to be 0.21 inch for the uphill side. The final crack depth is therefore calculated to be 1.21 inches and

$$a_f = 1.21 \text{ inches} < a_{allow} = 1.42 \text{ inches}$$

The allowable flaw depth is computed to be 1.50 inches for the downhill side of the penetration. For the downhill flaw evaluation, the limiting service condition is again the cooldown transient with flooding for which the smallest allowable flaw depth is calculated (i.e., a_{allow} = 1.52 inches). The maximum flaw growth for the postulated initial flaw (a_o = 1.0 inches) for a 40-year design life is computed to be 0.25 inch for the uphill side. The final crack depth is therefore calculated to be 1.25 inches and

$$a_f = 1.25 \text{ inches} < a_{allow} = 1.52 \text{ inches}$$

Therefore, the calculated final flaw depths for both uphill and downhill locations are acceptable for a 40-year design life. Based on this evaluation, any flaws remaining in the J-groove region will be acceptable to the safety margin requirements of ASME Section XI under IWB-3600.

3.0 ANALYSIS ASSUMPTIONS

The following assumptions were made in performing the design analysis calculations:

1. The flaw evaluation was completed using the 1995 Edition of ASME Section XI as guidance. Flaw evaluation procedures given under IWB-3600 and Appendix A of ASME Section XI are generally applicable.

2. Weld residual stresses are considered in the assessment. For elastic-plastic considerations, the maximum stress in the J-groove region is assumed to be limited by the yield strength of the material. A maximum yield strength of 60 ksi is assumed.

3. The hoop stresses at the inside surface of the bottom head due to external sleeve loads are assumed to be negligible (see Ref. 6).

4. Acceptance criteria for normal/upset and accident conditions are considered in the evaluation.

5. Maximum stress conditions for the outermost heater sleeves are assumed for all sleeve locations (bounding for all heater sleeves covered by this calculation).

6. Weld indications are assumed to be crack-like. The crack model is assumed to completely penetrate the J-groove weld and enter the low alloy steel shell.

7. Crack growth rate for reactor water for R = 0.25 is assumed in the evaluation for fatigue crack growth outside the J-groove region. Given the large initial postulated crack and nature of stress cycles (i.e., near zero or negative R ratios), this assumption will be conservative.

8. Cooldown transient with flooding is assumed to occur with each shutdown. This assumption is very conservative given the higher stresses of this transient and that low likelihood of occurrence given current plant operation.

8. Irradiation embrittlement of the PZR bottom head is negligible.

In general, use of the above assumptions will result in a conservative analysis of the flaw for normal operating conditions. Conservative means any condition that will result in a smaller calculated critical flaw size or in accelerated crack growth rates under normal operation.

4.0 METHODOLOGY

4.1 Technical Approach

The evaluation procedures of ASME Section XI, Appendix A, are used to analyze the postulated flaw geometries. The flaw is evaluated as a sharp crack and normal to the maximum principal stress direction (hoop direction) of the bottom head. The flaws are postulated as axially oriented cracks originating in the J-groove, as shown in Figure 4-1. It is conservatively assumed that the flaws will grow radially through the J-groove and into the low alloy steel head/shell material. The initial flaw assumed in the evaluation is a large quarter circular crack that just resides in the low alloy steel. This assumption conservatively ignores any crack growth life through the J-groove material.

The evaluation procedure is described in Article A-5000 of Section XI, Appendix A. Both theoretical solutions and numerical methods are used to evaluate the flaw, given the flaw size and geometry data, material properties, and the transient stresses and temperatures at the penetration location. These methods are used to calculate the following Section XI flaw parameters:

a_f — The maximum size to which the detected flaw is calculated to grow in a specified time period

a_c — The minimum critical size of the flaw under normal/upset operating conditions

a_i — The minimum critical size of the flaw under emergency/faulted accident conditions

Stress results from a three-dimensional finite element analysis (Ref. 7) are used to define stress distributions at the J-groove weld. The BIGIF computer program (Ref. 8) is used in the stress intensity factor and FCG analyses. The accuracy of the BIGIF program has been verified for both fracture and FCG analyses.

In addition to flaw evaluation procedures under IWB-3600, an alternate evaluation is performed to the procedure of IWB-3730 and Appendix K, which covers the situation of having adequate fracture toughness margins at upper shelf conditions. The methods of Appendix K are used for determining an allowable flaw size where assumptions regarding weld residual stress and concerns for brittle fracture can be more directly addressed. These procedures and acceptance criteria are discussed in Section 4.5

4.2 Flaw Acceptance Criteria

Flaws are acceptable if the critical flaw parameters satisfy the criteria of IWB-3611. These flaw size acceptance criteria are:

$$a_f < 0.1a_c \tag{4-1}$$

$$a_f < 0.5a_i \tag{4-2}$$

where a_f, a_c, and a_i are defined in Section 4.1.1. Equation 4-1 is the requirement for normal conditions and Eq. 4-2 governs the emergency/faulted conditions.

Alternatively, if the applied stress intensity factor and the flaw size, a_f, satisfy the following IWB-3612 criteria

$$a_f < a_{allow} \tag{4-3}$$

where a_{allow} is the minimum value of "a" determined from the following equations:

$$K_I(a) < K_{Ia}/\sqrt{10}, \quad \text{(normal/upset)} \tag{4-4a}$$

$$K_I(a) < K_{Ic}/\sqrt{2}, \quad \text{(emergency/faulted)}, \tag{4-4b}$$

then the flaw is acceptable based on load. For Eq. 4-4a, K_I is the maximum applied stress intensity factor under normal conditions, and K_{Ia} is the available fracture toughness based on crack arrest for the corresponding crack tip temperature. For Eq. 4-4b, K_I is the maximum stress intensity factor under emergency and faulted conditions, and K_{Ic} is the available fracture toughness based on fracture initiation for the corresponding crack tip temperature.

For the case at flange and shell discontinuities, and when the system pressure is less than 20% of the design pressure and the metal temperature exceeds RT_{NDT} + 60°F, the criteria of IWB-3613 states:

$$K_I(a) < K_{Ia}/\sqrt{2}, \tag{4-4c}$$

then the flaw is acceptable based on load under these limited service conditions.

Satisfying either the flaw size criteria or the applied load criteria and checking that the appropriate primary stress limits are satisfied will demonstrate acceptance of the flaw to ASME Section XI for the design conditions. It is expected that the acceptance criteria for normal conditions will govern the allowable flaw size because of the higher required safety margins imposed by ASME Section XI.

4.3. Calculation Flaw Size Parameters

4.3.1 Calculation of End-of-Life Flaw Size (a_f)

The expected end-of-life flaw size (a_f) is computed by a cumulative FCG analysis for normal operating conditions for the remainder of the expected service life of the component, according to Article A-5200 of Section XI, Appendix A. Normal conditions include all transients expected to occur during testing and normal operation. Included in normal operation are upset conditions that are anticipated to occur frequently enough as to warrant their consideration during design.

The FCG rate (da/dN) of the shell material is characterized by the following relation:

$$da/dN = C_0 \Delta K_I^n \qquad (4\text{-}5)$$

where da/dN is the crack growth rate (i.e., inches per cycle of loading), C_o and n are material constants, and ΔK_I is the range in stress intensity factor for the load cycle ($\Delta K_I = K_{max} - K_{min}$).

The material constants for alloy steel head material are given in Appendix A of ASME Section XI. The BIGIF computer program performs the FCG analysis by integrating Eq. 4-5. The number of applied load cycles, N, for the design transients is calculated from

$$N = \int_{a_0}^{a_f} \frac{da}{da/dN} \qquad (4\text{-}6)$$

where a_o is the starting crack depth and a_f is the final crack depth.

4.3.2 Calculation of Minimum Critical Flaw Size (a_c) for Normal/Upset Conditions

The procedure to compute the minimum critical flaw size for normal operation (a_c) as specified by Article A-5200 of Section XI, Appendix A is outlined below:

1. Determine the maximum end-of-life irradiation level at the flaw location (embrittlement of the PZR bottom head due to neutron radiation is negligible, i.e., $\Delta RT_{NDT} = 0$).

2. Using fracture toughness data, determine the crack-arrest fracture toughness (K_{Ia}) as a function of temperature.

3. Calculate stress intensity factors, K_I, for various geometrically similar crack depths of the assumed flaw.

4. Compare the calculated stress intensity factors to the material fracture toughness (K_{Ia}) for the appropriate temperature to determine a_c for the transient.

5. Proceed to the next transient.

The calculated values for the stress intensity factor as a function of crack depth, $K_I(a)$, are utilized in the determination of a_c from

$$K_I(a_c)=K_{Ia}(T,RT_{NDT}) \qquad (4\text{-}7)$$

where T is temperature at the crack tip and RT_{NDT} is the nil ductility temperature for the shell material. Equation 4-7, therefore, represents the intersection of the toughness distribution and the applied K_I field. The smallest value of a_c determined by the above procedure after all transients have been considered is the minimum critical flaw size for normal operation. This minimum value of a_c is checked against the flaw acceptability criteria of IWB-3600 (see Section 4.2).

4.3.3 Calculation of Minimum Initiating Flaw Size (a_i) for Accident Conditions

The procedure to compute the minimum initiating flaw size (a_i) for emergency/faulted conditions as specified by Article A-5300 of Section XI, Appendix A, is outlined below:

1. Determine the maximum end-of-life irradiation level at the flaw location (embrittlement of the pressurizer bottom head due to neutron radiation is assumed to be negligible, i.e., $\Delta RT_{NDT} = 0$).

2. Using fracture toughness data, determine the initiation fracture toughness (K_{Ic}) as a function of temperature.

3. Calculate stress intensity factors, K_I, for various geometrically similar crack depths of the assumed flaw.

4. Compare the calculated stress intensity factors to the material fracture toughness (K_{Ic}) for the appropriate temperature to determine a_i for the transient.

5. Proceed to the next transient.

The calculated values for the stress intensity factor as a function of crack depth, $K_I(a)$, are utilized in the determination of a_i from

$$K_I(a_i)=K_{Ic}(T,RT_{NDT}) \tag{4-8}$$

where T is the temperature at the crack tip and RT_{NDT} is the nil ductility temperature for the shell

material. Equation 4-8, therefore, represents the intersection of the toughness distribution and the applied K_I field. The smallest value of a_i determined by the above procedure after all accident conditions have been considered is the minimum initiating flaw size for emergency/faulted conditions. This minimum value of a_i is checked against the flaw acceptability criteria of IWB-3600 (see Section 4.2).

4.4 Calculation of Stress Intensity Factor

The stress intensity factor is defined as

$$K_I=\sigma F\sqrt{\pi a/Q} \tag{4-9}$$

where σ is the applied stress, F is a function which accounts for flaw geometry and loading mode, "a" is the crack depth, and Q is the flaw shape parameter. The explicit calculation of K_I is performed numerically by the BIGIF program.

4.5 Fracture Toughness Criteria of Appendix K

For the condition of preventing failure on the upper shelf, adequate toughness is evaluated by demonstrating flaw stability. The equilibrium equation for stable flaw extension is:

$$J = J_R \tag{4-10}$$

where J is the applied J-integral for the applied loads on the flaw and J_R is the fracture toughness resistance curve against ductile tearing. The condition for stable ductile tearing is defined by the inequality:

$$\frac{\partial J}{\partial a} < \frac{dJ}{da} J_R \tag{4-11}$$

where $\partial J/\partial a$ is the partial derivative of the applied J-integral with respect to flaw depth (load held constant), and dJ/da is the slope of the J_R curve for the material. Under increasing load, stable flaw extension will continue as long as $\partial J/\partial a$ in Eq. 4-11 remains valid.

For Service Level A and B (normal/upset conditions), adequacy of the upper shelf toughness is confirmed when, for a 1/4t flaw depth plus an additional 0.1 inch in depth to account for crack extension, and a factor of 1.15 on accumulation pressure, and a factor of 1.0 on thermal loads, the $J_{applied}$ is less than $J_{0.1}$,

$$J_{applied} < J_{0.1} \tag{4-12}$$

where $J_{0.1}$ is the J_R value at 0.1 inch crack extension. For limiting ductile tearing, flaw extensions at 1.25 times the accumulation pressure and 1.0 on thermal loads, shall remain ductile and stable.

Translating these criteria to flaw evaluation in terms of preventing crack initiation, the structural factors from Eq. 4-12 are equivalent to a factor of 1.4 on operating pressure (accumulation pressure is 1.10 times design pressure and operating pressure is 0.9 times design pressure). Provided that the postulated flaw depth is on the order of 25% of the wall thickness, preventing fracture initiation can be represented by

$$J_{applied} < J_{Ic} \tag{4-13}$$

In order to maintain the same margin on primary load that ASME Section XI Appendix A requires, the elastic-plastic parameters of Eq. 4-13 can be evaluated for the condition of constrained plasticity based on fracture initiation with the following relationships:

$$J_{applied} = 1000(3.16K_{Ip} + K_{It})^2 / E' \tag{4-14}$$

$$J_{Ic} = 1000 K_{Ia}{}^2 / E' \tag{4-15}$$

$$a_e = a + \frac{1}{6\pi}\left[\frac{K_{Ip} + K_{It}}{\sigma_y}\right]^2 \tag{4-16}$$

where

3.16 factor is simply $10^{1/2}$ structural factor from IWB-3612 acceptance criteria

K_{Ip} is the stress intensity factor for pressure loading for crack depth "a" determined from the plastic-zone corrected crack depth a_e in Eq. 4-16,

K_{It} is the stress intensity factor for thermal loading for crack depth "a" determined from the plastic-zone corrected crack depth a_c in Eq. 4-16,

σ_y is the yield strength for the material

E' is $E/(1-\nu^2)$ where E is the modulus of elasticity and ν is Poisson's ratio.

Satisfying Eq. 4-13 will be sufficient to meet the criteria of Appendix K in that crack extension is being prevented by the increased structural factor on pressure load (additional factor of 3.16/1.40 or 2.25) and the use of the initiation toughness based on K_{Ia} lower bound curve. Therefore tearing stability criterion will automatically be satisfied if Eq. 4-13 is met.

4.6 Definition of Stresses in the J-Groove Region

The distribution of hoop stresses at the sleeve penetration and throughout the PZR bottom head was obtained from the results of a three-dimensional finite element analysis (Ref. 7). An illustration of the finite element model is shown in Figure 4-2. Additional views of the model are given in Figures 4-3 and 4-4. This model geometry represents the outermost heater sleeve location (i.e., 52 degree penetration angle). The model represents a 90 degree segment of the PZR lower shell and bottom head. The model includes the surge nozzle and support skirt. The other heater sleeve penetrations are also modeled but the sleeves were omitted from the model to simplify the analysis since they will not affect the local stress results in the area of the outermost sleeve.

Close-up views of the sleeve, original J-groove weld, and repair weld/pad on the outside of the bottom head is shown in Figures 4-3 and 4-4. The results from this analysis will be bounding for sleeves at other locations.

A summary of input stress distributions are given in Appendix A of this calculation. These stress results are used as input to the BIGIF program in the calculation of allowable flaw depth and final flaw depth due to cyclic (fatigue) loading.

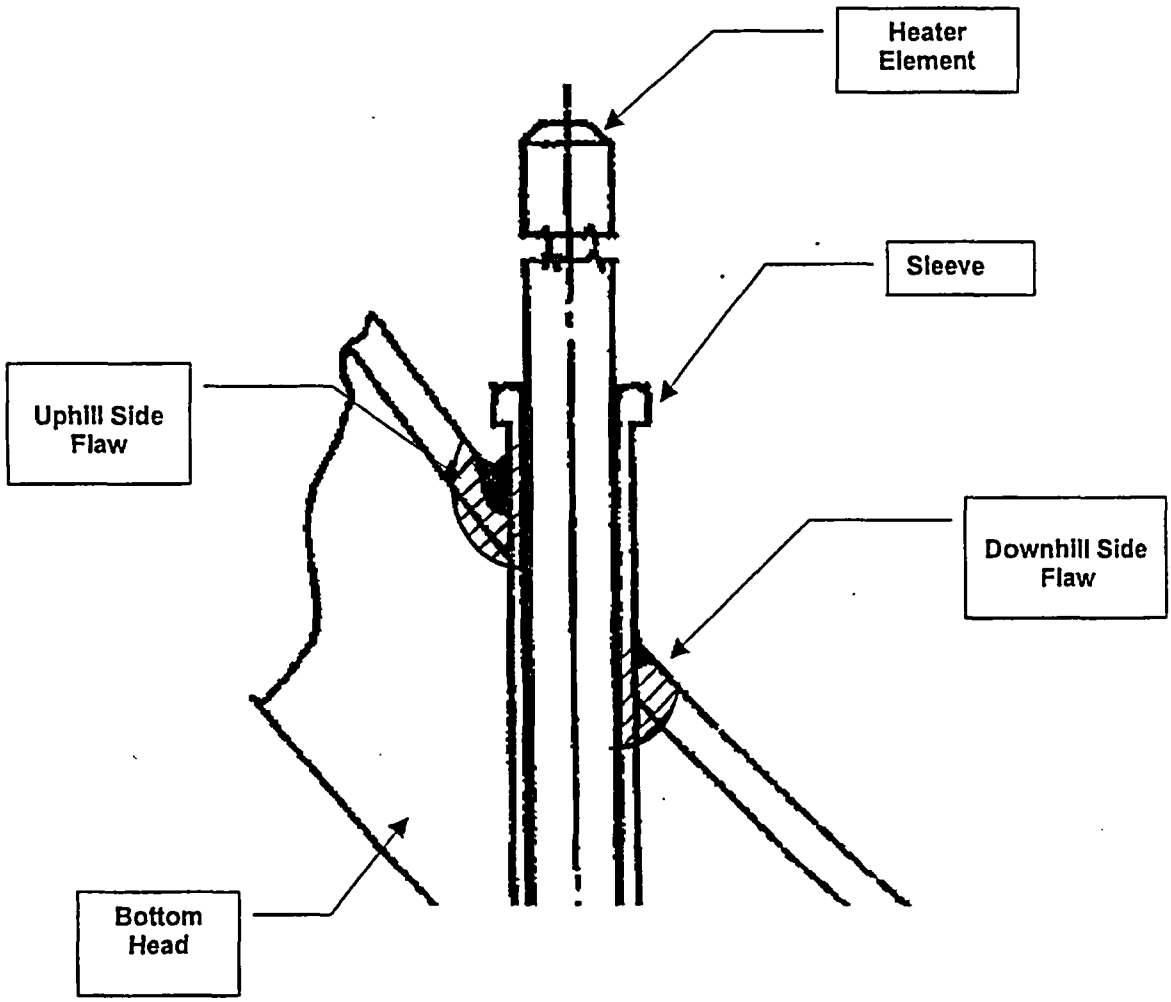

Figure 4-1 — Postulated Flaw in Heater Sleeve Weld Region.

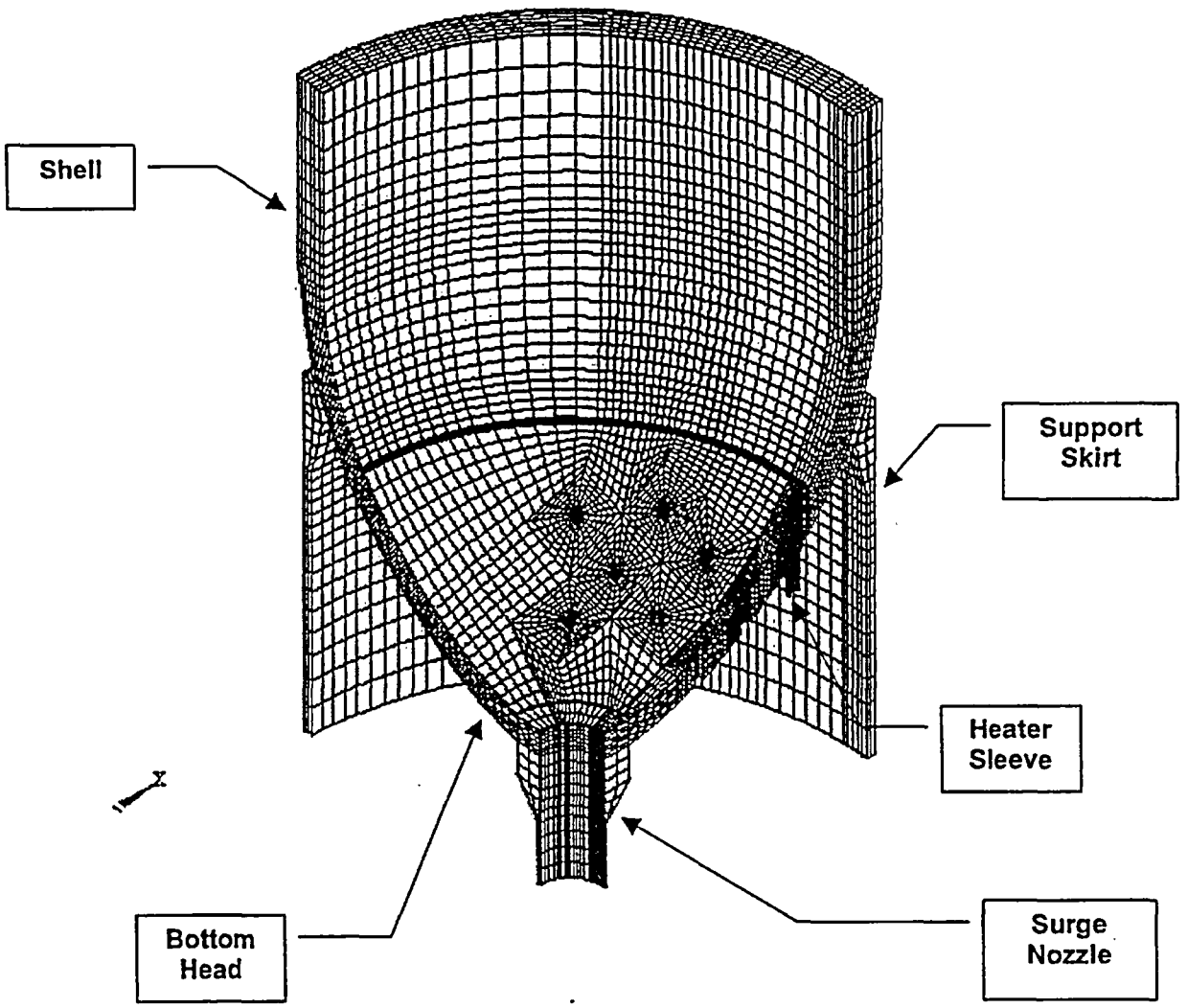

Figure 4-2 — Finite Element Model of PZR Bottom Head.

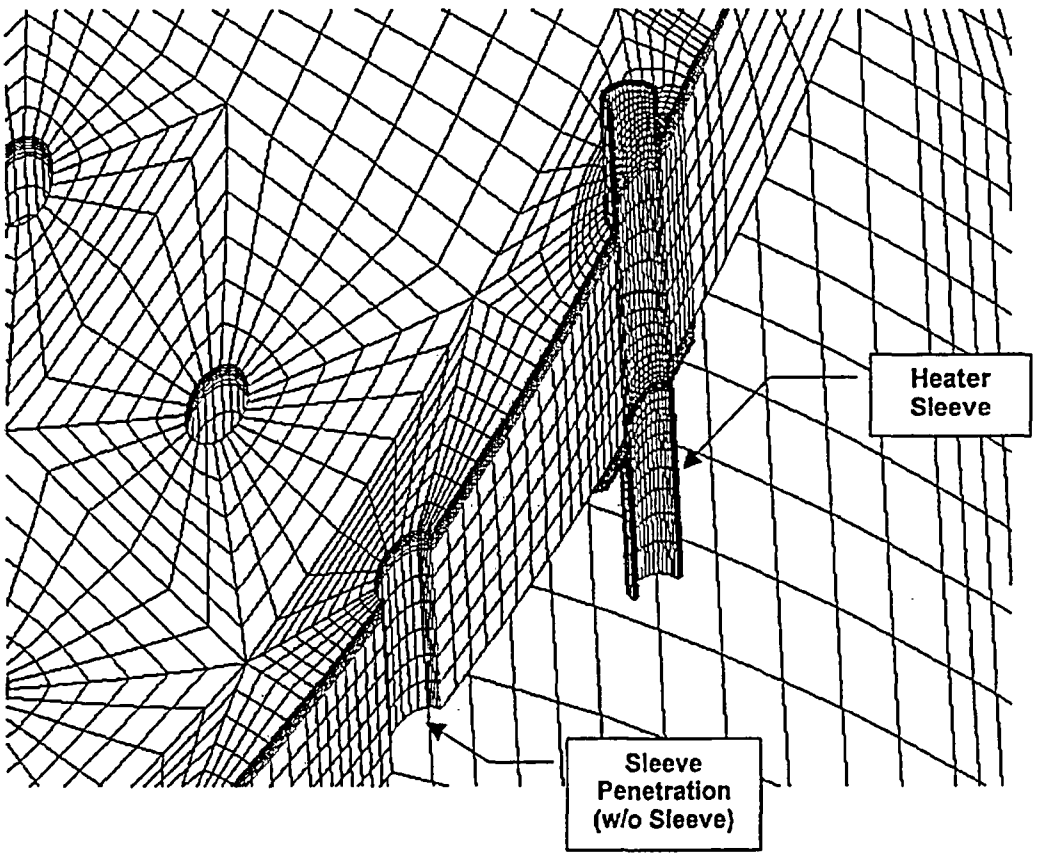

Figure 4-3— Local View of Heater Sleeve Region.

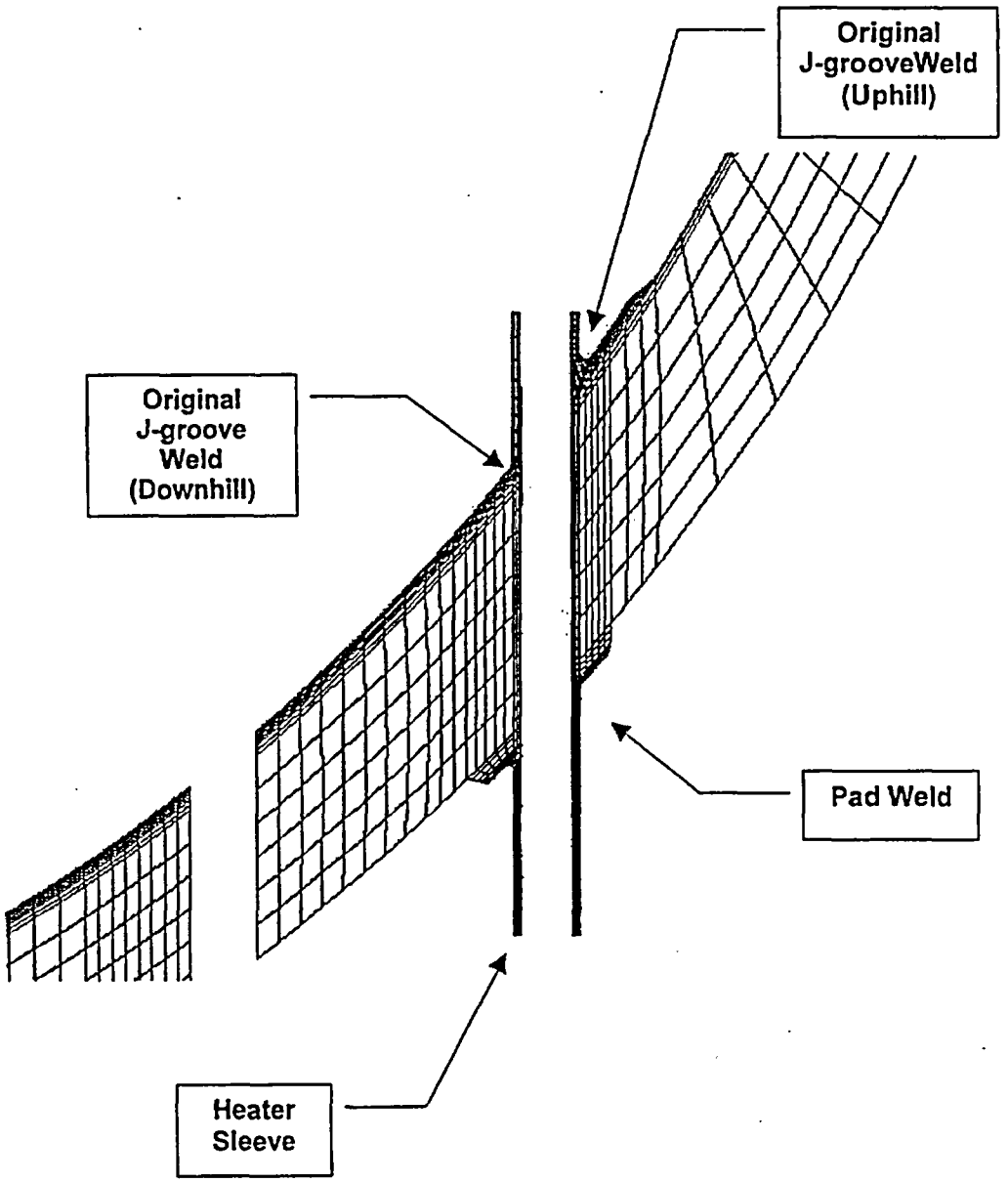

Figure 4-4— Edge View of Heater Sleeve Region.

5.0 DESIGN INPUT

5.1 Sleeve and Bottom Head Geometry

The heater sleeve is 1.660-inch nominal outside diameter size. The heater sleeve completely penetrates the PZR bottom head wall. The penetration through the spherical head is vertical. A schematic illustration of the nozzle geometry is shown in Figure 5-1a (Ref. 2). The components of this penetration are described as follows (Refs. 1, 2, 6):

Sleeve:

Outer radius:	r_o = 0.830 inch (max)
Inner radius:	r_I = 0.6365 inch (min)
Wall thickness:	t = 0.1935 inch (max)

Bottom Head:

Outer radius:	R_o = 52 5/16 inches
Inner radius:	R_i = 48 7/16 inches (excluding clad)
Wall thickness:	t_h = 3 7/8 inches (min, w/o clad)
Clad thickness:	t_c = 7/16 inch
Hole diameter:	D_h = 1.672 inches (min) counter bore
	= 1.662 inches (min) through hole

The half-nozzle repair geometry is illustrated in Figure 5-1b (Ref. 9).

5.2 Design and Operating Conditions

The design data for the primary side of the RCS from Refs. 10 and 11 are as follows:

Design pressure	= 2500 psia
Design temperature	= 700°F
Operating pressure	= 2250 psia
Operating temperature	= 653°F
Hydrotest pressure	= 1.25 P_D = 3125 psia (3110 psig)

Thermal transients are given in Table 5-1 (Refs. 10 and 11). Seven thermal cases are conservatively assumed that envelop the thermal transients. These are:

1. Isothermal steady-state load of 653°F; corresponding reactor coolant pressure is 2235 psig.
2. Heatup/cooldown at a rate of 200°F per hour; corresponding change in reactor coolant of 2235 psig.
3. Cooldown with flooding.
4. Plant loading/unloading and step changes of ±20°F; corresponding change in reactor coolant of ±100 psig.
5. Reactor trip (loss of load, etc).
6. Loss of secondary pressure (emergency condition).
7. Leak and hydro test heatup/cooldown at 100°F per hour; corresponding change in reactor coolant pressure is 2235 and 3110 psig.

Except for Case 5, all design basis conditions are classified as normal or upset conditions. Case 5 is classified as emergency condition and is the only accident condition relevant for the bottom head heater sleeve penetrations. The transient temperature conditions for Cases 3, 4 and 5 above are illustrated in Figures 5-2, 5-3 and 5-5. Specified changes in reactor coolant pressure for cooldown with flooding, reactor trips, and loss in secondary pressure are shown in Figures 5-2, 5-4 and 5-6

5.3 Material Properties

5.3.1 Mechanical Strength

The materials that comprise the head and sleeves (Refs. 10 and 11) are as follows:

Bottom Head:	SA-533, Grade B, Class 1
Sleeve:	SB-167, Alloy 600
Head Cladding:	Alloy 600
Shell/Nozzle Cladding	Type 304 stainless steel
Surge Nozzle	SA-508, Class II
Support Skirt:	SA-516 Grade 70

In the stress analysis, the cladding is included. The mechanical strength properties at the design temperature are summarized below (Ref. 3):

MECHANICAL STRENGTH AT 700°F		
	Sleeve/Weld (Alloy 600)	Bottom Head (SA-533B-1)
S_m (ksi)	23.3	26.7
S_y (ksi)	27.0	43.1
S_u (ksi)	80.0	80.0

Also, S_y for Alloy 600 at 100°F is 35 ksi. In the assessment of yielding and imposed weld residual stress, a maximum yield strength of 60 ksi is assumed.

5.3.2 Fracture Toughness

Definition of fracture toughness at the flaw location as a function of temperature was obtained from Article A-4000 of Appendix A to Section XI (Ref. 4). Section XI defines lower-bound behavior for K_{Ia} and K_{Ic} for SA-533B-1, SA-508-2, and SA-508-3 steels and associated welds, as shown in Figure 5-7. The equational formats of these reference curves are given below:

$$K_{Ia} = 26.8 + 12.445 \exp[0.0145 (T - RT_{NDT})] \quad (5\text{-}1)$$

$$K_{Ic} = 33.2 + 20.734 \exp[0.02 (T - RT_{NDT})] \quad (5\text{-}2)$$

where T is the metal temperature in °F, RT_{NDT} is the reference nil ductility temperature in °F, and K_{Ia} and K_{Ic} are fracture toughness in ksi in$^{1/2}$. The toughness parameter, K_{Ic}, is based on the lower bound of static initiation critical K_I values measured from specimens tested at several temperatures. Similarly, K_{Ia} is based on the lower bound of crack-arrest toughness data. It is assumed that the transition behavior of SA-533B-1 will be such that the normal operation of the PZR bottom head will be on the upper shelf during times when maximum pressure stresses are imposed.

The pressure-temperature (P-T) operation of the RCS will be controlled by the P-T limit curves for the RPV and, therefore, maximum operating stresses will not be experienced by the PZR at lower shelf toughness temperatures. This assumption is justified by the fact that RT_{NDT} of SA-533B-1 will be less than +20°F, which is the mean plus two standard deviations (upper bound) reported in Ref. 12. An RT_{NDT} = +20°F will cause the onset of upper shelf conditions at T > 120°F for initiation toughness. For this condition, the upper shelf toughness is 200 ksi in$^{1/2}$, as reflected in Figure 5-7, and is based on data evaluations in Ref. 13.

5.3.3 Fatigue Crack Growth Rate for the PZR Bottom Head

The reference curve for crack growth rate (da/dN) in a reactor water environment is given in Figure A-4300-2 of ASME Section XI, Appendix A, and is shown in Figure 5-8 for two R-ratio regimes. The crack growth behavior for the R-ratio range ($0 \leq R \leq 0.25$) is used in this evaluation. The equation for crack growth is:

$$da/dN = 1.02 \times 10^{-12}\ \Delta K^{5.95} \qquad \Delta K \leq 17.74 \text{ ksi in}^{1/2} \qquad (5\text{-}3)$$

$$da/dN = 1.01 \times 10^{-7}\ \Delta K^{1.95} \qquad \Delta K > 17.74 \text{ ksi in}^{1/2} \qquad (5\text{-}4)$$

where ΔK is in units of ksi in$^{1/2}$ and da/dN is in units of inches/cycle. These crack growth rates are used as input to the FCG analysis for the PZR bottom head. The basis for the use of Eqs. 5-3 and 5-4 is discussed in under the analysis assumptions.

Table 5-1

THERMAL TRANSIENT CONDITIONS (Refs. 6, 10 & 11)

Symbol	Transient Condition		Occurrence
A1	Plant Heatup	200°F/hr	500
B1	Steady State	653°F, 2250 psia	-
C1	Cooldown	-200°F/hr	500
CF1	Cooldown with Flooding	Fig. 5-2	
D1	Plant Loading/Step Increase	+20°F + 100 psia	1,000,000
E1	Plant Unloading/Step Decrease	-20°F -100 psia	
F1	Reactor Trip	Figs. 5-3 & 5-4	480
G1	Loss of Secondary Pressure	Figs. 5-5 & 5-6	5
H1	Plant Leak Test, Heatup	100°F/hr 2250 psia	200
H2	Plant Leak test, Cooldown	-100°F/hr 2250 psia	200
J1	Hydrostatic Test, Heatup	100°F/hr 3125 psia	10
J1	Hydrostatic Test, Cooldown	-100°F/hr 3125 psia	

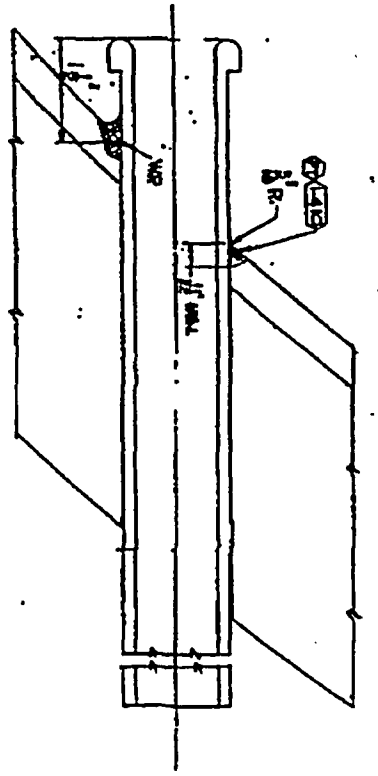

Figure 5-1a — Illustration of the Heater Sleeve Geometry (Original J-Groove Configuration).

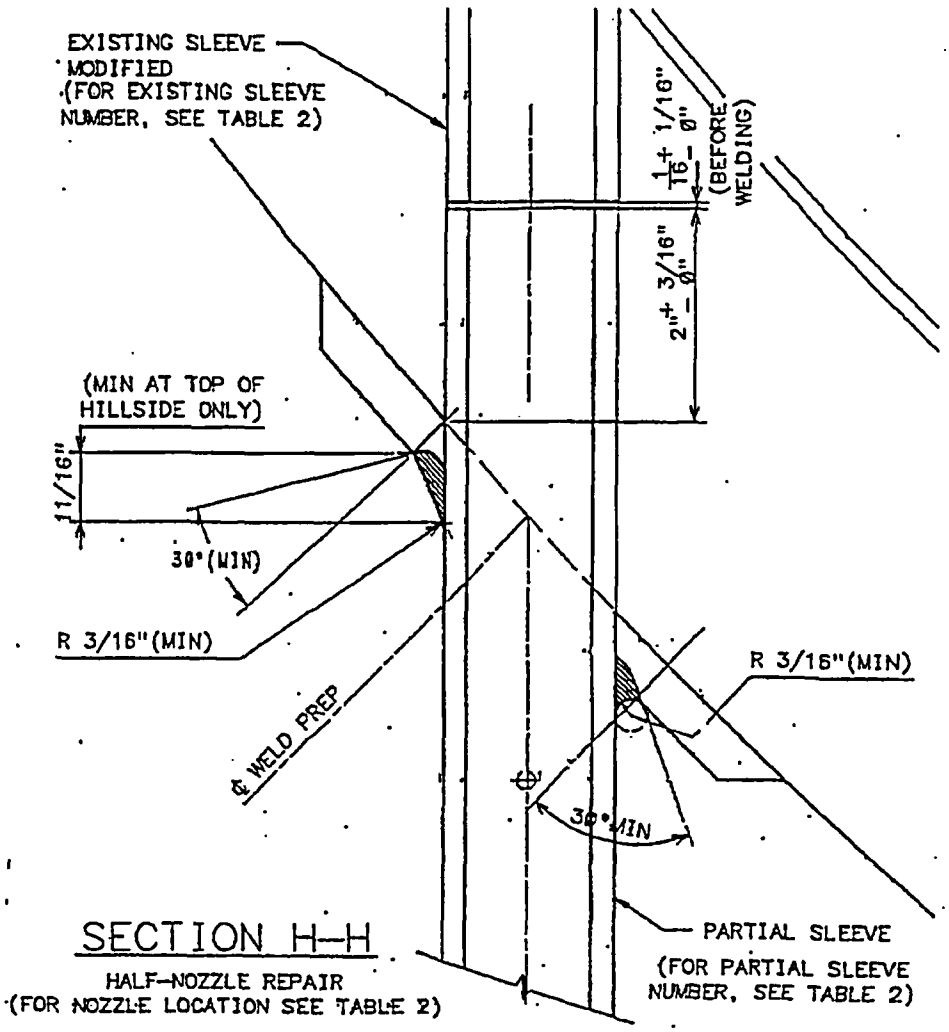

Figure 5-1b — Illustration of the Half-Nozzle Repair Configuration.

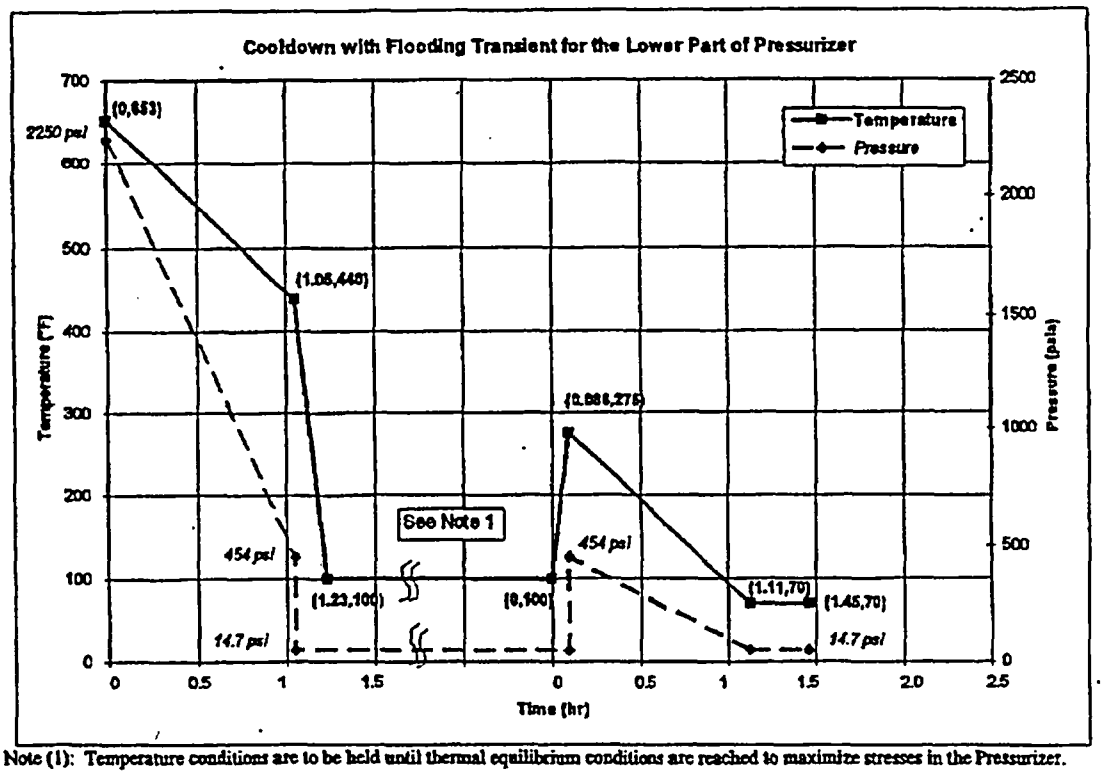

Note (1): Temperature conditions are to be held until thermal equilibrium conditions are reached to maximize stresses in the Pressurizer.

Figure 5-2 — Transient Condition — Cooldown with Flooding Transient (Figure 10 of Ref. 10).

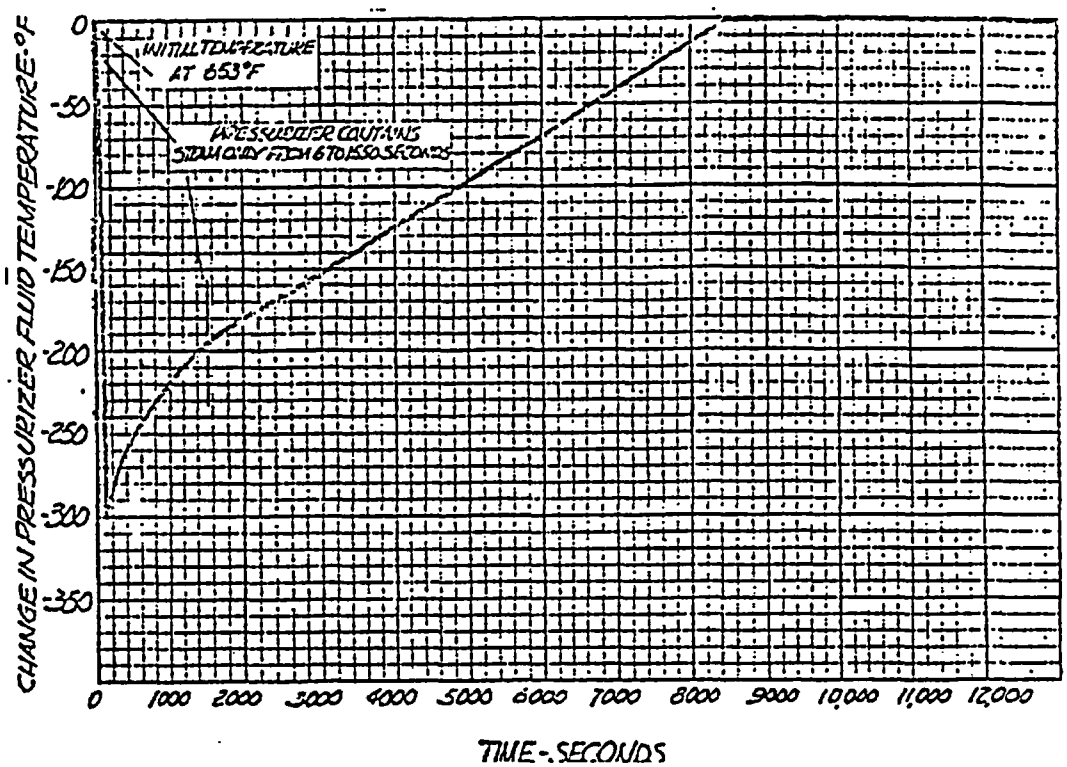

Figure 5-3 — Temperature Change in Reactor Coolant During Reactor Trip Transients (Figure 4 of Ref. 11).

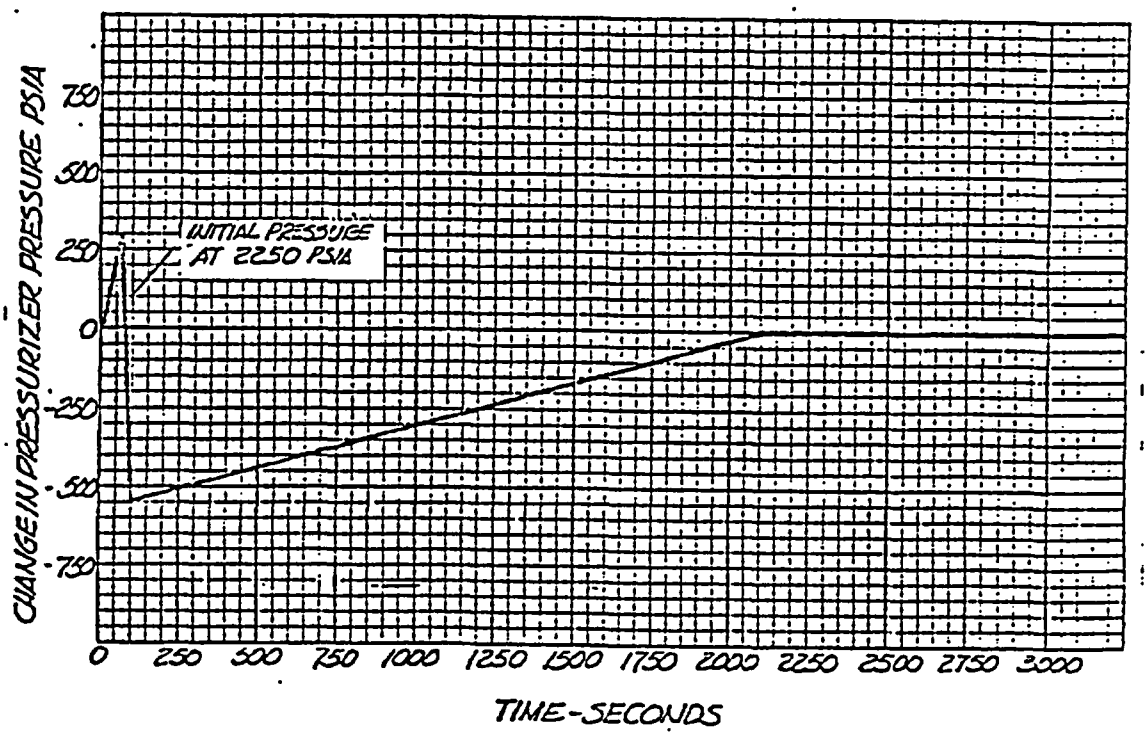

Figure 5-4 — Pressure Change in Reactor Coolant During Reactor Trip Transients (Figure 3 of Ref. 11).

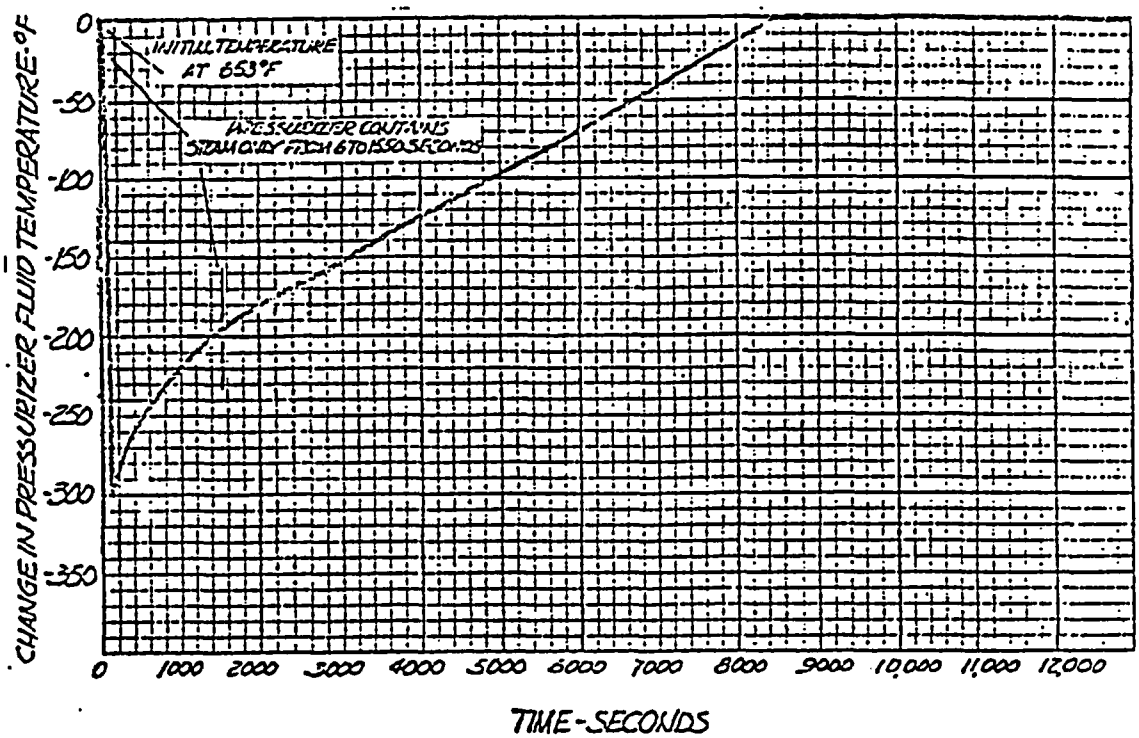

Figure 5-5 — Temperature Change in Reactor Coolant During Loss of Secondary Pressure Transient (Figure 4 of Ref. 11).

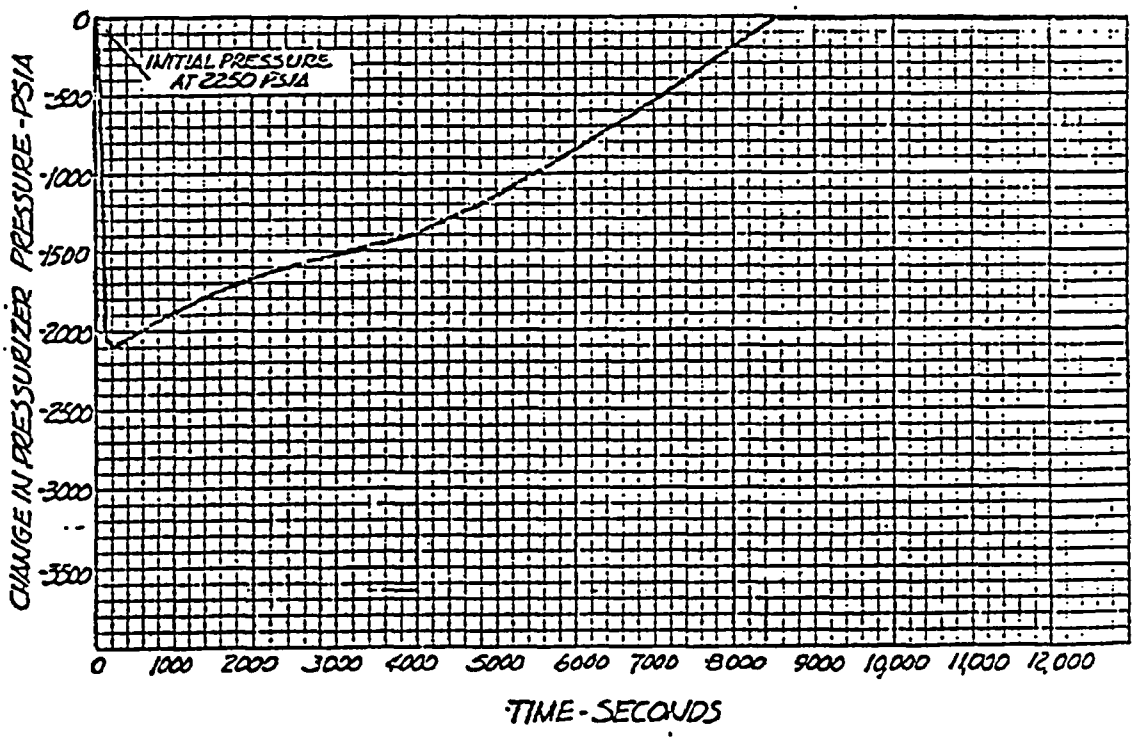

Figure 5-6 — Pressure Change in Reactor Coolant During Loss of Secondary Pressure Transient (Figure 4 of Ref. 11).

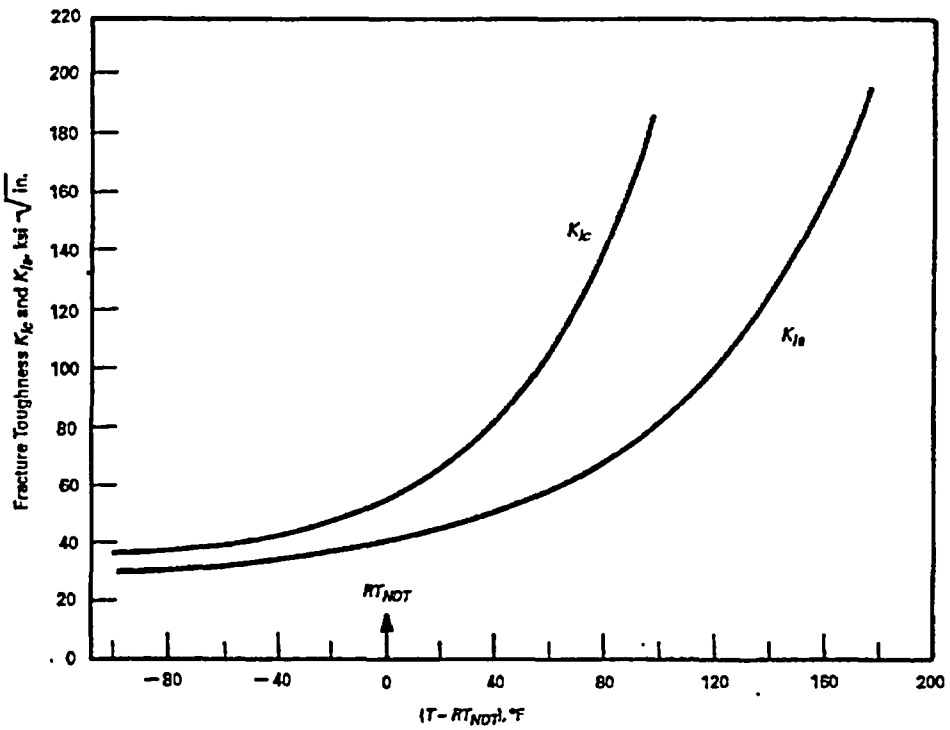

Figure 5-7 - Lower Bound Fracture Toughness from Tests of SA-533B-1, SA-508-2, and SA-508-3 (Figure A-4200-1 from ASME Section XI, Appendix A, in Ref. 4).

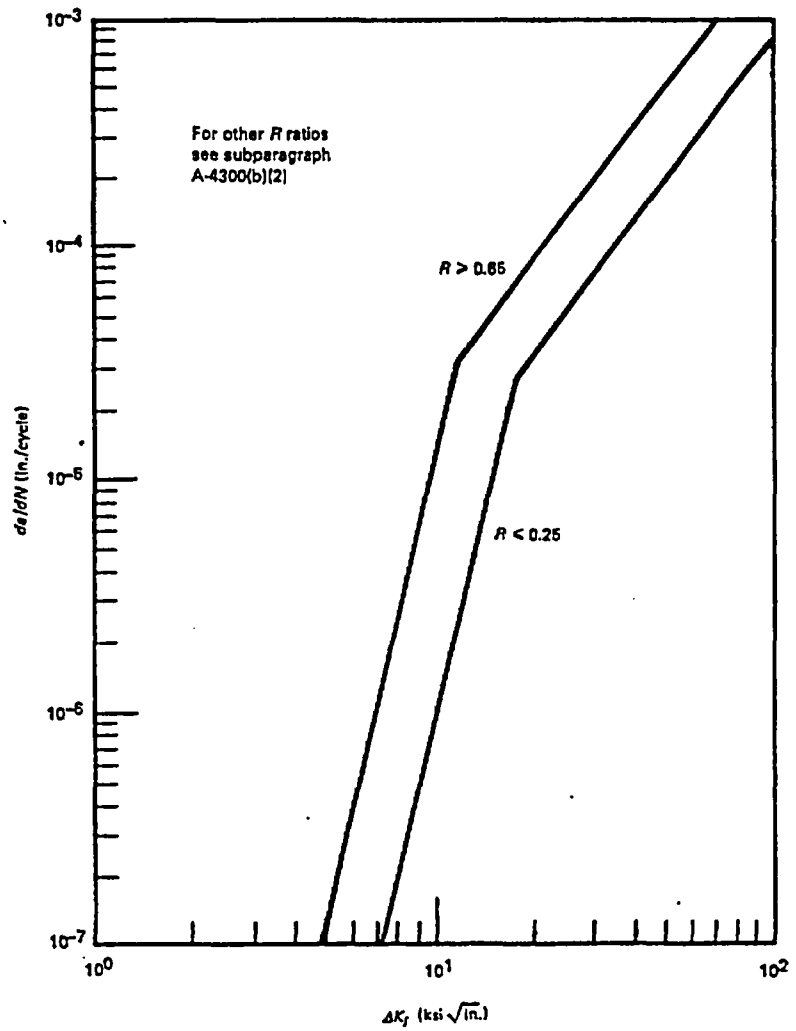

Figure 5-8 — Reference Fatigue Crack Growth Curves for Carbon and Low Alloy Ferritic Steels Exposed to Water Environments (Figure A-4300-2 from ASME Section XI, Appendix A, in Ref. 4).

6.0 REFERENCES

1. Drawing 235-121, Rev. 3, "Pressurizer General Arrangement San Onofre III," SO23-919-79-0 (October 10, 1976) (ECD-11 from Project AES 97103213-1Q).

2. Drawing 235-130, Rev. 4, "Heater Arrangement and Assembly Sa Onofre III," SO23-909-86-01 (March 31, 1981) (ECD-12 from Project AES 97103213-1Q)).

3. ASME Boiler and Pressure Vessel Code, Section III, "Rules for Construction of Nuclear Power Plant Components," 1971 Edition through 1971 Summer Addenda.

4. ASME Boiler and Pressure Vessel Code, Section XI, "Rules for Inservice Inspection of Nuclear Power Plant Components," 1995 Edition with 1996 Addenda.

5. "Evaluation of Half-Nozzle Repair for Pressurizer and Steam Generator Instrumentation Nozzles Under Long-Term Service Conditions," Calculation No. AES-C-3247-1, Aptech Engineering Services, Inc. (ICD-2 for Project AES 97123247-1Q) (May 11, 1998)

6. "Analytical Report for Southern California, San Onofre, Unit 2, Pressurizer," CENC-1275, CDCC No. 21986, Combustion Engineering, September 1976 (ECD-5 from Project AES 97103213-1Q).

7. "SONGS 2 and 3 Pressurizer Bottom Head Stress Analysis," ANSYS Results transmitted electronically, Southern California Edison (July 2004) (ECD-2 through 10).

8 Cipolla, R. C., P. M. Besuner, and D. C. Peters, "BIGIF — Fracture Mechanics Code for Structures," Manual 2, User's Guide, EPRI NP-838 (August 1978).

9. "Half-Nozzle Repair Drawing," DOC No. S023-919-86, Revision 1, Southern California Edison, Transmitted September 15, 2004, (ECD-15).

10. "Project Specification for a Pressurizer Assembly for San Onofre Units Nos. II & No. III," Specification No. 01370-PE-130, Revision 10, Combustion Engineering, SCE S023-919-3, Rev. 8 (January 4, 1999) (ECD-1).

11. "General Specification for a Pressurizer Assembly," Specification No. 00000-PE-130, Revision 3, Combustion Engineering, SCE S023-919-4-1, (October 25, 1972) (ECD-2 from Project AES 97103213-1Q).

12. NUREG-0577, "Potential for Low Fracture Toughness and Lamellar Tearing on PWR Steam Generator and Reactor Coolant Pump Supports," Appendix C (October 1979).

13. "Flaw Evaluation Procedures — Background and Application of ASME Section XI Appendix A," EPRI NP-719-SR, Electric Power Research Institute (August 1973).

14. "Operability Assessment for CEOG Plants with Hypothetical Circumferential Flaw Indications in Pressurizer Heater Sleeves," Draft WCAP-16180, Rev. 0, Westinghouse Electric (November 2003).

15. "Evaluation of Modified Pressurizer Heater Sleeves - SONGS Unit 2 and 3," Calculation No. AES-C-5212-1, Project AES-03105212-1Q, Aptech Engineering Services, (September 17, 2004) (ICD-1).

7.0 NOMENCLATURE

a	= Flaw depth, inch
a_{allow}	= Allowable flaw depth, inch
a_c	= Minimum critical crack size for normal/upset conditions, inch
a_f	= Final flaw depth, inch
a_i	= Minimum critical crack size for accident conditions, inch
a_o	= Initial flaw depth, inch
Δa	= Change in flaw depth, inch
C_o	= Material constant in the reference FCG equation
D	= Depth of corrosion groove, inch
d_h	= Diameter of hole penetration, inch
D_o	= Outer diameter, inch
E	= modulus of elasticity (ksi)
F	= Flaw correction factor
J	= J-integral value, in-lbs/in
$J_{applied}$	= Applied J-integral curve, in-lbs/in
J_R	= J resistance toughness curve for ductile tearing, in-lbs/in
K	= Stress intensity factor, ksi $in^{1/2}$
K_I	= Mode I stress intensity factor, ksi $in^{1/2}$
K_{Ia}	= Fracture toughness for crack arrest, ksi $in^{1/2}$
K_{Ic}	= Static fracture toughness for initiation, ksi $in^{1/2}$
K_{max}	= Maximum value of K in stress cycle, ksi $in^{1/2}$
K_{min}	= Minimum value of K in stress cycle, ksi $in^{1/2}$
ΔK	= Range in stress intensity factor ($K_{max} - K_{min}$), ksi $in^{1/2}$
n	= Exponent in the reference FCG equation
N	= Number of cycles
P	= Pressure, psi
P_D	= Design pressure, psi
P_{max}	= Maximum pressure in transient, psi
P_{min}	= Minimum pressure in transient, psi

ΔP	=	Pressure fluctuation, psi
Q	=	Flaw shape parameter
R	=	Radial distance, inch
r_o	=	Outer radius of sleeve, inch
r_i	=	Inner radius of sleeve, inch
R	=	Mean radius, inch
R	=	R-ratio (K_{min} / K_{max})
R_o	=	Outer radius of head or shell, inch
R_i	=	Inner radius of head or shell, inch
S_m	=	Allowable stress intensity, psi
S_u	=	Specified minimum ultimate tensile strength, ksi
S_y	=	Specified minimum yield strength, ksi
t	=	Wall thickness, inch
T	=	Temperature, °F
ΔT	=	Temperature difference, °F
t_c	=	Clad thickness, inch
t_h	=	Head or shell thickness, inch
ν	=	Poisson's ratio
σ_y	=	Yield strength, ksi

8.0 CALCULATIONS

8.1 Heater Sleeve Penetration Stresses

The hoop stresses for the heater sleeve penetration were obtained from the finite element analysis contained in Ref. 7. These stress summaries are given in Appendix A of this calculation. The loading conditions and corresponding stress results for the outer heater sleeve penetration are bounding due to the more severe geometric discontinuity between the sleeve and head. Therefore, the stress distributions from this stress analysis are conservatively used to establish the maximum and cyclic stress behavior for all heater sleeve penetrations.

The following load cases from Ref. 7 were used to bound the maximum stresses and stress ranges at the postulated flaw locations:

1.	Internal	P = 2500 psi
2.	Heatup	$\Delta T = 200°F/hr$
3.	Cooldown	(P = 2235 psig)
4.	Cooldown with Flooding	Fig. 5-2
5.	Isothermal	T = 653°F
6.	Plant Load/Unload Transient	$\Delta P = \pm 100$ psi, $\Delta T = \pm 20°F$)
7.	Reactor Trip	Figs. 5-3 & 5-4
8.	Loss of Secondary Pressure	Figs 5-5 & 5-6
9.	Leak/Hydro Test	$\Delta T = \pm 100°F/hr$

Weld residual stress was developed from literature results and added to the mechanical and thermal stresses when computing allowable flaw depths.

The stress combinations for the fatigue stress ranges for the eight plant transient conditions were developed from the load cases. The seven plant transient conditions (Refs. 10 and 11) are listed below:

Plant Condition	N	Pressure (psig) P_{max}	P_{min}	ΔT	N/Month
1. Startup/Shutdown	500	2235	0	±200°F/hr	1.042
2.. Startup/Shutdown/Flooding		2235	0	Fig. 5-2	
3. Plant Load Changes	10^6	2235	2135	+20°F	1042
4. Plant Unload Changes		2235	2135	-20°F	1042
5. Reactor Trip	480	2535	1635	Fig. 5-3	1.00
6. Loss of Secondary Pressure	5	2235	135	Fig. 5-5	0.010
7. Leak Test	200	2235	385	±100°F/hr	0.417
8. Hydro Test	10	3110	0	±100°F/hr	0.021

A stress summary for cyclic stress ranges for each transient is given in Appendix A of this calculation. These stresses are used as input to the BIGIF computer program.

8.2 Consideration of Weld Residual Stresses

The magnitude and distribution of weld residual stress were evaluated to determine if residual stress needs to be explicitly included in the flaw evaluation. The effect of weld residual stress is two-fold. First, it will increase the stress local to the weld zone, which can affect the critical flaw size. Second, there can be a higher mean stress in the tensile areas of residual stress that can lead to faster FCG rates. Therefore, the effect of residual stress must be considered and addressed in some format.

8.2.1 Fracture Resistance

The weld residual stress can potentially lower the brittle fracture resistance of the ferritic head material. Because of the ductile nature and austenitic structure of Alloy 600, the nozzle and J-groove weld will not be significantly affected by the presence of high residual stresses. Therefore, the consideration of residual stress on fracture is only an issue for the PZR bottom head.

Calculations that simulate the weld process for the sleeve has been performed for a similar plant design (Ref. 14). Figure 8-2 illustrates the stress contours for the weld residual plus operating stress state local to the J-groove region. This stress contour plot indicates that the peak residual stresses are local to the weld and that the magnitude of stress away from the weld is very low. Further, compressive stresses are also developed local to the weld region.

From these stress analyses, the following considerations was used to construct a residual stress fields in the hoop direction for the uphill and downhill weld regions:

1. Peak residual tensile stress occurs at the surface of the J-groove weld and attenuates with distance from the surface. The magnitude of the tensile residual stress is on the order of the yield strength of the material. The tensile field is contained within the Alloy 600 material.

2. Compressive residual stresses are developed at a depth near the clad to base metal region for the uphill side (larger weld prep area), and within the clad for the downhill side (smaller weld prep area). The magnitude of the compressive stresses is on the order of 50% of the yield strength.

3. The compressive residual stress attenuates slowly below the clad and becomes near zero within a distance of three times the clad thickness.

4. In general, the alloy steel head material will be under compressive residual stress at the clad interface.

On the basis of the stress attenuation and compressive nature of the weld residuals, the effect of weld residual stress on head fracture was included in the analysis for maximum stress intensity factor for the more limiting plant transients.

8.2.2 Fatigue Crack Growth Rate

The FCG rate for both Alloy 600 and ferritic pressure vessel steels will exhibit a faster rate when high mean stresses (high R-ratio where $R = K_{min}/K_{max}$) are present. Since residual stress is not explicitly evaluated in the FCG analysis, the affect of R on growth rate is addressed by assuming an R-ratio equal to 0.25 for all transients and flaw depths. This assumption is judged to be conservative since the combination of residual stress and compressive stresses from thermal stresses will cause R to be more in the range of $-1.0 < R < 0.0$. This assumption is made in Sections 5.3.3 and the FCG equations were modified accordingly. Therefore, the effect of mean stress is conservatively treated in the FCG analysis.

8.3 Definition of Cycle Stresses

The FCG evaluation requires the stress range ($\Delta\sigma$) for each transient condition. The values for $\Delta\sigma$ are developed in Appendix A (Tables A-1 and A-2) for the J-groove weld region. The following table of scaling factors was used to define $\Delta\sigma$ from the eight loading cases:

Plant Condition	Load Case									
	P_{MAX}/ P_{MIN}	ISO	HU	CD	CDF	+/- STEP	TRIP	LOSP	LTHU	LTCD
1. Startup/shutdown	0.894/0.0	0.0	1.0	1.0	0.0	0.0	0.0	0.0	0.0	0.0
2. Startup/Shutdown/Flooding	0.894/0.182	0.0	1.0	0.0	1.0	0.0	0.0	0.0	0.0	0.0
3. Steady State Operation	0.894/0.894	1.0	0.0	0.0	0.0	0.0	0.0	0.0	0.0	0.0
4. Plant Load Change	0.934/0.894	0.0	0.0	0.0	0.0	1.0	0.0	0.0	0.0	0.0
5. Plant Unload Change	0.894/0.854	0.0	0.0	0.0	0.0	1.0	0.0	0.0	0.0	0.0
6. Reactor Trip	1.014/0.674	0.0	0.0	0.0	0.0	0.0	1.0	0.0	0.0	1.0
7. Loss of Secondary Pressure	0.894/0.054	0.0	0.0	0.0	0.0	0.0	0.0	1.0	0.0	0.0
8. Leak Test	0.894/0.0	0.0	0.0	0.0	0.0	0.0	0.0	0.0	1.0	1.0
9. Hydro Test	1.243/0.0	0.0	0.0	0.0	0.0	0.0	0.0	0.0	1.0	1.0

The time step at which the maximum/minimum stress occurs during the transient was determined from the time where the linearized membrane plus bending stress was at maximum or minimum. This was accomplished by an analysis of the transient stress output given in Ref. 7 (see Appendix A).

8.4 Evaluation of Postulated Flaws at the J-Groove Weld

8.4.1 Flaw Model

To evaluate the integrity of the heater sleeve repair geometry, it is postulated that an axial flaw(s) remains in the nozzle stub at the original J-groove weld. It is further assumed that the postulated flaw has extended through the weld and clad and penetrated into the low alloy steel base metal. An illustration of the flaw model representing the postulated flaw geometry is shown in Figure 8-1. This represents the worst flaw orientation and size that could develop by stress corrosion cracking.

The initial flaw is conservatively assumed to be located at the corner of the hole and semicircular in shape with a depth of "a." The crack is conservatively assumed to penetrate the sleeve wall as shown in Figure 8-1. The initial flaw depth is assumed to be 1.0-inch (i.e., a_o = 1.0 inch). For this depth, the flaw tip will be well within the low alloy steel since the nominal J-groove prep is approximately 11/32-inch, and the clad thickness is 7/16 inch. A review of the finite element analysis details indicates that the vertical depth of the clad at the outermost sleeve is about 5/8-inch. Hence, it will be conservative to assume a 1.0-inch deep flaw as an initial flaw depth for the evaluation.

8.4.2 J-Groove Weld Stresses

The stresses at the J-groove weld were obtained from the finite element stress results in Appendix A of this calculation. The stress distribution in two dimensions, i.e., radial and circumferential with respect to the PZR bottom head, was used in the BIGIF program. This program uses linear interpolation within the two-dimensional stress table to calculate K using a weight function solution.

Since the flaw is conservatively modeled to penetrate the sleeve and the weld, the cyclic stress ranges from the finite element analysis are combined accordingly to cover the appropriate flaw area. The tabular input for each transient is listed in the BIGIF output data in Appendices B and C of this calculation.

8.4.3 Allowable Flaw Depth Evaluations

8.4.3.1 Appendix A Evaluation

The evaluation of allowable flaw depth following the ASME Section XI Appendix A method requires the solution of K_I, and K_{Ia} or K_{Ic} in accordance with Eqs. 4-7 and 4-8. For determining the allowable flaw depth, the fracture toughness acceptance criteria require that

$$K_I < K_{Ia}/\sqrt{10} = 200/\sqrt{10} = 63.2 \text{ ksi in}^{1/2} \qquad (8\text{-}1)$$

for normal, upset, and test conditions, and

$$K_I < K_{Ic}/\sqrt{2} = 200/\sqrt{2} = 141.4 \text{ ksi in}^{1/2} \qquad (8\text{-}2)$$

for emergency and faulted conditions. Since seismic loading will have a negligible effect on stress at the flaw location, the limiting criterion for defining allowable flaw depth is Eq. 8-1.

When defining the maximum stress for computing the allowable flaw depths, the combination of residual plus pressure plus thermal stresses produce stress levels in excess of the specified minimum yield strength. This situation was particularly true for the cooldown with flooding transient where local thermal stresses are high. Therefore, an elastic-plastic consideration was applied where the maximum stress was limited to the yield strength of the material, after all stress sources were elastically combined. The yield stress assumed as a limit to the stress is 60 ksi. Additional considerations that led to this evaluation with respect to the cooldown/flooding transient are:

1) The cooldown with flooding transient is a less likely event than a normal plant cooldown.

2) For toughness considerations, the bottom head will remain on the upper shelf during cooldown transient with flooding transient affording ductile behavior during the transient.

3) Higher stress conditions occur when the RCS pressure is below 20% of the design pressure. Maximum stress occurs when the RCS pressure is near zero. Therefore, the significant stress conditions for the cooldown/flooding transient when P is less than 20% P_D. ASME Section XI flaw acceptance criteria under IWB-3613 permit a relaxation in structural factors from $10^{1/2}$ to $2^{1/2}$ for such a situation.

The solution for K_I for the eight plant transient conditions defined in Section 8.1 was determined with the BIGIF computer program. The semicircular corner crack flaw model (IFI = 303 model in Ref. 8) was used. A listing of the input file and the solution output are given in Appendices B and C. Appendix B gives the results for the uphill side weld location and Appendix C gives the results for the downhill side.

The highest K_I for all design conditions is computed for the cooldown with flooding transient. A plot of K_I versus flaw depth is given in Figures 8-3 and 8-4 for the case of cooldown/flooding, hydrotest, and loss of secondary pressure. The somewhat irregular shape of K_I is due to the stress distribution behavior in the transition between the weld and the head. The flaw on the uphill side reaches the allowable K_I of $K_{Ia}/\sqrt{10}$ = 63.2 ksi in$^{1/2}$ at the smallest depth. The following allowable flaw depths are computed:

Location	Allowable Depth, a_{allow} (inches)
Uphill Side	1.42
Downhill Side	1.52

8.4.3.2 Appendix K Evaluation

With regard to the cooldown with flooding transient, an alternate analysis using Appendix K procedures was performed to confirm the assumptions and inputs for the allowable flaw depths computed in Section 8.4.3.1. The purpose of the alternate calculations is to address the uncertainties of weld residual stress and simplified elastic-plastic assumptions used in the Appendix A calculations. The logic used to apply Appendix K methods and acceptance criteria is based on the following:

1) The Appendix K procedures use a "postulated" flaw to evaluate margins to failure for upper shelf conditions. This evaluation of the PZR bottom head is similar in that a 1.0 inch flaw is postulated to evaluate material resistance to fracture.

2) The Appendix K procedures are applicable since the PZR bottom head will be at upper shelf conditions for all design loads including the cooldown with flooding transient.

3) The 1.0-inch postulated flaw depth is on the order of the postulated depth for the Appendix K analysis (i.e. 25% of the wall thickness). Therefore margins on flaw depth are comparable.

4) In the Appendix K analysis, residual stress are not considered since they are not highly influential to upper shelf behavior. Applied stresses are treated as elastic with the structural factors applied separately to pressure and thermal loading (see Section 4.5).

From the analysis procedures for $J_{applied}$ based on small-scale yielding (Eq. 4-14), the crack tip driving force in terms of K_I are plotted in Figure 8-5. The allowable flaw depth is the depth where K_I exceeds K_{Ia} = 200 ksi in$^{1/2}$. From this analysis, the allowable flaw depths are large relative to the postulated flaw depth and exceed the allowable values determined from the Appendix A evaluation. Therefore, the allowable flaw depths from the Appendix A procedure are conservative.

8.4.4 Fatigue Evaluation

An FCG analysis was performed to determine the final crack depth (a_f) after 40 years of service. The following conservative analysis input data and assumptions were used:

1. Initial flaw depth equal to 1.0 inch is assumed to exist at the start of service.

2. Reference FCG curve for reactor water environment with conservative R-ratio behavior is assumed.

3. All plant cooldowns are conservatively assumed to include flooding.

The cyclic stresses were determined on a pure elastic basis (i.e., elastic superposition of pressure and thermal stresses). The stress summaries are given in Appendix A of this calculation. The 40-year service cycles were divided into one-month block loading, as given in Section 8.1. Therefore, 480 blocks equals 40 years of operation. The fatigue life results from the BIGIF program are given in Appendices B and C of this calculation. From these results, the change in crack depth with service time is provided. The FCG is comparable for the downhill and uphill side flaw locations.

The calculated flaw growth and final depths for N = 480 months are summarized below:

Location	Growth, Δa (inches)	Final Depth, a_f (inches)
Uphill Side	0.21	1.21
Downhill Side	0.25	1.25

Therefore, it is determined that $a_f < a_{allow}$ at either weld location. Axial oriented flaws remaining in the heater sleeve J-groove will be acceptable to the ASME Section XI flaw evaluation rules.

8.5 Evaluation of Borated Water Corrosion

The potential of borated water corrosion (BWC) of the low alloy steel material was conservatively evaluated in Ref. 5 for the half-nozzle repair geometries for the steam generator and PZR. Local corrosion was modeled as a planar circumferential groove within the hole penetration. The rate for BWC was conservatively established from industry data discussed in Ref. 5. A limit load based analysis determined that the allowable depth of corrosion was large compared to the computed groove depths from BWC. In summary, the total corrosion depths were computed to be less than the allowable corrosion depths established for the PZR bottom head region. Therefore, the ASME Section margins are satisfied based on the previous analysis of the half-nozzle repair design.

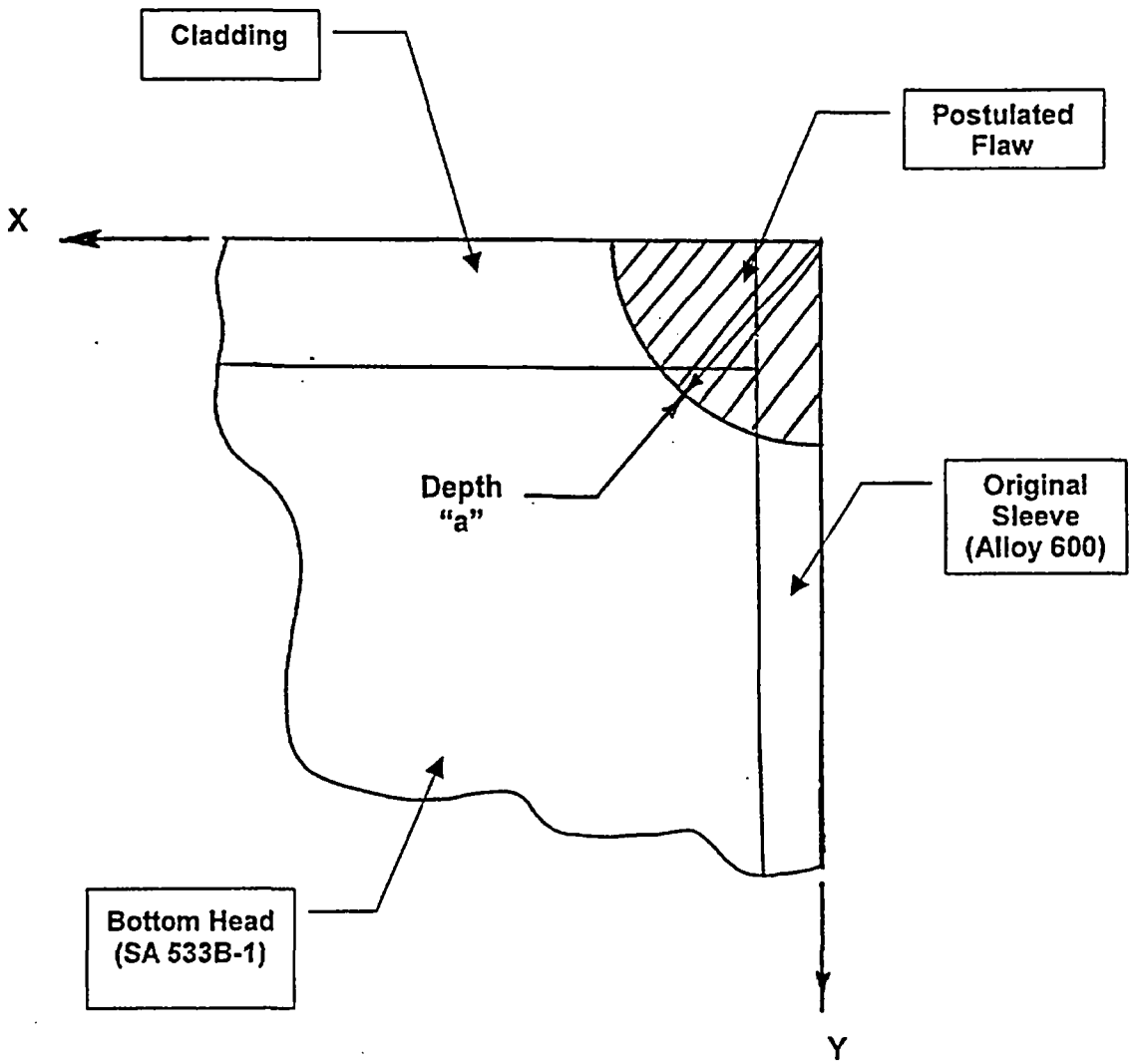

Figure 8-1 — Heater Sleeve J-Groove Flaw Model.

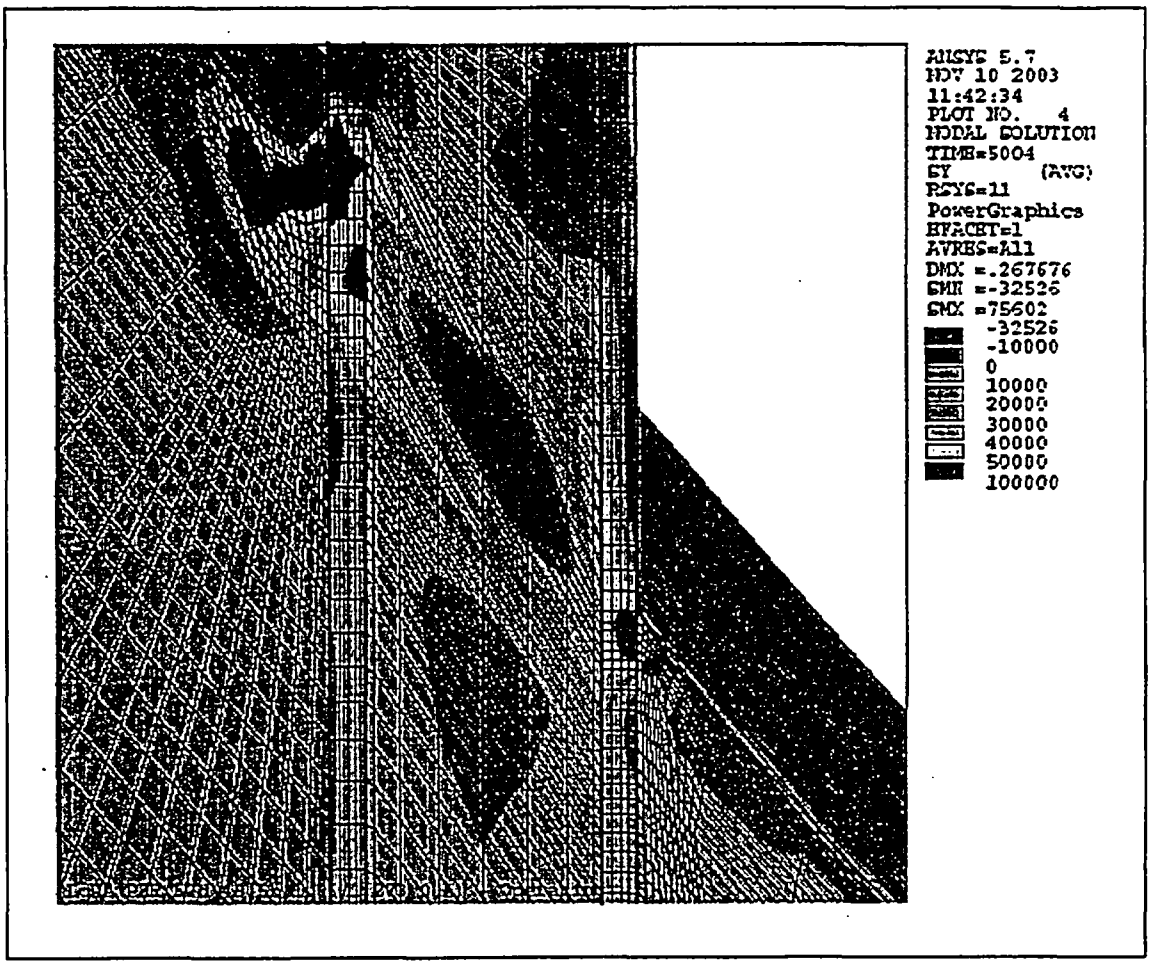

Figure 8-2 — Weld Residual Stress Distribution at Operating Conditions (Outermost 52° Angle)

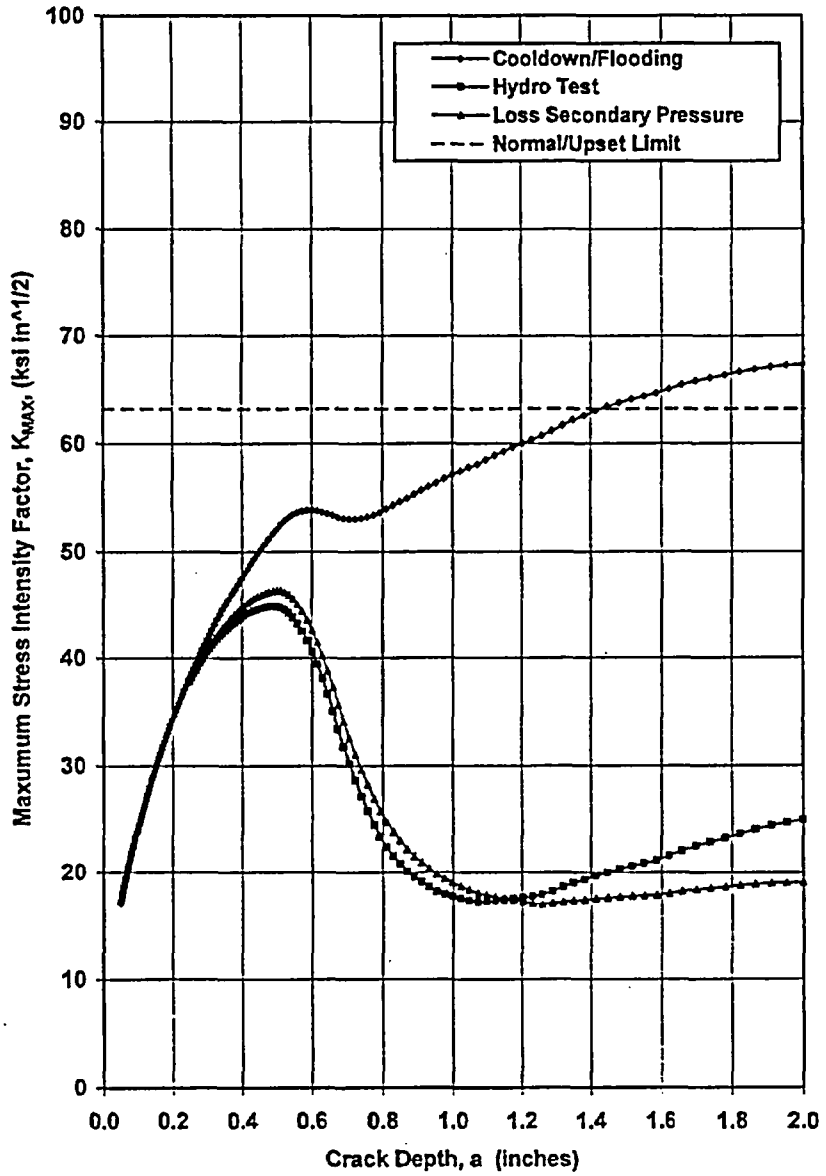

Figure 8-3 — Stress Intensity Factor Versus Flaw Depth for Corner Flaw in J-Groove Weld Location – Uphill Side.

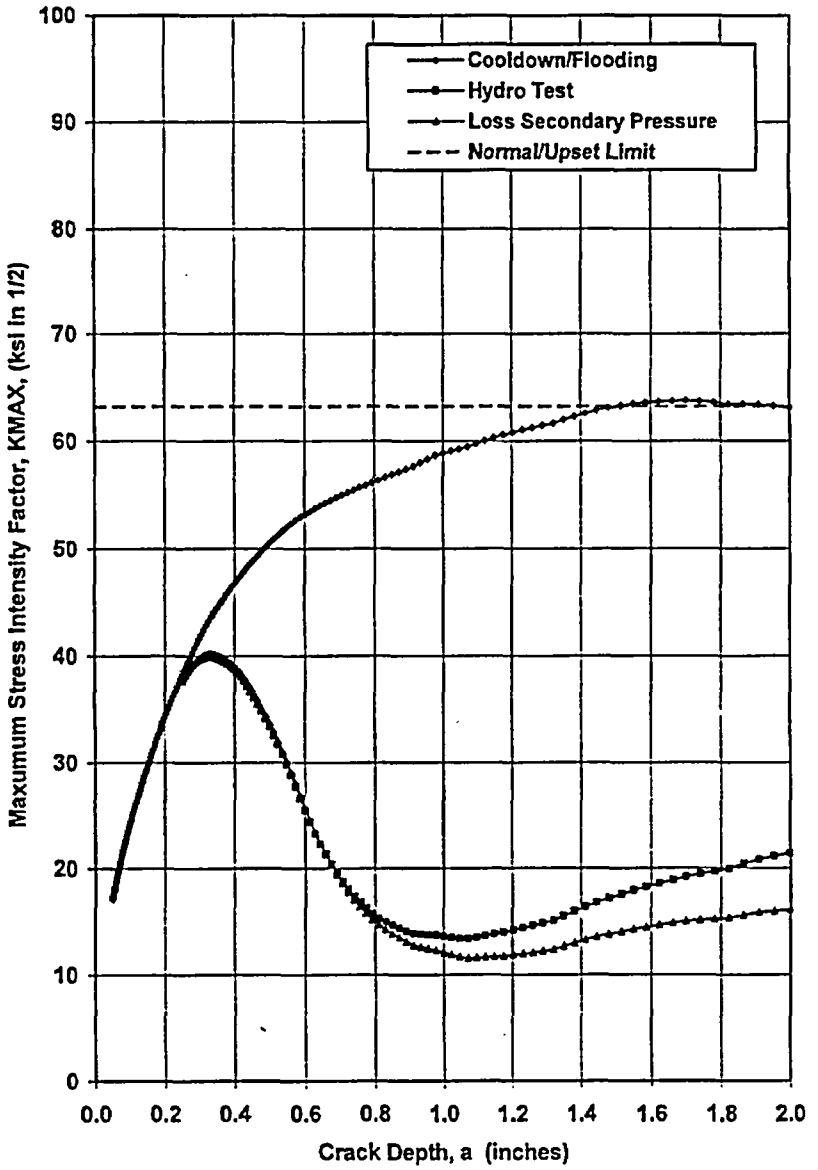

Figure 8-4 — Stress Intensity Factor Versus Flaw Depth for Corner Flaw in J-Groove Weld Location – Downhill Side (Appendix A Evaluation)

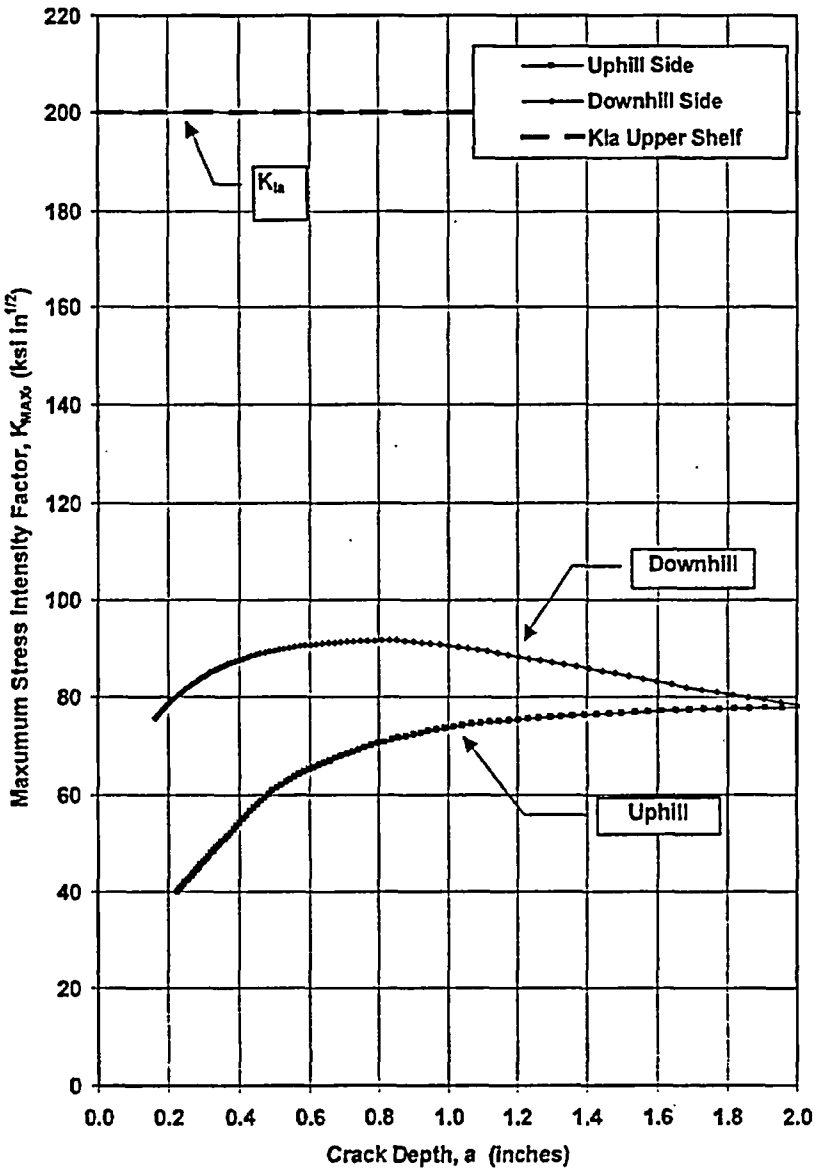

Figure 8-5 — Stress Intensity Factor Versus Flaw Depth for Corner Flaw in J-Groove Weld Location (Appendix K Evaluation)

Appendix A

SUMMARY OF HEATER SLEEVE CYCLIC STRESSES

A.1 ANALYSIS GEOMETRY

The stress results from the three-dimensional finite element analysis of the PZR bottom head penetrations (Ref. 7) were used to define the hoop stress distributions within the J-groove weld. The outermost sleeve is used to define the stresses for all heater sleeve penetrations. Further description of the finite element model is given in Section 4.6 and in Ref. 14.

The finite element model geometry is described in Section 4.6. The node numbers on the Y-Z symmetry plane of the model are used to define the x, y coordinates for input to BIGIF (Ref. 8). Two generic BIGIF models are developed: one for the uphill side and a second for the downhill side. In order to match the rectangular coordinate system of the BIGIF program, the skewed geometry of the ANSYS model was simply mapped to create a rectangular block where $0 \leq X' \leq w$ and $0 \leq Y' \leq t$, where w is the linearized arc length along the inside circumferential surface and t is the wall thickness. For the uphill side, this is accomplished by pivoting the sleeve about Node 3699 until the nozzle aligns along the head radius.

For the downhill side, the nozzle is rotated clockwise about Node 4253 to achieve a radial alignment. The inside surface circumferential length was selected to be reasonable since the local discontinuity stresses will remain concentrated near the hole penetration at the weld location.

The geometry transformation for the PZR bottom head nodes is shown in the tables. The radial coordinate transformation uses the Y coordinate in the ANSYS model and projects the length to a perpendicular radial line. This creates the "Y" input to the BIGIF program. The circumferential transformation simply uses the element spacing to develop the "X" input to the BIGIF program.

A.2 STRESS SUMMARY

A.2.1 Finite Element Data

The hoop stresses for each load case are summarized in Tables A-1 through A-11 for the nodes within the sleeve/J-groove weld. The ANSYS loading cases are defined as follows:

Case	Description	Filename	Transient Time, t (sec)	
			Uphill (Max/Min)	Downhill (Max)
P	Internal pressure, P = 2500 psi	hnpres2.p11	na/na	na/na
HU	Plant heatup, 200°F/hr	hnhu.p11	10494/na	10495/na
CD	Plant cooldown, -200°F/hr	hncd.p11	10495/na	10495/na
CDF	Plant cooldown with flooding	hncdf.p11	4440/na	4440/na
SS	Isothermal, T=653°F	hniso.p11	na/na	na/na
LD	Plant loading, ΔT = +20°F	hnstu.p11	210/na	210/na
UNLD	Plant unloading, ΔT = -20°F	hnstd.p11	210/na	210/na
TRIP	Reactor trip (loss of load)	hnlol.p11	601/2020	601/2020
LSP	Loss of secondary pressure	hnlsp.p11	400/6200	350/6200
LKHU	Leak test heatup, 100°F/hr	hnltu.p11	10801/na	10801/na
LKCD	Leak test cooldown, -100°F/hr	hnltd.p11	10801/na	10801/na

The coordinates x, y for each reference node are the coordinates established in the transformation shown in Tables A-1 and A-2.

A.3 Cyclic Stress for the PZR Bottom Head

The stress ranges for the eight transient loading conditions were obtained by linear combination of the minimum and maximum values of the individual load cases in Tables A-1 and A-2. Absolute values of the maximum range is conservatively taken. A description of each transient case and the manner in which the stress range was determined is given below:

1. Startup/Shutdown: The maximum stress during startup/shutdown is the maximum stress from pressure (P=2235 psi) plus heatup, or pressure (P=2235 psi) plus cooldown. The minimum stress state is zero. Therefore, the stress range is

$$\Delta\sigma = \left|\mathrm{MAX}[(P+HU),(P+CD)]-[0]\right|$$

2. Startup/Shutdown with Flooding: The maximum stress during startup/shutdown with flooding is the maximum stress from pressure (P=2235 psi) plus heatup, or pressure (P=2235 psi) plus cooldown with flooding. The minimum stress state is zero. Therefore, the stress range is

$$\Delta\sigma = \left|\mathrm{MAX}[(P+HU),(P+CDF)]-[0]\right|$$

3. Plant Loading: The plant loading transient causes a change in stress from a steady-state condition from a +100 psi pressure and +20°F temperature change. Therefore, the corresponding stress range is the maximum stress difference between steady-state operation and for an upload condition. Therefore, the stress range is the larger of:

$$\Delta\sigma = \left|[P_{SS} + SS] - [P_{Load} + LOAD]\right|$$

4. Plant Unloading: The plant unloading transient causes a change in stress from a steady-state condition from a -100 psi pressure and -20°F temperature change. Therefore, the corresponding stress range is the maximum stress difference between steady-state operation and a download condition. Therefore, the stress range is:

$$\Delta\sigma = \left|[P_{SS} + SS] - [P_{Unload} + UNLOAD]\right|$$

5. Reactor Trip: The reactor trip causes a major stress cycle from a steady-state operating condition. The cycle associated with a reactor trip assumes a return to steady-state. Therefore, the stress range for a trip is the maximum of:

$$\Delta\sigma = \left|[P_{Max} + TRIP_{Max}] - [P_{Min} + TRIP_{Min}]\right|$$

or

$$\Delta\sigma = \left|[P_{Max} + TRIP_{Min}] - [P_{Min} + TRIP_{Max}]\right|$$

6. Loss of Secondary Pressure: This transient trip causes a stress cycle from a steady-state operating condition to the absolute maximum stress resulting from the thermal transient. The cycle associated with a loss of secondary pressures assumes a return to steady-state conditions. Therefore, the stress range for this transient is:

$$\Delta\sigma = \left|[P_{SS} + SS] - [P_{LSP} + LSP]\right|$$

7. Leak Test: The plant leak test is performed for a pressure from 0 psig to 2235 psig and at a temperature change of 400°F. Therefore, the stress range is determined as follows:

$$\Delta\sigma = \left|MAX[(P_{Leak} + LKHU), (P_{Leak} + LKCD)] - [0]\right|$$

8. Hydro Test: The hydro test is performed at $1.25P_d$ at a temperature change of 400°F. Therefore, the stress range is calculated as:

$$\Delta\sigma = \left|MAX[(P_{Hydro} + LKHU), (P_{Hydro} + LKCD)] - [0]\right|$$

The stress range was computed for each plant condition as described above. The results of the combined cases are given in Tables A-12 and A-13. Linear interpolation with respect to the X′ coordinate was used to define the stress values for nodes where stress results were not reported. For the surface nodes along the clad surface, the surface stress was equated to the stress value of the next node into the head (i.e., node at the clad-to-base metal interface). This is a reasonable assumption for pressure load cases and is acceptable for thermal transient cases since peak stresses will be localized only to the surface layer. The stress values in Tables A-12 and A-13, along with the nozzle stresses described in Section A.4 are used as input to the BIGIF program for evaluating the fatigue crack growth in the head material.

Table A-1a

SUMMARY OF STRESSES FOR UPHILL J-GROOVE (Internal Pressure P = 2500 psi)

Uphill Side						
Node	SX	SY	SZ	SXY	SYZ	SXZ
3699	-1863	18970	-4346	-2323	-2271	1472
3682	-2626	31392	7998	-1775	-2663	3785
4385	-1900	29283	17219	-2590	-1041	1606
4366	-2030	22388	11253	-1727	-908	-682
5930	-1964	2874	2791	-812	456	-756
5929	-2416	-1887	-2543	-396	193	-87
3755	-590	13039	2440	-496	-396	5172
3677	6054	22396	14376	-573	647	10878
4578	1571	21493	-5826	-1321	-1747	4131
4553	-1105	25590	2717	-2239	-1327	3014
6972	-111	33704	9182	-2937	-1301	1596
6971	527	35662	12648	-3200	-1175	1244
3745	13970	11332	3693	305	9	5996
4520	2299	14296	6124	-203	-41	6591
4585	2396	15243	5949	-216	-112	7165
4555	1578	15279	5012	-371	-290	5995
7002	2399	16851	6400	-369	-329	5346
6996	3914	16752	7561	-235	-292	5387
4509	3436	13155	7572	76	9	7347
4509	3436	13155	7572	76	9	7347
4510	3789	13306	7419	63	-36	7045
4504	3307	13052	7119	-63	-61	6580
6943	2884	14463	7118	-172	-128	6143
6944	3785	15649	7554	-169	-182	5934
6433	7117	13956	10020	-77	60	10637
6433	7117	13956	10020	-77	60	10637
6508	4694	13178	9698	-94	68	9279
6493	3802	12621	9288	-91	58	8555
7252	2853	12033	8338	-77	37	7248
7253	2831	12239	8198	-72	3	6751

Table A-1b

SUMMARY OF STRESSES FOR DOWNHILL J-GROOVE
(Internal Pressure P = 2500 psi)

Downhill Side						
Node	SX	SY	SZ	SXY	SYZ	SXZ
4253	-1583	45446	10012	3014	-3203	-3264
4237	-1224	36726	-3095	2640	-2999	-2953
4461	-216	15383	-5533	1216	-1765	676
6117	-3281	-2143	-2693	141	-119	0
6115	-1635	-2768	-1580	12	-18	-309
4157	6621	24651	19687	541	1174	-15214
4162	10972	32813	23122	619	555	-12694
4737	650	38808	15714	2722	-1828	-3240
6612	1060	38132	11537	3024	-1729	-1889
6611	1228	36607	11512	3100	-1342	-1767
4987	3435	13332	5490	55	-31	-6441
4767	6422	24011	9397	-189	-1088	-9314
4742	2467	22974	7980	700	-1165	-4374
6628	2258	23725	7820	1059	-1100	-3016
6629	2702	23781	8071	1273	-915	-2845
4989	4689	12744	7742	-544	444	-8078
4769	4646	16480	6647	-436	-512	-7022
4744	4667	17057	6737	-194	-491	-6419
6618	4735	17352	6529	-13	-489	-5617
6619	5235	17498	6497	118	-410	-5388
4967	3622	12584	5150	-319	5	-7044
4722	4527	14929	5747	-251	-248	-7206
4727	4793	15246	5870	-173	-276	-6893
6553	5073	15355	5725	-87	-279	-6500
6554	5450	15472	5680	11	-200	-6532
6345	4223	13481	5848	-176	106	-7286
6379	4531	14526	5641	-193	-156	-7295
6525	4872	14629	5535	-160	-212	-7047
7339	5163	14679	5414	-89	-205	-6835
7338	5454	14852	5494	10	-140	-6828

Table A-2a

SUMMARY OF STRESSES FOR UPHILL J-GROOVE (Plant Heatup at 10494s)

Uphill Side						
Node	SX	SY	SZ	SXY	SYZ	SXZ
3699	-874	5554	-39174	-1684	-3239	-3391
3682	-278	-7665	-49527	-4279	-2976	-2478
4385	-1802	-20432	-44295	-1194	-552	-4120
4366	-1305	-12732	-33842	837	-674	-2852
5930	-1513	-4947	-7708	441	395	-2126
5929	-523	-1536	-5840	-150	-112	-646
3755	-3104	-3337	-25605	-4773	-523	-357
3677	-10942	-14510	-35103	-10033	940	-669
4578	-5859	-712	-37276	-2192	-1363	-1906
4553	-4201	-7415	-40498	-3818	1037	-1992
6972	-5744	-8456	-40261	-2362	1280	-1931
6971	-2896	-6387	-29919	637	-106	-2596
3745	-16359	-4669	-21544	-5459	21	961
4520	-3550	-5731	-24753	-5993	167	133
4585	-4421	-4772	-25006	-6366	149	113
4555	-4353	-2662	-23286	-4696	-93	89
7002	-4879	-1996	-20130	-2650	-42	94
6996	-4743	-391	-15230	-838	-41	166
4509	-4148	-5998	-25673	-4641	50	-12
4509	-4148	-5998	-25673	-4641	50	-12
4510	-4430	-5305	-24380	-3762	58	-40
4504	-4701	-3857	-22406	-3355	49	-98
6943	-4050	-1732	-18059	-2798	50	48
6944	-4429	-225	-14609	-1167	10	175
6433	-4732	-4790	-28518	-4187	-21	-280
6433	-4732	-4790	-28518	-4187	-21	-280
6508	-3520	-3734	-26568	-3209	-19	-241
6493	-3357	-2362	-23846	-2735	-34	-174
7252	-2928	-231	-17699	-1997	-13	-75
7253	-2832	1259	-13735	-1026	-27	21

Table A-2b

SUMMARY OF STRESSES FOR DOWNHILL J-GROOVE (Plant Heatup at 10495s)

Downhill Side						
Node	SX	SY	SZ	SXY	SYZ	SXZ
4253	-1376	-14349	-75262	-4569	4218	4555
4237	-2066	3455	-60821	-2877	4348	4003
4461	-3304	-2141	-29231	-251	2431	2557
6117	533	-588	-3490	76	340	433
6115	-716	-930	393	-187	107	245
4157	-13724	-27378	-41556	-19854	-2446	-342
4162	-10701	-20256	-42902	-10477	-583	321
4737	-2116	-18050	-50253	-3053	1203	3453
6612	-2408	-6205	-35176	-1139	954	2633
6611	-2062	-3100	-23296	-459	306	1821
4987	-9892	-13466	-31858	-10490	-803	-288
4767	-9911	-12426	-36875	-9243	311	-290
4742	-5014	-6458	-29356	-4483	775	392
6628	-3558	-4063	-21357	-1808	434	658
6629	-2383	-1539	-13800	-707	15	459
4989	-9250	-12707	-26952	-10566	-569	-742
4769	-8153	-9333	-25539	-7755	177	-553
4744	-6793	-7189	-21806	-5927	160	-333
6618	-4347	-3848	-14836	-2987	70	-196
6619	-2602	-1519	-9257	-975	-65	-173
4967	-8874	-11069	-25411	-9929	-165	-430
4722	-7681	-8834	-22366	-7828	33	-339
4727	-6287	-6851	-18730	-6002	44	-262
6553	-4036	-3833	-12533	-3054	14	-182
6554	-2239	-1533	-7563	-699	-32	-167
6345	-9099	-11300	-24854	-10046	-176	-317
6379	-7455	-8657	-21019	-7801	-13	-259
6525	-6129	-6734	-17444	-5997	15	-226
7339	-3830	-3735	-11467	-2972	1	-169
7338	-2043	-1333	-6675	-581	-22	-172

Table A-3a

SUMMARY OF STRESSES FOR UPHILL J-GROOVE (Plant Cooldown at 10494s)

Uphill Side						
Node	SX	SY	SZ	SXY	SYZ	SXZ
3699	542	-2458	24200	1347	2210	2051
3682	13	5810	28993	2631	1882	1462
4385	1080	12924	25641	710	427	2350
4366	686	7826	18831	-546	447	1627
5930	834	2881	3587	-289	-221	1130
5929	218	717	2973	67	36	250
3755	1951	2678	16128	4193	427	277
3677	6092	9315	20311	6593	-420	361
4578	2648	202	19368	1709	748	1018
4553	2384	4753	21150	2251	-631	960
6972	2943	4488	18765	1163	-732	854
6971	982	2612	11559	-547	51	1151
3745	14475	4888	15494	5093	39	-562
4520	2763	5060	15337	4563	-59	50
4585	2439	3983	14351	4447	-71	53
4555	2009	1988	12145	2904	59	20
7002	2323	1253	9434	1346	21	-10
6996	2055	21	6068	96	21	-70
4509	3868	5951	16131	4514	2	-22
4509	3868	5951	16131	4514	2	-22
4510	3770	4938	14561	3509	12	-2
4504	3073	3228	12176	2499	20	49
6943	1946	1194	8347	1317	-10	7
6944	1898	-7	5841	279	-4	-72
6433	5439	6260	18390	5449	1	224
6433	5439	6260	18390	5449	1	224
6508	4215	5649	17035	4369	-8	204
6493	3648	4450	14849	3496	22	143
7252	1204	268	7694	1203	25	43
7253	1025	-643	5375	224	31	-16

Table A-3b

SUMMARY OF STRESSES FOR DOWNHILL J-GROOVE (Plant Cooldown at 10495s)

Downhill Side						
Node	SX	SY	SZ	SXY	SYZ	SXZ
4253	873	9485	45925	3024	-2897	-2809
4237	1265	-1379	36211	1822	-2768	-2481
4461	2068	1534	16908	214	-1438	-1654
6117	-393	243	2012	-100	-225	-235
6115	446	666	-174	131	-62	-141
4157	9348	19099	27242	13957	1373	120
4162	7188	13949	26459	7218	300	-282
4737	1205	11586	28790	2079	-786	-2028
6612	873	2860	15825	481	-432	-1299
6611	807	1062	8697	218	-72	-715
4987	6975	9590	20960	7598	374	37
4767	6487	8843	22421	6630	-211	190
4742	2954	4355	16750	3044	-470	-203
6628	1609	2143	9641	855	-177	-343
6629	847	503	4993	297	50	-157
4989	6652	9218	18168	7645	271	357
4769	5695	6884	16297	5687	-113	245
4744	4265	4896	12675	4012	-75	140
6618	1871	1866	6494	1413	-5	65
6619	836	567	3248	304	62	63
4967	6432	8087	17246	7271	21	206
4722	5532	6556	14672	5809	-30	152
4727	3934	4550	10897	3963	-14	108
6553	1814	1940	5551	1412	10	61
6554	732	633	2619	76	30	59
6345	6698	8314	17056	7408	52	153
6379	5469	6450	14016	5797	-5	119
6525	3841	4430	10179	3897	-1	95
7339	1746	1902	5088	1354	12	60
7338	681	523	2242	-16	18	68

Table A-4a

SUMMARY OF STRESSES FOR UPHILL J-GROOVE (Plant Cooldown with Flooding at 4440s)

Uphill Side						
Node	SX	SY	SZ	SXY	SYZ	SXZ
3699	1248	-5767	70976	5837	7451	6078
3682	-135	23353	86506	8826	6202	4417
4385	2899	43722	76516	2556	2012	7036
4366	2041	27146	56120	-1370	2019	4872
5930	2379	9444	7108	-1015	-467	3219
5929	330	1373	7783	67	77	152
3755	3827	8810	48491	19248	1340	932
3677	16839	31461	59784	24233	-973	1025
4578	6368	-3617	53030	8022	2729	2965
4553	6829	15027	59276	9000	-1821	2146
6972	7986	13546	41529	3330	-2033	1495
6971	80	4345	10265	-2722	328	2124
3745	77251	29324	65674	23775	544	-1763
4520	10783	22105	47631	16466	-103	911
4585	6841	17785	42544	16279	-181	790
4555	5150	10785	35636	11670	290	450
7002	4925	5553	21373	4534	159	234
6996	3055	-423	6376	-932	91	-54
4509	17344	26214	49805	19934	94	-290
4509	17344	26214	49805	19934	94	-290
4510	16619	21042	42734	15496	268	-286
4504	12071	15228	34286	11135	340	3
6943	5296	6699	19405	4487	160	183
6944	2574	-174	6227	-510	37	-28
6433	30720	37168	66064	30839	9	902
6433	30720	37168	66064	30839	9	902
6508	21089	31461	55508	23570	-10	778
6493	15348	23526	43444	17819	126	505
7252	4963	6796	18636	6664	102	131
7253	1161	-707	5168	-187	153	-39

Table A-4b

SUMMARY OF STRESSES FOR DOWNHILL J-GROOVE (Plant Cooldown with Flooding at 10494s)

Downhill Side						
Node	SX	SY	SZ	SXY	SYZ	SXZ
4253	3281	35529	156220	11843	-11466	-9654
4237	4035	-1734	112900	5899	-9173	-8263
4461	6455	5141	45604	470	-3951	-5499
6117	-1304	1211	7015	-256	-778	-785
6115	1343	2278	793	406	-206	-585
4157	38886	81283	104180	60197	4667	233
4162	25497	53513	85567	26931	1135	-1205
4737	3603	42572	83668	7376	-2470	-6289
6612	1029	7742	37482	2275	-1314	-3240
6611	1235	27	8233	514	-148	-937
4987	29864	41757	80240	33550	925	-438
4767	22753	34501	70957	25286	-684	746
4742	8736	15948	48172	10896	-1503	-579
6628	4182	7740	24180	3617	-614	-954
6629	428	173	3706	800	275	-146
4989	28556	39692	70741	33003	727	1005
4769	20082	26404	53299	21388	-295	398
4744	13323	17689	37744	14190	-164	79
6618	5410	7638	17330	5833	41	-99
6619	245	1337	2129	623	279	-56
4967	27328	34773	67935	31281	-160	471
4722	19682	24683	48862	21485	-93	194
4727	13025	16615	33637	14152	-2	49
6553	5780	7924	15355	5761	85	-64
6554	632	1870	1721	-332	130	-37
6345	28237	35140	67504	31478	-58	326
6379	19658	24118	47254	21327	-42	132
6525	13119	16294	32200	14000	13	59
7339	5857	7748	14341	5442	72	-18
7338	800	1541	1112	-719	78	35

Table A-5a

SUMMARY OF STRESSES FOR UPHILL J-GROOVE
(Steady State Isothermal T = 653°F)

Uphill Side						
Node	SX	SY	SZ	SXY	SYZ	SXZ
3699	-355	2664	-14544	-264	-982	-1241
3682	-174	-1297	-18344	-1375	-948	-902
4385	-719	-6229	-16462	-353	-51	-1536
4366	-510	-3811	-12896	329	-119	-1058
5930	-592	-1603	-3757	136	195	-830
5929	-272	-694	-2326	-79	-38	-374
3755	-1347	-724	-9150	-375	-142	-81
3677	-4259	-4267	-13060	-2706	436	-257
4578	-2648	-891	-15193	-178	-425	-737
4553	-1591	-2260	-16168	-1011	384	-895
6972	-2297	-2898	-18018	-919	510	-933
6971	-1687	-2870	-15956	4	14	-1211
3745	-132	877	-4891	-292	70	365
4520	-614	-422	-8570	-1351	95	195
4585	-1615	-322	-9226	-1560	76	171
4555	-1821	90	-8988	-1145	-9	120
7002	-2207	-239	-8910	-884	2	91
6996	-2379	-111	-7964	-558	-9	93
4509	-188	-21	-8917	-82	40	-47
4509	-188	-21	-8917	-82	40	-47
4510	-408	-168	-8877	-70	65	-60
4504	-1125	1	-8649	-357	70	-56
6943	-1658	62	-7943	-961	53	56
6944	-2272	2	-7623	-695	14	102
6433	1163	2009	-8794	1560	-13	-63
6433	1163	2009	-8794	1560	-13	-63
6508	670	1999	-8775	1286	-15	-53
6493	122	1943	-8433	883	-9	-42
7252	-977	1014	-7828	-174	3	-26
7253	-1514	807	-7240	-569	5	10

Table A-5b

SUMMARY OF STRESSES FOR DOWNHILL J-GROOVE
(Steady State Isothermal T = 653°F)

Downhill Side						
Node	SX	SY	SZ	SXY	SYZ	SXZ
4253	-421	-4163	-25838	-1264	1095	1536
4237	-737	1877	-22394	-947	1451	1368
4461	-1164	-873	-11804	-103	931	812
6117	164	-183	-1053	22	101	156
6115	-236	-213	572	-48	43	71
4157	-3415	-6196	-12007	-4382	-904	-207
4162	-3052	-4968	-14693	-2717	-188	34
4737	-834	-4988	-19091	-813	388	1232
6612	-1266	-2572	-15785	-346	379	1132
6611	-1017	-1741	-12523	-181	157	943
4987	-2286	-2968	-9412	-2189	-388	-244
4767	-2978	-2914	-13039	-2216	85	-64
4742	-1823	-1657	-11178	-1181	252	152
6628	-1547	-1303	-9399	-561	164	262
6629	-1348	-820	-7597	-285	40	252
4989	-2024	-2703	-7698	-2260	-247	-315
4769	-2285	-2125	-8541	-1865	61	-284
4744	-2245	-1824	-8024	-1581	67	-191
6618	-1833	-1161	-6468	-942	42	-129
6619	-1491	-628	-5157	-456	-3	-107
4967	-1991	-2402	-7182	-2144	-122	-201
4722	-2057	-2067	-7260	-1899	4	-180
4727	-1980	-1770	-6754	-1627	22	-151
6553	-1596	-1114	-5390	-986	17	-115
6554	-1219	-559	-4229	-424	-4	-101
6345	-2025	-2497	-6928	-2199	-113	-153
6379	-1937	-2047	-6694	-1912	-15	-141
6525	-1874	-1753	-6194	-1646	7	-127
7339	-1464	-1083	-4905	-982	8	-101
7338	-1078	-496	-3799	-408	-5	-94

Table A-6a

SUMMARY OF STRESSES FOR UPHILL J-GROOVE (Plant Loading at 210s)

Uphill Side						
Node	SX	SY	SZ	SXY	SYZ	SXZ
3699	-427	2959	-18713	-634	-1441	-1605
3682	-161	-2850	-23552	-1927	-1337	-1169
4385	-885	-9001	-21065	-519	-186	-1960
4366	-631	-5548	-16246	408	-255	-1353
5930	-733	-2202	-4108	199	217	-1022
5929	-286	-782	-2826	-82	-45	-371
3755	-1568	-1309	-12040	-1616	-226	-143
3677	-5278	-6287	-16667	-4261	487	-319
4578	-2994	-596	-18287	-723	-603	-914
4553	-2015	-3223	-19678	-1601	494	-1009
6972	-2774	-3755	-20275	-1116	629	-1006
6971	-1640	-3097	-16162	194	-13	-1322
3745	-5036	-1006	-8858	-1794	39	466
4520	-1336	-1885	-11454	-2412	96	132
4585	-2059	-1526	-11799	-2615	82	116
4555	-2142	-685	-11140	-1916	-31	86
7002	-2469	-615	-10063	-1164	-10	73
6996	-2509	-79	-8125	-476	-15	93
4509	-1334	-1754	-11892	-1404	33	-25
4509	-1334	-1754	-11892	-1404	33	-25
4510	-1517	-1589	-11446	-1133	45	-38
4504	-1909	-1065	-10703	-1140	45	-53
6943	-1967	-404	-8989	-1239	40	42
6944	-2370	17	-7777	-634	11	100
6433	-858	-474	-12699	-495	-13	-117
6433	-858	-474	-12699	-495	-13	-117
6508	-722	-148	-12074	-326	-13	-100
6493	-925	248	-11060	-364	-16	-74
7252	-1283	517	-8786	-615	-3	-34
7253	-1542	842	-7293	-534	-5	13

Table A-6b

SUMMARY OF STRESSES FOR DOWNHILL J-GROOVE (Plant Loading at 210s)

Downhill Side						
Node	SX	SY	SZ	SXY	SYZ	SXZ
4253	-618	-6348	-35121	-1984	1798	2112
4237	-978	1916	-29089	-1314	2007	1865
4461	-1561	-1154	-14493	-133	1170	1159
6117	243	-259	-1524	39	152	206
6115	-324	-357	506	-71	58	113
4157	-5781	-11203	-18299	-8079	-1175	-210
4162	-4659	-8385	-19920	-4427	-258	112
4737	-1065	-7741	-24213	-1305	547	1621
6612	-1295	-2987	-17855	-488	464	1316
6611	-1055	-1666	-12669	-205	166	977
4987	-4094	-5502	-14202	-4230	-433	-207
4767	-4393	-5103	-17363	-3828	132	-111
4742	-2361	-2690	-14137	-1902	349	189
6628	-1786	-1782	-10767	-791	203	319
6629	-1342	-804	-7612	-326	21	255
4989	-3770	-5139	-11943	-4281	-289	-372
4769	-3544	-3813	-11824	-3226	79	-300
4744	-3102	-2997	-10390	-2524	77	-189
6618	-2153	-1646	-7459	-1318	39	-118
6619	-1464	-687	-5134	-482	-22	-100
4967	-3648	-4513	-11248	-4045	-107	-225
4722	-3302	-3643	-10283	-3269	10	-186
4727	-2832	-2874	-8884	-2572	22	-149
6553	-1952	-1622	-6282	-1358	11	-107
6554	-1223	-655	-4206	-389	-12	-96
6345	-3740	-4634	-10973	-4113	-106	-168
6379	-3185	-3587	-9625	-3273	-12	-144
6525	-2739	-2838	-8248	-2582	7	-127
7339	-1829	-1581	-5744	-1335	3	-97
7338	-1095	-574	-3750	-349	-11	-93

Table A-7a

SUMMARY OF STRESSES FOR UPHILL J-GROOVE (Plant Unloading at 210s)

Uphill Side						
Node	SX	SY	SZ	SXY	SYZ	SXZ
3699	-270	2275	-9865	115	-489	-834
3682	-182	301	-12498	-776	-527	-603
4385	-528	-3242	-11288	-175	87	-1058
4366	-372	-1944	-9099	238	20	-727
5930	-431	-950	-3278	68	165	-610
5929	-249	-588	-1762	-74	-31	-364
3755	-1077	-112	-5939	880	-53	-16
3677	-3092	-2094	-8999	-1057	370	-186
4578	-2209	-1130	-11565	376	-234	-535
4553	-1115	-1215	-12158	-388	259	-757
6972	-1752	-1981	-15310	-697	370	-839
6971	-1688	-2589	-15356	-186	38	-1071
3745	4772	2729	-755	1223	98	252
4520	131	1061	-5389	-239	90	251
4585	-1111	901	-6331	-445	68	220
4555	-1445	853	-6570	-340	13	148
7002	-1887	126	-7538	-587	14	107
6996	-2187	-152	-7607	-630	-3	90
4509	966	1723	-5632	1248	45	-66
4509	966	1723	-5632	1248	45	-66
4510	715	1270	-6002	998	83	-79
4504	-307	1065	-6338	431	93	-56
6943	-1308	508	-6706	-665	65	68
6944	-2114	-25	-7281	-742	16	101
6433	3154	4434	-4588	3573	-13	-7
6433	3154	4434	-4588	3573	-13	-7
6508	2045	4089	-5177	2863	-16	-3
6493	1165	3573	-5562	2102	-2	-10
7252	-650	1467	-6686	264	10	-19
7253	-1450	739	-7015	-595	14	7

Table A-7b

SUMMARY OF STRESSES FOR DOWNHILL J-GROOVE (Plant Unloading at 210s)

Downhill Side						
Node	SX	SY	SZ	SXY	SYZ	SXZ
4253	-209	-1835	-15652	-500	353	906
4237	-470	1767	-14928	-547	843	825
4461	-729	-567	-8721	-71	659	439
6117	79	-100	-557	4	47	102
6115	-140	-62	611	-22	27	28
4157	-928	-974	-5287	-530	-601	-196
4162	-1339	-1386	-8961	-918	-112	-47
4737	-576	-2110	-13409	-293	219	808
6612	-1205	-2103	-13325	-198	286	920
6611	-954	-1778	-12064	-153	146	886
4987	-393	-326	-4275	-66	-328	-272
4767	-1461	-629	-8263	-527	36	-15
4742	-1228	-580	-7882	-422	148	111
6628	-1269	-801	-7798	-321	122	198
6629	-1320	-823	-7392	-239	58	242
4989	-204	-168	-3160	-157	-197	-249
4769	-945	-360	-4948	-435	41	-259
4744	-1321	-599	-5409	-593	56	-188
6618	-1469	-658	-5316	-550	45	-137
6619	-1482	-562	-5051	-423	15	-111
4967	-262	-203	-2840	-164	-133	-170
4722	-738	-415	-3966	-459	-2	-169
4727	-1070	-617	-4410	-634	22	-148
6553	-1203	-590	-4364	-596	23	-120
6554	-1187	-459	-4146	-452	5	-104
6345	-234	-267	-2616	-204	-116	-132
6379	-617	-431	-3507	-480	-18	-133
6525	-954	-618	-3942	-661	8	-124
7339	-1066	-569	-3944	-611	13	-103
7338	-1037	-413	-3752	-461	0	-92

Table A-8a

SUMMARY OF STRESSES FOR UPHILL J-GROOVE (Reactor Trip at 601s)

Uphill Side						
Node	SX	SY	SZ	SXY	SYZ	SXZ
3699	-126	1552	-2594	620	228	-197
3682	-172	2528	-3280	128	107	-135
4385	-223	1238	-3104	95	273	-301
4366	-143	882	-3013	94	216	-201
5930	-168	59	-2348	-28	119	-240
5929	-196	-422	-821	-60	-10	-319
3755	-606	772	-1007	2515	72	77
3677	-1173	1184	-2538	1344	241	-69
4578	-1383	-1345	-5441	1117	58	-202
4553	-357	376	-5440	529	63	-489
6972	-795	-415	-9954	-289	144	-634
6971	-1511	-1847	-12984	-432	84	-770
3745	11003	5003	4935	3178	128	78
4520	1161	3028	-501	1332	76	306
4585	-284	2546	-1714	1158	51	269
4555	-770	1883	-2567	829	44	176
7002	-1234	713	-4809	-68	32	120
6996	-1696	-116	-6301	-631	9	79
4509	2467	3995	-587	2978	48	-86
4509	2467	3995	-587	2978	48	-86
4510	2207	3184	-1449	2403	98	-98
4504	877	2501	-2503	1513	114	-50
6943	-664	1174	-4238	-131	76	80
6944	-1677	18	-6020	-691	21	91
6433	5603	7366	1607	6023	-13	66
6433	5603	7366	1607	6023	-13	66
6508	3755	6601	261	4784	-17	62
6493	2509	5525	-1058	3617	6	34
7252	-73	2089	-4302	918	17	-5
7253	-1188	683	-5869	-517	27	4

Table A-8b

SUMMARY OF STRESSES FOR DOWNHILL J-GROOVE
(Reactor Trip at 601s)

Downhill Side						
Node	SX	SY	SZ	SXY	SYZ	SXZ
4253	98	1493	-380	592	-695	-34
4237	-68	1432	-3437	61	-63	12
4461	-86	-249	-3815	-36	219	-112
6117	-38	48	219	-11	-28	21
6115	13	198	805	27	11	-26
4157	2548	6291	4372	4800	-140	-174
4162	1172	3812	-250	1671	13	-153
4737	-211	2167	-4387	447	-35	144
6612	-978	-1094	-8470	59	124	528
6611	-707	-1516	-10040	-62	111	707
4987	2211	3292	3047	2820	-225	-291
4767	773	2608	-1002	1860	-39	65
4742	-285	1021	-2611	670	-14	44
6628	-746	72	-4718	79	44	86
6629	-1152	-671	-6277	-105	73	202
4989	2294	3306	3238	2724	-110	-132
4769	977	2107	406	1564	6	-201
4744	74	1180	-1295	835	31	-167
6618	-792	199	-3100	102	42	-137
6619	-1288	-304	-4294	-272	39	-110
4967	2105	2795	3278	2535	-136	-113
4722	1125	1890	890	1551	-12	-137
4727	282	1059	-760	799	18	-133
6553	-506	286	-2418	59	27	-118
6554	-967	-161	-3510	-389	16	-101
6345	2207	2773	3447	2511	-110	-93
6379	1231	1819	1156	1514	-21	-110
6525	401	1024	-465	761	7	-109
7339	-366	286	-2130	15	17	-97
7338	-807	-157	-3214	-434	7	-82

Table A-9a

SUMMARY OF STRESSES FOR UPHILL J-GROOVE (Loss of Secondary Pressure at 350s)

Uphill Side						
Node	SX	SY	SZ	SXY	SYZ	SXZ
3699	-433	2814	-19377	-800	-1580	-1671
3682	-141	-3588	-24456	-2085	-1450	-1220
4385	-895	-9894	-21837	-577	-256	-2030
4366	-645	-6143	-16715	415	-318	-1404
5930	-749	-2388	-3889	216	202	-1049
5929	-265	-752	-2864	-76	-52	-331
3755	-1545	-1571	-12620	-2228	-254	-170
3677	-5404	-6987	-17289	-4832	471	-328
4578	-2928	-347	-18452	-1004	-661	-939
4553	-2079	-3553	-20119	-1833	507	-1001
6972	-2847	-4104	-20208	-1163	633	-977
6971	-1483	-3127	-15137	294	-40	-1296
3745	-7594	-2087	-10429	-2544	15	477
4520	-1671	-2628	-12144	-2844	86	78
4585	-2153	-2157	-12288	-3032	75	68
4555	-2164	-1173	-11546	-2245	-43	51
7002	-2452	-903	-10108	-1290	-19	52
6996	-2400	-142	-7710	-421	-20	85
4509	-1925	-2664	-12604	-2099	25	-10
4509	-1925	-2664	-12604	-2099	25	-10
4510	-2078	-2334	-11979	-1707	28	-20
4504	-2239	-1678	-11095	-1563	24	-47
6943	-2027	-761	-9073	-1365	28	28
6944	-2245	-55	-7395	-584	6	90
6433	-2003	-1929	-13914	-1701	-11	-135
6433	-2003	-1929	-13914	-1701	-11	-135
6508	-1503	-1437	-13001	-1280	-10	-117
6493	-1504	-842	-11802	-1121	-17	-86
7252	-1427	50	-8932	-903	-6	-37
7253	-1475	696	-7016	-527	-11	10

Table A-9b

SUMMARY OF STRESSES FOR DOWNHILL J-GROOVE (Loss of Secondary Pressure at 350s)

Downhill Side						
Node	SX	SY	SZ	SXY	SYZ	SXZ
4253	-676	-7036	-37191	-2230	2052	2248
4237	-1023	1753	-30165	-1412	2142	1976
4461	-1634	-1108	-14581	-129	1204	1253
6117	262	-287	-1689	39	166	214
6115	-349	-440	272	-88	55	121
4157	-6671	-13235	-20335	-9593	-1216	-180
4162	-5209	-9776	-21135	-5072	-284	151
4737	-1067	-8802	-25070	-1478	598	1712
6612	-1223	-3082	-17720	-559	480	1324
6611	-1041	-1552	-11807	-228	157	924
4987	-4801	-6521	-15646	-5070	-409	-157
4767	-4841	-5985	-18207	-4456	151	-138
4742	-2479	-3115	-14612	-2173	382	196
6628	-1791	-1985	-10748	-893	216	330
6629	-1214	-754	-7009	-353	10	235
4989	-4485	-6151	-13255	-5118	-286	-372
4769	-3969	-4486	-12574	-3744	86	-280
4744	-3346	-3473	-10828	-2882	78	-170
6618	-2184	-1874	-7469	-1477	35	-100
6619	-1333	-732	-4713	-492	-31	-86
4967	-4315	-5376	-12520	-4824	-87	-216
4722	-3734	-4259	-11011	-3786	15	-171
4727	-3091	-3316	-9300	-2925	21	-133
6553	-2025	-1867	-6314	-1513	7	-92
6554	-1147	-735	-3856	-362	-16	-84
6345	-4428	-5496	-12252	-4887	-91	-160
6379	-3625	-4181	-10351	-3779	-8	-131
6525	-3013	-3266	-8663	-2926	6	-115
7339	-1922	-1821	-5780	-1475	1	-85
7338	-1047	-640	-3413	-307	-12	-85

Table A-10a

SUMMARY OF STRESSES FOR UPHILL J-GROOVE (Leak Test Heatup at 10801s)

Uphill Side						
Node	SX	SY	SZ	SXY	SYZ	SXZ
3699	-443	2838	-19806	-827	-1620	-1708
3682	-147	-3717	-24991	-2134	-1485	-1247
4385	-917	-10158	-22309	-590	-263	-2075
4366	-658	-6316	-17067	426	-325	-1436
5930	-765	-2478	-3968	220	206	-1075
5929	-272	-814	-2971	-78	-56	-340
3755	-1573	-1634	-12916	-2309	-260	-175
3677	-5512	-7175	-17675	-4950	480	-337
4578	-2988	-390	-18867	-1034	-677	-963
4553	-2116	-3685	-20651	-1878	515	-1039
6972	-2919	-4325	-21022	-1204	636	-1026
6971	-1541	-3379	-15974	294	-50	-1366
3745	-7922	-2204	-10761	-2652	12	488
4520	-1713	-2737	-12449	-2929	88	76
4585	-2189	-2246	-12581	-3114	78	66
4555	-2209	-1247	-11864	-2310	-43	48
7002	-2541	-1013	-10535	-1360	-19	52
6996	-2504	-240	-8138	-471	-20	89
4509	-1991	-2799	-12953	-2192	27	-9
4509	-1991	-2799	-12953	-2192	27	-9
4510	-2134	-2445	-12289	-1768	30	-21
4504	-2299	-1766	-11412	-1608	27	-49
6943	-2098	-855	-9467	-1436	29	28
6944	-2334	-142	-7808	-641	6	93
6433	-2141	-2083	-14409	-1838	-11	-140
6433	-2141	-2083	-14409	-1838	-11	-140
6508	-1599	-1554	-13425	-1372	-11	-119
6493	-1556	-884	-12162	-1181	-18	-87
7252	-1497	-23	-9340	-975	-6	-39
7253	-1528	643	-7415	-576	-12	10

Table A-10b

SUMMARY OF STRESSES FOR DOWNHILL J-GROOVE (Leak Test Heatup at 10801s)

Downhill Side						
Node	SX	SY	SZ	SXY	SYZ	SXZ
4253	-689	-7152	-37858	-2278	2095	2289
4237	-1042	1783	-30676	-1432	2177	2013
4461	-1665	-1148	-14834	-133	1222	1275
6117	267	-291	-1745	38	170	220
6115	-350	-448	247	-91	55	124
4157	-6834	-13571	-20754	-9842	-1236	-181
4162	-5295	-9958	-21480	-5181	-291	152
4737	-1067	-8995	-25521	-1492	606	1747
6612	-1277	-3228	-18307	-578	487	1366
6611	-1079	-1657	-12388	-235	161	963
4987	-4920	-6694	-15927	-5202	-413	-157
4767	-4934	-6130	-18478	-4544	153	-144
4742	-2533	-3195	-14862	-2202	390	199
6628	-1844	-2068	-11076	-915	223	338
6629	-1275	-830	-7355	-363	12	243
4989	-4586	-6289	-13410	-5235	-289	-380
4769	-4042	-4577	-12705	-3810	90	-289
4744	-3400	-3541	-10950	-2920	82	-179
6618	-2245	-1955	-7670	-1511	39	-109
6619	-1392	-804	-4931	-510	-30	-96
4967	-4415	-5501	-12632	-4931	-90	-222
4722	-3793	-4336	-11077	-3844	16	-178
4727	-3127	-3376	-9355	-2954	23	-141
6553	-2070	-1941	-6454	-1546	9	-100
6554	-1189	-805	-4024	-378	-15	-92
6345	-4520	-5612	-12335	-4988	-94	-165
6379	-3670	-4247	-10378	-3830	-8	-137
6525	-3036	-3315	-8680	-2951	8	-121
7339	-1956	-1890	-5892	-1506	2	-92
7338	-1081	-701	-3554	-321	-10	-93

Table A-11a

SUMMARY OF STRESSES FOR UPHILL J-GROOVE (Leak Test Cooldown at 10801s)

Uphill Side						
Node	SX	SY	SZ	SXY	SYZ	SXZ
3699	200	-1119	9746	575	895	842
3682	32	2499	12166	1131	789	614
4385	426	5521	10811	321	196	1001
4366	305	3446	8116	-201	215	692
5930	354	1289	1489	-124	-84	490
5929	91	317	1254	24	19	98
3755	683	1022	6501	1793	154	107
3677	2567	3990	8549	2866	-193	157
4578	1229	41	8487	804	348	444
4553	993	2033	9224	1078	-264	411
6972	1283	1977	8138	528	-306	362
6971	400	1132	4883	-248	34	496
3745	6689	2318	6820	2149	29	-240
4520	1144	2135	6338	1858	-31	30
4585	1060	1768	6102	1901	-34	29
4555	922	995	5381	1347	29	12
7002	983	585	4100	630	14	-2
6996	858	27	2569	64	11	-28
4509	1589	2464	6600	1851	-3	-14
4509	1589	2464	6600	1851	-3	-14
4510	1585	2088	6019	1449	2	-6
4504	1387	1460	5196	1093	7	18
6943	862	594	3679	649	1	3
6944	794	23	2478	139	0	-28
6433	2484	2871	7905	2421	3	91
6433	2484	2871	7905	2421	3	91
6508	1760	2402	7031	1864	2	79
6493	1364	1663	5870	1415	12	53
7252	701	415	3592	667	8	19
7253	443	-223	2283	122	13	-5

Table A-11b

SUMMARY OF STRESSES FOR DOWNHILL J-GROOVE (Leak Test Cooldown at 10801s)

Downhill Side						
Node	SX	SY	SZ	SXY	SYZ	SXZ
4253	383	4035	19663	1330	-1261	-1201
4237	525	-629	15135	751	-1150	-1044
4461	842	569	6770	58	-576	-680
6117	-153	168	884	-22	-92	-104
6115	180	268	-8	54	-25	-65
4157	4184	8556	11936	6280	612	61
4162	3004	5966	11053	3039	147	-117
4737	521	4914	11875	865	-309	-846
6612	398	1303	7101	293	-200	-559
6611	372	440	3803	95	-44	-312
4987	3132	4324	9194	3429	165	13
4767	2738	3758	9351	2788	-82	85
4742	1229	1826	6920	1264	-193	-84
6628	742	997	4385	456	-92	-146
6629	356	209	2164	142	16	-71
4989	2965	4100	7937	3409	120	160
4769	2352	2882	6758	2370	-43	103
4744	1728	2022	5246	1649	-31	54
6618	908	953	3060	735	-6	24
6619	368	276	1420	163	27	24
4967	2848	3593	7550	3228	13	88
4722	2261	2717	6056	2387	-10	60
4727	1633	1914	4571	1653	-6	41
6553	874	967	2613	736	4	23
6554	333	312	1153	63	13	23
6345	2937	3650	7447	3259	22	64
6379	2227	2658	5772	2374	0	45
6525	1613	1879	4302	1643	-1	37
7339	846	944	2401	703	5	24
7338	315	262	990	21	8	27

Table A-12

SUMMARY OF CYCLIC STRESSES FOR UPHILL J-GROOVE

Node	X' (in)	Y' (in)	Cyclic Stresses, Δσ (ksi)							
			Startup/ Shutdown	Startup/ Shutdown (w/Flooding)	Plant Loading	Plant UnLoading	Reator Trip	Loss of Secondary Pressure	Leak Test	Hydro Test
3699	0.000	0.000	20.31	70.19	4.52	5.03	21.84	5.07	5.86	4.35
3682	0.000	0.476	36.14	87.96	4.57	5.21	18.37	5.68	19.32	22.10
4385	0.000	0.634	41.03	79.64	3.23	3.80	9.64	4.45	26.20	32.20
4366	0.000	0.792	28.89	58.16	2.45	2.90	8.72	3.21	18.18	22.09
5930	0.000	1.744	6.08	7.61	0.13	0.26	2.05	0.02	3.98	4.96
5929	0.000	2.697	0.70	7.32	0.70	0.77	4.48	0.68	1.02	1.90
3755	0.194	0.000	18.31	48.93	2.70	3.02	10.60	3.34	8.68	9.53
3677	0.194	0.476	33.16	62.39	2.46	2.91	7.09	3.45	21.40	26.40
4578	0.194	0.634	14.16	51.97	3.56	4.09	21.97	3.57	3.28	1.25
4553	0.194	0.792	23.58	59.77	3.29	3.79	17.66	3.80	11.65	12.60
6972	0.194	1.744	26.97	43.20	1.52	1.97	13.36	1.69	16.35	19.54
6971	0.194	2.697	22.87	12.56	0.81	0.41	6.39	1.50	16.19	20.59
3745	0.735	0.000	18.80	66.34	3.67	3.84	7.32	5.34	10.12	11.41
4520	0.735	0.476	20.81	48.74	2.39	2.69	7.57	3.24	11.81	13.94
4585	0.735	0.634	19.67	43.62	2.10	2.42	7.87	2.74	11.42	13.49
4555	0.735	0.792	16.63	36.55	1.75	2.02	7.72	2.29	9.86	11.61
7002	0.735	1.744	15.16	22.54	0.64	0.86	5.40	0.85	9.82	12.05
6996	0.735	2.697	12.83	7.75	0.44	0.25	2.43	0.66	9.33	11.96
4509	1.304	0.000	22.90	51.18	2.37	2.68	7.04	3.28	13.37	16.00
4509	1.304	0.476	22.90	51.18	2.37	2.68	7.04	3.28	13.37	16.00
4510	1.304	0.634	21.19	44.08	1.98	2.28	6.56	2.70	12.65	15.23
4504	1.304	0.792	18.54	35.58	1.48	1.74	5.86	2.06	11.56	14.04
6943	1.304	1.744	14.71	20.70	0.48	0.67	3.89	0.75	10.04	12.52
6944	1.304	2.697	12.59	7.60	0.45	0.26	2.11	0.64	9.23	11.86
6433	3.276	0.000	27.35	67.88	3.10	3.40	6.54	4.58	16.86	20.35
6433	3.276	0.476	27.35	67.88	3.10	3.40	6.54	4.58	16.86	20.35
6508	3.276	0.634	25.70	57.27	2.52	2.82	5.92	3.70	15.70	19.08
6493	3.276	0.792	23.15	45.13	1.88	2.13	4.98	2.87	14.17	17.41
7252	3.276	1.744	15.15	20.15	0.29	0.47	2.84	0.65	11.05	13.95
7253	3.276	2.697	12.70	6.66	0.60	0.43	1.21	0.67	9.61	12.47

Table A-13

SUMMARY OF CYCLIC STRESSES FOR DOWNHILL SIDE

Node	X' (in)	Y' (in)	Cyclic Stresses, Δσ (ksi)							
			Startup/ Shutdown	Startup/ Shutdown (w/Flooding)	Plant Loading	Plant UnLoading	Reator Trip	Loss of Secondary Pressure	Leak Test	Hydro Test
4253	0.000	0.000	54.88	165.17	8.48	9.39	29.44	19.76	28.61	32.10
4237	0.000	0.266	33.44	110.13	6.94	7.71	31.62	5.17	12.37	11.29
4461	0.000	0.565	11.96	40.66	3.13	3.53	18.16	1.87	1.82	0.11
6117	0.000	1.660	0.40	4.61	0.69	0.71	3.40	1.63	1.52	2.46
6115	0.000	2.756	1.02	0.62	0.19	0.17	0.66	1.03	1.17	1.72
4157	0.194	0.000	44.84	121.78	4.72	5.15	6.21	24.87	29.54	36.40
4162	0.194	0.266	47.13	106.24	3.38	3.88	4.93	25.86	31.72	39.78
4737	0.194	0.565	42.84	97.72	3.86	4.42	13.80	19.18	25.92	31.40
6612	0.194	1.660	26.14	47.80	1.15	1.54	9.56	11.63	17.42	21.44
6611	0.194	2.756	18.99	18.52	0.77	0.46	4.04	8.95	14.09	18.11
4987	0.619	0.000	25.87	85.15	4.35	4.70	11.37	10.85	14.10	16.02
4767	0.619	0.266	30.82	79.36	3.57	4.02	11.43	13.06	17.75	21.03
4742	0.619	0.565	23.88	55.31	2.32	2.66	8.85	10.14	14.05	16.83
6628	0.619	1.660	16.63	31.17	0.74	0.98	5.24	7.92	11.38	14.10
6629	0.619	2.756	12.21	10.92	0.63	0.44	1.63	6.19	9.38	12.19
4989	1.301	0.000	25.09	77.66	3.63	3.92	7.57	12.06	14.86	17.56
4769	1.301	0.266	22.24	59.24	2.75	3.06	7.77	9.62	12.70	15.02
4744	1.301	0.565	18.70	43.77	1.83	2.08	6.01	8.46	11.27	13.62
6618	1.301	1.660	12.33	23.17	0.47	0.63	2.92	6.49	8.90	11.17
6619	1.301	2.756	9.06	7.94	0.54	0.41	0.41	5.01	7.23	9.49
4967	1.985	0.000	21.85	72.54	3.65	3.93	8.61	9.66	12.15	13.95
4722	1.985	0.266	19.81	54.00	2.56	2.83	6.87	8.58	11.19	13.20
4727	1.985	0.565	16.14	38.88	1.66	1.87	5.13	7.48	9.82	11.86
6553	1.985	1.660	10.67	20.47	0.43	0.57	2.35	5.73	7.73	9.73
6554	1.985	2.756	7.70	6.80	0.48	0.37	0.11	4.40	6.23	8.21
6345	2.491	0.000	22.28	72.73	3.58	3.84	7.89	10.24	12.67	14.71
6379	2.491	0.266	19.06	52.30	2.48	2.74	6.31	8.40	10.81	12.78
6525	2.491	0.565	15.13	37.15	1.61	1.81	4.74	7.12	9.25	11.18
7339	2.491	1.660	9.93	19.18	0.41	0.53	2.05	5.42	7.24	9.13
7338	2.491	2.756	7.15	6.02	0.49	0.39	0.20	4.23	5.90	7.82

Appendix B

BIGIF COMPUTER OUTPUT FOR J-GROOVE FLAW EVALUATION (UPHILL SIDE)

```
SONGS PZR HEATER SLEEVE REPAIR EVALUATION BOTTOM HEAD FLAW UPHILL SIDE

BIGIF:  BOUNDARY INTEGRAL EQUATION          IBM PC VERSION   REV. 0 - SEPTEMBER 23, 1985
        GENERATED INFLUENCE FUNCTIONS
        FOR USE IN FRACTURE MECHANICS
        PROBLEMS

          ANALYSIS SELECTION (IFAT)

                    1 FATIGUE ANALYSIS

          CRACK GEOMETRY MODEL INDEX NUMBER (IFI)

                  303 SURFACE 1/4 CIRCULAR CRACK

          VARIABLE THICKNESS SPECIFICATION (WTH)

                    0 CONSTANT BODY THICKNESS

          CRACK GROWTH RATE RULE (IDADN)

                    2 INPUT TABULAR DA/DN, DELTA-K DATA

          INTEGRATION INCREMENT SCHEME (INUM)

                    3 REFINED

          SINGLE OR MULT INTEGRATION SCHEMES (INCL)

                    0 SINGLE

          INCREMENTS USED TO DOUBLE CRACK SIZE (NDUB)

                      USER SPECIFIED NDUB =    30
```

```
        GEOMETRY AND MATERIAL                    SONGS PZR HEATER SLEEVE REPAIR EVALUATION BOTTOM HEAD FLAW UPHILL SIDE
CRACK GROWTH INPUT

NUMBER OF DEGREES OF FREEDOM =  1

            INITIAL A-VALUES FOR EACH DEGREE OF FREEDOM

                CRACK LENGTH AI(1) =   1.0000



             GEOMETRY FACTORS

                G(1)    2.7000          BODY WIDTH
                G(2)    .00000
                G(3)    .00000
                G(4)    .00000
                G(5)    .00000
                G(6)    .00000          X-COORD. TO CRACK CENTER (XC)
                G(7)    .00000          Y-COORD. TO CRACK CENTER (YC)
                G(8)    .00000          CRACK ORIENTATION ANGLE (PHI, DEGREES)

            DA/DN OPTION SELECTED:  2

                KIC =  1000.0       FRACTURE TOUGHNESS

           THERE ARE SETS OF INPUT DATA FOR  1 R-RATIOS

           R-RATIO =   .25000           3 POINTS INPUT
                DELTA-K     DA/DN
             1.0000     1.02000E-12
             17.740     2.75000E-05
             100.00     8.02000E-04
```

```
LOAD TRANSIENTS:   8 TRANSIENT(S) IN PROBLEM        SONGS PZR HEATER SLEEVE REPAIR EVALUATION BOTTOM HEAD FLAW UPHILL SIDE

                                                    NUMBER OF
                                                      CYCLES
      NUMBER            NAME                        PER BLOCK   SPECIFIER   AGLD        IPSRD  IPLD  KAME  IWO   NPX   NPY

        1      STARTUP/SHUTDOWN                     .00000         1      1.0000        2     5     0     0     5     6
               BIVARIATE STRESS TABLE

   X           Y           SIGMA(X,Y)

 .00000      .00000        20.310
 .00000      .47600        36.140
 .00000      .63400        41.030
 .00000      .79200        28.890
 .00000      1.7440        6.0800
 .00000      2.6970        .70000
 .19400      .00000        18.310
 .19400      .47600        33.160
 .19400      .63400        14.160
 .19400      .79200        23.580
 .19400      1.7440        26.970
 .19400      2.6970        22.870
 .73500      .00000        18.800
 .73500      .47600        20.810
 .73500      .63400        19.670
 .73500      .79200        16.630
 .73500      1.7440        15.160
 .73500      2.6970        12.830
 1.3040      .00000        22.900
 1.3040      .47600        22.900
 1.3040      .63400        21.190
 1.3040      .79200        18.540
 1.3040      1.7440        14.710
 1.3040      2.6970        12.590
 3.2760      .00000        27.350
 3.2760      .47600        27.350
 3.2760      .63400        25.700
 3.2760      .79200        23.150
 3.2760      1.7440        15.150
 3.2760      2.6970        12.700
THE DATA FOR THE STRESS FIELD HAS BEEN READ CORRECTLY
                                                                  2      .00000        3     0     0     0     0     0

 4      2      STARTUP/SHUTDOWN/FLOODING            1.0420         1      1.0000        2     5     0     0     5     6
               BIVARIATE STRESS TABLE

   X           Y           SIGMA(X,Y)

 .00000      .00000        70.190
 .00000      .47600        87.960
 .00000      .63400        79.640
 .00000      .79200        58.160
 .00000      1.7440        7.6100
 .00000      2.6970        7.3200
 .19400      .00000        48.930
 .19400      .47600        62.390
 .19400      .63400        51.970
 .19400      .79200        59.770
 .19400      1.7440        43.200
 .19400      2.6970        12.560
 .73500      .00000        66.340
 .73500      .47600        48.740
 .73500      .63400        43.620
 .73500      .79200        36.550
 .73500      1.7440        22.540
 .73500      2.6970        7.7500
 1.3040      .00000        51.180
 1.3040      .47600        51.180
 1.3040      .63400        44.080
 1.3040      .79200        35.580
 1.3040      1.7440        20.700
 1.3040      2.6970        7.6000
 3.2760      .00000        67.880
 3.2760      .47600        67.880
 3.2760      .63400        57.270
```

```
3.2760        .79200        45.130
3.2760        1.7440        20.150
3.2760        2.6970        6.6600
THE DATA FOR THE STRESS FIELD HAS BEEN READ CORRECTLY

                                                2      .00000      3    0    0    0    0    0

      3     PLANT LOAD/STEP                1042.0     1     1.0000     2    5    0    0    5    6

            BIVARIATE STRESS TABLE

  X           Y           SIGMA(X,Y)

.00000      .00000       4.5200
.00000      .47600       4.5700
.00000      .63400       3.2300
.00000      .79200       2.4500
.00000      1.7440       .13000
.00000      2.6970       .70000
.19400      .00000       2.7000
.19400      .47600       2.4600
.19400      .63400       3.5600
.19400      .79200       3.2900
.19400      1.7440       1.5200
.19400      2.6970       .81000
.73500      .00000       3.6700
.73500      .47600       2.3900
.73500      .63400       2.1000
.73500      .79200       1.7500
.73500      1.7440       .64000
.73500      2.6970       .44000
1.3040      .00000       2.3700
1.3040      .47600       2.3700
1.3040      .63400       1.9800
1.3040      .79200       1.4800
1.3040      1.7440       .48000
1.3040      2.6970       .45000
3.2760      .00000       3.1000
3.2760      .47600       3.1000
3.2760      .63400       2.5200
3.2760      .79200       1.8800
3.2760      1.7440       .29000
3.2760      2.6970       .60000
THE DATA FOR THE STRESS FIELD HAS BEEN READ CORRECTLY

                                                2      .00000      3    0    0    0    0    0

      4     PLANT UNLOAD/STEP              1042.0     1     1.0000     2    5    0    0    5    6

            BIVARIATE STRESS TABLE

  X           Y           SIGMA(X,Y)

.00000      .00000       5.0300
.00000      .47600       5.2100
.00000      .63400       3.8000
.00000      .79200       2.9000
.00000      1.7440       .26000
.00000      2.6970       .77000
.19400      .00000       3.0200
.19400      .47600       2.9100
.19400      .63400       4.0900
.19400      .79200       3.7900
.19400      1.7440       1.9700
.19400      2.6970       .41000
.73500      .00000       3.8400
.73500      .47600       2.6900
.73500      .63400       2.4200
.73500      .79200       2.0200
.73500      1.7440       .86000
.73500      2.6970       .25000
1.3040      .00000       2.6800
1.3040      .47600       2.6800
1.3040      .63400       2.2800
1.3040      .79200       1.7400
1.3040      1.7440       .67000
1.3040      2.6970       .26000
3.2760      .00000       3.4000
3.2760      .47600       3.4000
```

```
3.2760        .63400        2.8200
3.2760        .79200        2.1300
3.2760        1.7440        .47000
3.2760        2.6970        .43000
THE DATA FOR THE STRESS FIELD HAS BEEN READ CORRECTLY

                                                    2     .00000     3   0   0   0   0   0

      5    REACTOR TRIP                  1.0000     1     1.0000     2   5   0   0   5   6

           BIVARIATE STRESS TABLE

  X          Y          SIGMA(X,Y)

.00000     .00000       21.840
.00000     .47600       18.370
.00000     .63400       9.6400
.00000     .79200       8.7200
.00000     1.7440       2.0500
.00000     2.6970       4.4800
.19400     .00000       10.600
.19400     .47600       7.0900
.19400     .63400       21.970
.19400     .79200       17.660
.19400     1.7440       13.360
.19400     2.6970       6.3900
.73500     .00000       7.3200
.73500     .47600       7.5700
.73500     .63400       7.8700
.73500     .79200       7.7200
.73500     1.7440       5.4000
.73500     2.6970       2.4300
1.3040     .00000       7.0400
1.3040     .47600       7.0400
1.3040     .63400       6.5600
1.3040     .79200       5.8600
1.3040     1.7440       3.8900
1.3040     2.6970       2.1100
3.2760     .00000       6.5400
3.2760     .47600       6.5400
3.2760     .63400       5.9200
3.2760     .79200       4.9800
3.2760     1.7440       2.8400
3.2760     2.6970       1.2100
THE DATA FOR THE STRESS FIELD HAS BEEN READ CORRECTLY

                                                    2     .00000     3   0   0   0   0   0

      6    LOSS OF SECONDARY PRESSURE    1.05000E-02  1     1.0000     2   5   0   0   5   6

           BIVARIATE STRESS TABLE

  X          Y          SIGMA(X,Y)

.00000     .00000       5.0700
.00000     .47600       5.6800
.00000     .63400       4.4500
.00000     .79200       3.2100
.00000     1.7440       2.00000E-02
.00000     2.6970       .68000
.19400     .00000       3.3400
.19400     .47600       3.4500
.19400     .63400       3.5700
.19400     .79200       3.8000
.19400     1.7440       1.6900
.19400     2.6970       1.5000
.73500     .00000       5.3400
.73500     .47600       3.2400
.73500     .63400       2.7400
.73500     .79200       2.2900
.73500     1.7440       .85000
.73500     2.6970       .66000
1.3040     .00000       3.2800
1.3040     .47600       3.2800
1.3040     .63400       2.7000
1.3040     .79200       2.0600
1.3040     1.7440       .75000
1.3040     2.6970       .64000
3.2760     .00000       4.5800
3.2760     .47600       4.5800
```

```
3.2760        .63400        3.7000
3.2760        .79200        2.8700
3.2760        1.7440        .65000
3.2760        2.6970        .67000
THE DATA FOR THE STRESS FIELD HAS BEEN READ CORRECTLY

                                                    2     .00000     3   0   0   0   0   0

        7     PLANT LEAK TEST                .41700   1     1.0000     2   5   0   0   5   6

              BIVARIATE STRESS TABLE

  X           Y           SIGMA(X,Y)

 .00000       .00000       5.8600
 .00000       .47600       19.320
 .00000       .63400       26.200
 .00000       .79200       18.180
 .00000       1.7440       3.9800
 .00000       2.6970       1.0200
 .19400       .00000       8.6800
 .19400       .47600       21.400
 .19400       .63400       3.2800
 .19400       .79200       11.650
 .19400       1.7440       16.350
 .19400       2.6970       16.190
 .73500       .00000       10.120
 .73500       .47600       11.810
 .73500       .63400       11.420
 .73500       .79200       9.8600
 .73500       1.7440       9.8200
 .73500       2.6970       9.3300
 1.3040       .00000       13.370
 1.3040       .47600       13.370
 1.3040       .63400       12.650
 1.3040       .79200       11.560
 1.3040       1.7440       10.040
 1.3040       2.6970       9.2300
 3.2760       .00000       16.860
 3.2760       .47600       16.860
 3.2760       .63400       15.700
 3.2760       .79200       14.170
 3.2760       1.7440       11.050
 3.2760       2.6970       9.6100
THE DATA FOR THE STRESS FIELD HAS BEEN READ CORRECTLY

                                                    2     .00000     3   0   0   0   0   0

        8     HYDROTEST                  2.10000E-02   1     1.0000     2   5   0   0   5   6

              BIVARIATE STRESS TABLE

  X           Y           SIGMA(X,Y)

 .00000       .00000       4.3500
 .00000       .47600       22.100
 .00000       .63400       32.200
 .00000       .79200       22.090
 .00000       1.7440       4.9600
 .00000       2.6970       1.9000
 .19400       .00000       9.5300
 .19400       .47600       26.400
 .19400       .63400       1.2500
 .19400       .79200       12.600
 .19400       1.7440       19.540
 .19400       2.6970       20.590
 .73500       .00000       11.410
 .73500       .47600       13.940
 .73500       .63400       13.490
 .73500       .79200       11.610
 .73500       1.7440       12.050
 .73500       2.6970       11.960
 1.3040       .00000       16.000
 1.3040       .47600       16.000
 1.3040       .63400       15.230
 1.3040       .79200       14.040
 1.3040       1.7440       12.520
 1.3040       2.6970       11.860
 3.2760       .00000       20.350
```

```
3.2760        .47600        20.350
3.2760        .63400        19.080
3.2760        .79200        17.410
3.2760        1.7440        13.950
3.2760        2.6970        12.470
THE DATA FOR THE STRESS FIELD HAS BEEN READ CORRECTLY

                                                2      .00000      3    0    0    0    0    0

DETAILED OUTPUT FOR ALL LOAD TRANSIENT(S) AND CRACK DEGREE(S) OF FREEDOM

                    ************
INTEGRATION BREAKUP * REFINED *          SONGS PZR HEATER SLEEVE REPAIR EVALUATION BOTTOM HEAD FLAW UPHILL SIDE
                    ************
```

TRANSIENT NUMBER	DEGREE OF FREEDOM	CYCLES /BLOCK	KMAX	KMIN	KMEAN	DEL-K	R-RAT	TRANSIENT DA/DN (PER CYCLE)	DA/DN (PER BLOCK)	DOF CRACK SIZE	N
1	1	.0000	28.45	.00	14.23	28.45	.000	6.9096E-05	4.347E-04	1.00	.0000
2	1	1.042	70.02	.00	35.01	70.02	.000	4.0021E-04			
3	1	1042.	3.56	.00	1.78	3.56	.000	1.9554E-09			
4	1	1042.	4.03	.00	2.01	4.03	.000	4.0461E-09			
5	1	1.000	13.50	.00	6.75	13.50	.000	5.4046E-06			
6	1	1.0500E-02	4.60	.00	2.30	4.60	.000	8.9711E-09			
7	1	.4170	15.66	.00	7.83	15.66	.000	1.3102E-05			
8	1	2.1000E-02	18.07	.00	9.04	18.07	.000	2.8520E-05			
1	1	.0000	28.69	.00	14.35	28.69	.000	7.0233E-05	4.386E-04	1.02	53.53
2	1	1.042	70.30	.00	35.15	70.30	.000	4.0338E-04			
3	1	1042.	3.57	.00	1.78	3.57	.000	1.9720E-09			
4	1	1042.	4.03	.00	2.02	4.03	.000	4.0960E-09			
5	1	1.000	13.56	.00	6.78	13.56	.000	5.5573E-06			
6	1	1.0500E-02	4.61	.00	2.31	4.61	.000	9.0650E-09			
7	1	.4170	15.83	.00	7.91	15.83	.000	1.3949E-05			
8	1	2.1000E-02	18.29	.00	9.14	18.28	.000	2.9162E-05			
1	1	.0000	28.93	.00	14.47	28.93	.000	7.1384E-05	4.423E-04	1.05	107.8
2	1	1.042	70.57	.00	35.28	70.57	.000	4.0634E-04			
3	1	1042.	3.57	.00	1.79	3.57	.000	1.9818E-09			
4	1	1042.	4.04	.00	2.02	4.04	.000	4.1325E-09			
5	1	1.000	13.61	.00	6.81	13.61	.000	5.6855E-06			
6	1	1.0500E-02	4.62	.00	2.31	4.62	.000	9.1362E-09			
7	1	.4170	16.00	.00	8.00	16.00	.000	1.4867E-05			
8	1	2.1000E-02	18.50	.00	9.25	18.50	.000	2.9837E-05			
1	1	.0000	29.16	.00	14.58	29.16	.000	7.2486E-05	4.456E-04	1.07	163.0
2	1	1.042	70.80	.00	35.40	70.80	.000	4.0897E-04			
3	1	1042.	3.57	.00	1.79	3.57	.000	1.9866E-09			
4	1	1042.	4.04	.00	2.02	4.04	.000	4.1590E-09			
5	1	1.000	13.66	.00	6.83	13.66	.000	5.8099E-06			
6	1	1.0500E-02	4.62	.00	2.31	4.62	.000	9.1818E-09			
7	1	.4170	16.16	.00	8.08	16.16	.000	1.5793E-05			
8	1	2.1000E-02	18.70	.00	9.35	18.70	.000	3.0491E-05			
1	1	.0000	29.41	.00	14.71	29.41	.000	7.3712E-05	4.489E-04	1.10	219.0
2	1	1.042	71.03	.00	35.51	71.03	.000	4.1152E-04			
3	1	1042.	3.57	.00	1.79	3.57	.000	1.9842E-09			
4	1	1042.	4.05	.00	2.02	4.05	.000	4.1751E-09			
5	1	1.000	13.71	.00	6.86	13.71	.000	5.9414E-06			
6	1	1.0500E-02	4.62	.00	2.31	4.62	.000	9.1865E-09			
7	1	.4170	16.34	.00	8.17	16.34	.000	1.6871E-05			
8	1	2.1000E-02	18.93	.00	9.47	18.93	.000	3.1225E-05			
1	1	.0000	29.66	.00	14.83	29.66	.000	7.4918E-05	4.519E-04	1.12	275.9
2	1	1.042	71.23	.00	35.62	71.23	.000	4.1386E-04			
3	1	1042.	3.57	.00	1.78	3.57	.000	1.9789E-09			
4	1	1042.	4.05	.00	2.02	4.05	.000	4.1862E-09			
5	1	1.000	13.77	.00	6.88	13.77	.000	6.0840E-06			
6	1	1.0500E-02	4.62	.00	2.31	4.62	.000	9.1695E-09			
7	1	.4170	16.52	.00	8.26	16.52	.000	1.7975E-05			
8	1	2.1000E-02	19.16	.00	9.58	19.16	.000	3.1944E-05			

APTECH ENGINEERING SERVICES, INC.

Calculation No.: AES-C-5212-2 SCE No. M-DSC-402, Rev. 0 Title: Pressurizer Heater Sleeve J-Groove Weld Flaw Evaluation — SONGS Units 2 and 3	Made by: RCC	Date: 9/17/04	Client: SCE
	Checked by: MTC	Date: 17 Sept 04	Project No.: AES 03105212-1Q
	Revision No.: 0	Document Control No.: I-2	Sheet No.: 90 of 110

1	1	.0000	29.90	.00	14.95	29.90	.000	7.6131E-05	4.547E-04	1.15	333.8
2	1	1.042	71.42	.00	35.71	71.42	.000	4.1598E-04			
3	1	1042.	3.57	.00	1.78	3.57	.000	1.9676E-09			
4	1	1042.	4.05	.00	2.02	4.05	.000	4.1851E-09			
5	1	1.000	13.81	.00	6.91	13.81	.000	6.2051E-06			
6	1	1.0500E-02	4.62	.00	2.31	4.62	.000	9.1310E-09			
7	1	.4170	16.69	.00	8.35	16.69	.000	1.9157E-05			
8	1	2.1000E-02	19.38	.00	9.69	19.38	.000	3.2687E-05			
1	1	.0000	30.15	.00	15.08	30.15	.000	7.7376E-05	4.573E-04	1.18	392.7
2	1	1.042	71.59	.00	35.79	71.59	.000	4.1789E-04			
3	1	1042.	3.56	.00	1.78	3.56	.000	1.9493E-09			
4	1	1042.	4.05	.00	2.02	4.05	.000	4.1698E-09			
5	1	1.000	13.85	.00	6.92	13.85	.000	6.2966E-06			
6	1	1.0500E-02	4.61	.00	2.31	4.61	.000	9.0672E-09			
7	1	.4170	16.88	.00	8.44	16.88	.000	2.0454E-05			
8	1	2.1000E-02	19.62	.00	9.81	19.62	.000	3.3474E-05			
1	1	.0000	30.39	.00	15.20	30.39	.000	7.8601E-05	4.596E-04	1.20	452.6
2	1	1.042	71.73	.00	35.86	71.73	.000	4.1949E-04			
3	1	1042.	3.55	.00	1.78	3.55	.000	1.9246E-09			
4	1	1042.	4.04	.00	2.02	4.04	.000	4.1412E-09			
5	1	1.000	13.87	.00	6.94	13.87	.000	6.3699E-06			
6	1	1.0500E-02	4.60	.00	2.30	4.60	.000	8.9759E-09			
7	1	.4170	17.06	.00	8.53	17.06	.000	2.1811E-05			
8	1	2.1000E-02	19.86	.00	9.93	19.86	.000	3.4268E-05			
1	1	.0000	30.62	.00	15.31	30.62	.000	7.9763E-05	4.615E-04	1.23	513.7
2	1	1.042	71.84	.00	35.92	71.84	.000	4.2070E-04			
3	1	1042.	3.54	.00	1.77	3.54	.000	1.8950E-09			
4	1	1042.	4.03	.00	2.02	4.03	.000	4.1017E-09			
5	1	1.000	13.90	.00	6.95	13.90	.000	6.4359E-06			
6	1	1.0500E-02	4.59	.00	2.30	4.59	.000	8.8597E-09			
7	1	.4170	17.24	.00	8.62	17.24	.000	2.3170E-05			
8	1	2.1000E-02	20.08	.00	10.04	20.08	.000	3.5033E-05			
1	1	.0000	30.86	.00	15.43	30.86	.000	8.0963E-05	4.631E-04	1.26	575.9
2	1	1.042	71.92	.00	35.96	71.92	.000	4.2172E-04			
3	1	1042.	3.53	.00	1.77	3.53	.000	1.8588E-09			
4	1	1042.	4.03	.00	2.01	4.03	.000	4.0480E-09			
5	1	1.000	13.91	.00	6.95	13.91	.000	6.4651E-06			
6	1	1.0500E-02	4.58	.00	2.29	4.58	.000	8.7223E-09			
7	1	.4170	17.42	.00	8.71	17.42	.000	2.4674E-05			
8	1	2.1000E-02	20.32	.00	10.16	20.32	.000	3.5852E-05			
1	1	.0000	31.13	.00	15.56	31.13	.000	8.2335E-05	4.652E-04	1.29	639.4
2	1	1.042	72.04	.00	36.02	72.04	.000	4.2300E-04			
3	1	1042.	3.52	.00	1.76	3.52	.000	1.8234E-09			
4	1	1042.	4.02	.00	2.01	4.02	.000	4.0005E-09			
5	1	1.000	13.94	.00	6.97	13.94	.000	6.5515E-06			
6	1	1.0500E-02	4.57	.00	2.28	4.57	.000	8.5664E-09			
7	1	.4170	17.62	.00	8.81	17.62	.000	2.6400E-05			
8	1	2.1000E-02	20.58	.00	10.29	20.58	.000	3.6747E-05			
1	1	.0000	31.40	.00	15.70	31.40	.000	8.3725E-05	4.669E-04	1.32	704.0
2	1	1.042	72.13	.00	36.07	72.13	.000	4.2413E-04			
3	1	1042.	3.51	.00	1.75	3.51	.000	1.7842E-09			
4	1	1042.	4.01	.00	2.00	4.01	.000	3.9442E-09			
5	1	1.000	13.96	.00	6.98	13.96	.000	6.6152E-06			
6	1	1.0500E-02	4.55	.00	2.28	4.55	.000	8.3987E-09			
7	1	.4170	17.82	.00	8.91	17.82	.000	2.7747E-05			
8	1	2.1000E-02	20.85	.00	10.42	20.85	.000	3.7672E-05			
1	1	.0000	31.66	.00	15.83	31.66	.000	8.5117E-05	4.683E-04	1.35	770.0
2	1	1.042	72.24	.00	36.12	72.24	.000	4.2532E-04			
3	1	1042.	3.49	.00	1.75	3.49	.000	1.7451E-09			
4	1	1042.	4.00	.00	2.00	4.00	.000	3.8854E-09			
5	1	1.000	13.97	.00	6.99	13.97	.000	6.6501E-06			
6	1	1.0500E-02	4.54	.00	2.27	4.54	.000	8.2439E-09			
7	1	.4170	18.03	.00	9.01	18.03	.000	2.8373E-05			
8	1	2.1000E-02	21.11	.00	10.56	21.11	.000	3.8621E-05			
1	1	.0000	31.91	.00	15.96	31.91	.000	8.6449E-05	4.696E-04	1.38	837.3
2	1	1.042	72.33	.00	36.16	72.33	.000	4.2636E-04			
3	1	1042.	3.48	.00	1.74	3.48	.000	1.7058E-09			
4	1	1042.	3.99	.00	1.99	3.99	.000	3.8243E-09			
5	1	1.000	13.99	.00	6.99	13.99	.000	6.6805E-06			
6	1	1.0500E-02	4.52	.00	2.26	4.52	.000	8.0885E-09			
7	1	.4170	18.22	.00	9.11	18.22	.000	2.8977E-05			
8	1	2.1000E-02	21.37	.00	10.69	21.37	.000	3.9541E-05			

1	1	.0000	32.17	.00	16.08	32.17	.000	8.7780E-05	4.709E-04	1.41	906.0
2	1	1.042	72.42	.00	36.21	72.42	.000	4.2744E-04			
3	1	1042.	3.47	.00	1.73	3.47	.000	1.6668E-09			
4	1	1042.	3.98	.00	1.99	3.98	.000	3.7610E-09			
5	1	1.000	13.99	.00	6.99	13.99	.000	6.6833E-06			
6	1	1.0500E-02	4.51	.00	2.25	4.51	.000	7.9460E-09			
7	1	.4170	18.42	.00	9.21	18.42	.000	2.9593E-05			
8	1	2.1000E-02	21.63	.00	10.82	21.63	.000	4.0484E-05			
1	1	.0000	32.41	.00	16.20	32.41	.000	8.9074E-05	4.719E-04	1.45	976.1
2	1	1.042	72.49	.00	36.25	72.49	.000	4.2824E-04			
3	1	1042.	3.45	.00	1.73	3.45	.000	1.6243E-09			
4	1	1042.	3.96	.00	1.98	3.96	.000	3.6897E-09			
5	1	1.000	13.98	.00	6.99	13.98	.000	6.6753E-06			
6	1	1.0500E-02	4.49	.00	2.25	4.49	.000	7.7851E-09			
7	1	.4170	18.61	.00	9.31	18.61	.000	3.0200E-05			
8	1	2.1000E-02	21.88	.00	10.94	21.88	.000	4.1415E-05			
1	1	.0000	32.65	.00	16.33	32.65	.000	9.0400E-05	4.730E-04	1.48	1048.
2	1	1.042	72.57	.00	36.29	72.57	.000	4.2914E-04			
3	1	1042.	3.44	.00	1.72	3.44	.000	1.5814E-09			
4	1	1042.	3.95	.00	1.97	3.95	.000	3.6147E-09			
5	1	1.000	13.97	.00	6.98	13.97	.000	6.6242E-06			
6	1	1.0500E-02	4.48	.00	2.24	4.48	.000	7.6382E-09			
7	1	.4170	18.81	.00	9.41	18.81	.000	3.0840E-05			
8	1	2.1000E-02	22.15	.00	11.08	22.15	.000	4.2404E-05			
1	1	.0000	32.90	.00	16.45	32.90	.000	9.1720E-05	4.737E-04	1.52	1121.
2	1	1.042	72.63	.00	36.31	72.63	.000	4.2979E-04			
3	1	1042.	3.42	.00	1.71	3.42	.000	1.5345E-09			
4	1	1042.	3.93	.00	1.97	3.93	.000	3.5301E-09			
5	1	1.000	13.94	.00	6.97	13.94	.000	6.5497E-06			
6	1	1.0500E-02	4.46	.00	2.23	4.46	.000	7.4737E-09			
7	1	.4170	19.02	.00	9.51	19.02	.000	3.1489E-05			
8	1	2.1000E-02	22.42	.00	11.21	22.42	.000	4.3413E-05			
1	1	.0000	33.13	.00	16.57	33.13	.000	9.2990E-05	4.741E-04	1.55	1196.
2	1	1.042	72.65	.00	36.33	72.65	.000	4.3011E-04			
3	1	1042.	3.40	.00	1.70	3.40	.000	1.4846E-09			
4	1	1042.	3.92	.00	1.96	3.92	.000	3.4380E-09			
5	1	1.000	13.91	.00	6.95	13.91	.000	6.4639E-06			
6	1	1.0500E-02	4.44	.00	2.22	4.44	.000	7.2923E-09			
7	1	.4170	19.21	.00	9.61	19.21	.000	3.2124E-05			
8	1	2.1000E-02	22.68	.00	11.34	22.68	.000	4.4405E-05			
1	1	.0000	33.37	.00	16.69	33.37	.000	9.4315E-05	4.750E-04	1.59	1272.
2	1	1.042	72.72	.00	36.36	72.72	.000	4.3084E-04			
3	1	1042.	3.38	.00	1.69	3.38	.000	1.4420E-09			
4	1	1042.	3.90	.00	1.95	3.90	.000	3.3615E-09			
5	1	1.000	13.90	.00	6.95	13.90	.000	6.4302E-06			
6	1	1.0500E-02	4.43	.00	2.21	4.43	.000	7.1347E-09			
7	1	.4170	19.41	.00	9.70	19.41	.000	3.2768E-05			
8	1	2.1000E-02	22.94	.00	11.47	22.94	.000	4.5404E-05			
1	1	.0000	33.65	.00	16.82	33.65	.000	9.5831E-05	4.762E-04	1.62	1350.
2	1	1.042	72.80	.00	36.40	72.80	.000	4.3182E-04			
3	1	1042.	3.37	.00	1.68	3.37	.000	1.3986E-09			
4	1	1042.	3.89	.00	1.94	3.89	.000	3.2851E-09			
5	1	1.000	13.89	.00	6.94	13.89	.000	6.4111E-06			
6	1	1.0500E-02	4.41	.00	2.21	4.41	.000	6.9696E-09			
7	1	.4170	19.63	.00	9.81	19.63	.000	3.3494E-05			
8	1	2.1000E-02	23.23	.00	11.61	23.23	.000	4.6527E-05			
1	1	.0000	33.92	.00	16.96	33.92	.000	9.7363E-05	4.772E-04	1.66	1430.
2	1	1.042	72.87	.00	36.44	72.87	.000	4.3261E-04			
3	1	1042.	3.35	.00	1.67	3.35	.000	1.3523E-09			
4	1	1042.	3.87	.00	1.94	3.87	.000	3.2015E-09			
5	1	1.000	13.88	.00	6.94	13.88	.000	6.3744E-06			
6	1	1.0500E-02	4.39	.00	2.20	4.39	.000	6.7911E-09			
7	1	.4170	19.85	.00	9.92	19.85	.000	3.4236E-05			
8	1	2.1000E-02	23.52	.00	11.76	23.52	.000	4.7680E-05			
1	1	.0000	34.19	.00	17.10	34.19	.000	9.8880E-05	4.779E-04	1.70	1511.
2	1	1.042	72.92	.00	36.46	72.92	.000	4.3314E-04			
3	1	1042.	3.33	.00	1.66	3.33	.000	1.3032E-09			
4	1	1042.	3.85	.00	1.93	3.85	.000	3.1101E-09			
5	1	1.000	13.85	.00	6.93	13.85	.000	6.3173E-06			
6	1	1.0500E-02	4.37	.00	2.19	4.37	.000	6.6005E-09			
7	1	.4170	20.07	.00	10.04	20.07	.000	3.4987E-05			
8	1	2.1000E-02	23.82	.00	11.91	23.82	.000	4.8853E-05			

1	1	.0000	34.46	.00	17.23	34.46	.000	1.0038E-04	4.787E-04	1.74	1594.
2	1	1.042	72.97	.00	36.49	72.97	.000	4.3380E-04			
3	1	1042.	3.31	.00	1.65	3.31	.000	1.2576E-09			
4	1	1042.	3.83	.00	1.92	3.83	.000	3.0244E-09			
5	1	1.000	13.83	.00	6.92	13.83	.000	6.2589E-06			
6	1	1.0500E-02	4.35	.00	2.18	4.35	.000	6.4292E-09			
7	1	.4170	20.29	.00	10.14	20.29	.000	3.5733E-05			
8	1	2.1000E-02	24.11	.00	12.05	24.11	.000	5.0020E-05			
1	1	.0000	34.72	.00	17.36	34.72	.000	1.0188E-04	4.794E-04	1.78	1679.
2	1	1.042	73.02	.00	36.51	73.02	.000	4.3430E-04			
3	1	1042.	3.29	.00	1.64	3.29	.000	1.2119E-09			
4	1	1042.	3.81	.00	1.91	3.81	.000	2.9362E-09			
5	1	1.000	13.81	.00	6.90	13.81	.000	6.1906E-06			
6	1	1.0500E-02	4.33	.00	2.17	4.33	.000	6.2582E-09			
7	1	.4170	20.51	.00	10.25	20.51	.000	3.6492E-05			
8	1	2.1000E-02	24.40	.00	12.20	24.40	.000	5.1212E-05			
1	1	.0000	34.98	.00	17.49	34.98	.000	1.0338E-04	4.798E-04	1.82	1766.
2	1	1.042	73.04	.00	36.52	73.04	.000	4.3459E-04			
3	1	1042.	3.27	.00	1.63	3.27	.000	1.1679E-09			
4	1	1042.	3.79	.00	1.90	3.79	.000	2.8460E-09			
5	1	1.000	13.77	.00	6.89	13.77	.000	6.0980E-06			
6	1	1.0500E-02	4.31	.00	2.16	4.31	.000	6.1033E-09			
7	1	.4170	20.73	.00	10.37	20.73	.000	3.7270E-05			
8	1	2.1000E-02	24.70	.00	12.35	24.70	.000	5.2443E-05			
1	1	.0000	35.23	.00	17.62	35.23	.000	1.0485E-04	4.799E-04	1.87	1855.
2	1	1.042	73.04	.00	36.52	73.04	.000	4.3458E-04			
3	1	1042.	3.25	.00	1.62	3.25	.000	1.1253E-09			
4	1	1042.	3.77	.00	1.89	3.77	.000	2.7550E-09			
5	1	1.000	13.73	.00	6.87	13.73	.000	5.9955E-06			
6	1	1.0500E-02	4.30	.00	2.15	4.30	.000	5.9555E-09			
7	1	.4170	20.95	.00	10.48	20.95	.000	3.8040E-05			
8	1	2.1000E-02	24.99	.00	12.50	24.99	.000	5.3669E-05			
1	1	.0000	35.48	.00	17.74	35.48	.000	1.0629E-04	4.797E-04	1.91	1946.
2	1	1.042	73.02	.00	36.51	73.02	.000	4.3434E-04			
3	1	1042.	3.23	.00	1.61	3.23	.000	1.0854E-09			
4	1	1042.	3.75	.00	1.88	3.75	.000	2.6650E-09			
5	1	1.000	13.69	.00	6.84	13.69	.000	5.8748E-06			
6	1	1.0500E-02	4.28	.00	2.14	4.28	.000	5.8256E-09			
7	1	.4170	21.17	.00	10.58	21.17	.000	3.8815E-05			
8	1	2.1000E-02	25.29	.00	12.64	25.29	.000	5.4909E-05			
1	1	.0000	35.72	.00	17.86	35.72	.000	1.0768E-04	4.798E-04	1.95	2039.
2	1	1.042	73.02	.00	36.51	73.02	.000	4.3430E-04			
3	1	1042.	3.21	.00	1.61	3.21	.000	1.0530E-09			
4	1	1042.	3.73	.00	1.87	3.73	.000	2.5871E-09			
5	1	1.000	13.64	.00	6.82	13.64	.000	5.7608E-06			
6	1	1.0500E-02	4.27	.00	2.13	4.27	.000	5.7383E-09			
7	1	.4170	21.38	.00	10.69	21.38	.000	3.9570E-05			
8	1	2.1000E-02	25.57	.00	12.79	25.57	.000	5.6121E-05			
1	1	.0000	35.95	.00	17.98	35.95	.000	1.0905E-04	4.795E-04	2.00	2134.
2	1	1.042	72.99	.00	36.49	72.99	.000	4.3397E-04			
3	1	1042.	3.19	.00	1.60	3.19	.000	1.0215E-09			
4	1	1042.	3.71	.00	1.86	3.71	.000	2.5078E-09			
5	1	1.000	13.59	.00	6.80	13.59	.000	5.6346E-06			
6	1	1.0500E-02	4.26	.00	2.13	4.26	.000	5.6564E-09			
7	1	.4170	21.59	.00	10.79	21.59	.000	4.0326E-05			
8	1	2.1000E-02	25.86	.00	12.93	25.86	.000	5.7338E-05			
1	1	.0000	36.18	.00	18.09	36.18	.000	1.1039E-04	4.789E-04	2.05	2232.
2	1	1.042	72.93	.00	36.47	72.93	.000	4.3333E-04			
3	1	1042.	3.18	.00	1.59	3.18	.000	9.9066E-10			
4	1	1042.	3.69	.00	1.85	3.69	.000	2.4263E-09			
5	1	1.000	13.53	.00	6.76	13.53	.000	5.4857E-06			
6	1	1.0500E-02	4.25	.00	2.12	4.25	.000	5.5812E-09			
7	1	.4170	21.80	.00	10.90	21.80	.000	4.1088E-05			
8	1	2.1000E-02	26.14	.00	13.07	26.14	.000	5.8577E-05			
1	1	.0000	36.41	.00	18.21	36.41	.000	1.1178E-04	4.781E-04	2.09	2332.
2	1	1.042	72.86	.00	36.43	72.86	.000	4.3247E-04			
3	1	1042.	3.16	.00	1.58	3.16	.000	9.5864E-10			
4	1	1042.	3.67	.00	1.84	3.67	.000	2.3395E-09			
5	1	1.000	13.45	.00	6.73	13.45	.000	5.2986E-06			
6	1	1.0500E-02	4.24	.00	2.12	4.24	.000	5.5072E-09			
7	1	.4170	22.02	.00	11.01	22.02	.000	4.1903E-05			
8	1	2.1000E-02	26.44	.00	13.22	26.44	.000	5.9909E-05			

1	1	.0000	36.64	.00	18.32	36.64	.000	1.1316E-04	4.769E-04	2.14	2434.
2	1	1.042	72.76	.00	36.38	72.76	.000	4.3129E-04			
3	1	1042.	3.14	.00	1.57	3.14	.000	9.2650E-10			
4	1	1042.	3.65	.00	1.82	3.65	.000	2.2501E-09			
5	1	1.000	13.36	.00	6.68	13.36	.000	5.0971E-06			
6	1	1.0500E-02	4.23	.00	2.11	4.23	.000	5.4329E-09			
7	1	.4170	22.24	.00	11.12	22.24	.000	4.2726E-05			
8	1	2.1000E-02	26.75	.00	13.37	26.75	.000	6.1263E-05			
1	1	.0000	36.90	.00	18.45	36.90	.000	1.1474E-04	4.761E-04	2.19	2539.
2	1	1.042	72.68	.00	36.34	72.68	.000	4.3039E-04			
3	1	1042.	3.13	.00	1.56	3.13	.000	8.9932E-10			
4	1	1042.	3.63	.00	1.81	3.63	.000	2.1715E-09			
5	1	1.000	13.30	.00	6.65	13.30	.000	4.9566E-06			
6	1	1.0500E-02	4.22	.00	2.11	4.22	.000	5.3733E-09			
7	1	.4170	22.48	.00	11.24	22.48	.000	4.3626E-05			
8	1	2.1000E-02	27.08	.00	13.54	27.08	.000	6.2728E-05			
1	1	.0000	37.18	.00	18.59	37.18	.000	1.1644E-04	4.757E-04	2.24	2647.
2	1	1.042	72.62	.00	36.31	72.62	.000	4.2976E-04			
3	1	1042.	3.11	.00	1.56	3.11	.000	8.7810E-10			
4	1	1042.	3.61	.00	1.80	3.61	.000	2.1049E-09			
5	1	1.000	13.26	.00	6.63	13.26	.000	4.8672E-06			
6	1	1.0500E-02	4.22	.00	2.11	4.22	.000	5.3362E-09			
7	1	.4170	22.72	.00	11.36	22.72	.000	4.4565E-05			
8	1	2.1000E-02	27.41	.00	13.70	27.41	.000	6.4248E-05			
1	1	.0000	37.45	.00	18.73	37.45	.000	1.1811E-04	4.754E-04	2.30	2757.
2	1	1.042	72.57	.00	36.29	72.57	.000	4.2918E-04			
3	1	1042.	3.10	.00	1.55	3.10	.000	8.6193E-10			
4	1	1042.	3.59	.00	1.79	3.59	.000	2.0463E-09			
5	1	1.000	13.22	.00	6.61	13.22	.000	4.7898E-06			
6	1	1.0500E-02	4.22	.00	2.11	4.22	.000	5.3289E-09			
7	1	.4170	22.96	.00	11.48	22.96	.000	4.5489E-05			
8	1	2.1000E-02	27.74	.00	13.87	27.74	.000	6.5744E-05			
1	1	.0000	37.72	.00	18.86	37.72	.000	1.1977E-04	4.747E-04	2.35	2870.
2	1	1.042	72.50	.00	36.25	72.50	.000	4.2827E-04			
3	1	1042.	3.09	.00	1.55	3.09	.000	8.4544E-10			
4	1	1042.	3.57	.00	1.79	3.57	.000	1.9848E-09			
5	1	1.000	13.18	.00	6.59	13.18	.000	4.6993E-06			
6	1	1.0500E-02	4.22	.00	2.11	4.22	.000	5.3218E-09			
7	1	.4170	23.20	.00	11.60	23.20	.000	4.6430E-05			
8	1	2.1000E-02	28.06	.00	14.03	28.06	.000	6.7274E-05			
1	1	.0000	38.00	.00	19.00	38.00	.000	1.2147E-04	4.736E-04	2.41	2986.
2	1	1.042	72.39	.00	36.19	72.39	.000	4.2701E-04			
3	1	1042.	3.08	.00	1.54	3.08	.000	8.2766E-10			
4	1	1042.	3.55	.00	1.78	3.55	.000	1.9181E-09			
5	1	1.000	13.13	.00	6.56	13.13	.000	4.5804E-06			
6	1	1.0500E-02	4.21	.00	2.11	4.21	.000	5.3129E-09			
7	1	.4170	23.46	.00	11.73	23.46	.000	4.7417E-05			
8	1	2.1000E-02	28.41	.00	14.20	28.41	.000	6.8890E-05			
1	1	.0000	38.28	.00	19.14	38.28	.000	1.2325E-04	4.722E-04	2.46	3105.
2	1	1.042	72.25	.00	36.12	72.25	.000	4.2545E-04			
3	1	1042.	3.07	.00	1.54	3.07	.000	8.0948E-10			
4	1	1042.	3.53	.00	1.76	3.53	.000	1.8481E-09			
5	1	1.000	13.05	.00	6.53	13.05	.000	4.4351E-06			
6	1	1.0500E-02	4.21	.00	2.11	4.21	.000	5.3076E-09			
7	1	.4170	23.72	.00	11.86	23.72	.000	4.8462E-05			
8	1	2.1000E-02	28.77	.00	14.38	28.77	.000	7.0607E-05			
1	1	.0000	38.56	.00	19.28	38.56	.000	1.2501E-04	4.704E-04	2.52	3227.
2	1	1.042	72.08	.00	36.04	72.08	.000	4.2349E-04			
3	1	1042.	3.06	.00	1.53	3.06	.000	7.9131E-10			
4	1	1042.	3.51	.00	1.75	3.51	.000	1.7761E-09			
5	1	1.000	12.98	.00	6.49	12.98	.000	4.2792E-06			
6	1	1.0500E-02	4.21	.00	2.11	4.21	.000	5.3027E-09			
7	1	.4170	23.98	.00	11.99	23.98	.000	4.9521E-05			
8	1	2.1000E-02	29.13	.00	14.57	29.13	.000	7.2358E-05			
1	1	.0000	38.84	.00	19.42	38.84	.000	1.2676E-04	4.682E-04	2.58	3353.
2	1	1.042	71.88	.00	35.94	71.88	.000	4.2117E-04			
3	1	1042.	3.05	.00	1.52	3.05	.000	7.7384E-10			
4	1	1042.	3.48	.00	1.74	3.48	.000	1.7039E-09			
5	1	1.000	12.89	.00	6.45	12.89	.000	4.1182E-06			
6	1	1.0500E-02	4.21	.00	2.11	4.21	.000	5.3005E-09			
7	1	.4170	24.25	.00	12.12	24.25	.000	5.0589E-05			
8	1	2.1000E-02	29.50	.00	14.75	29.50	.000	7.4132E-05			

1	1	.0000	39.11	.00	19.55	39.11	.000	1.2851E-04	4.656E-04	2.64	3482.
2	1	1.042	71.64	.00	35.82	71.64	.000	4.1843E-04			
3	1	1042.	3.04	.00	1.52	3.04	.000	7.5624E-10			
4	1	1042.	3.46	.00	1.73	3.46	.000	1.6302E-09			
5	1.	1.000	12.80	.00	6.40	12.80	.000	3.9498E-06			
6	1	1.0500E-02	4.21	.00	2.11	4.21	.000	5.2960E-09			
7	1	.4170	24.51	.00	12.26	24.51	.000	5.1670E-05			
8	1	2.1000E-02	29.86	.00	14.93	29.86	.000	7.5936E-05			

NOTE: CRACK SIZE OF 1ST DOF WILL EXCEED BODY WIDTH, G(1), ON NEXT ITERATION. PROCESSING TERMINATED.

REFINED BREAKUP

SONGS PZR HEATER SLEEVE REPAIR EVALUATION BOTTOM HEAD FLAW UPHILL SIDE

FATIGUE CRACK GROWTH ANALYSIS SUMMARY

CRACK DIMENSION(S) A(I)	MAXIMUM STRESS INTENSITY FACTOR(S) FOR WORST INPUT LOAD TRANSIENT KMAX	TOTAL CRACK GROWTH RATE(S) DADN(I)	NUMBER OF CYCLES OR BLOCKS TO GROW CRACK FROM INITIAL SIZE N
A1	K1	DADN1	N
1.000	70.019	4.3474E-04	.0000
1.023	70.304	4.3864E-04	53.53
1.047	70.567	4.4229E-04	107.8
1.072	70.801	4.4558E-04	163.0
1.097	71.027	4.4885E-04	219.0
1.122	71.234	4.5192E-04	275.9
1.149	71.421	4.5474E-04	333.8
1.176	71.589	4.5735E-04	392.7
1.203	71.729	4.5961E-04	452.6
1.231	71.835	4.6145E-04	513.7
1.260	71.925	4.6310E-04	575.9
1.289	72.036	4.6517E-04	639.4
1.320	72.135	4.6689E-04	704.0
1.350	72.238	4.6834E-04	770.0
1.382	72.329	4.6962E-04	837.3
1.414	72.423	4.7093E-04	906.0
1.447	72.492	4.7190E-04	976.1
1.481	72.570	4.7295E-04	1048.
1.516	72.626	4.7371E-04	1121.
1.551	72.655	4.7410E-04	1196.
1.587	72.718	4.7499E-04	1272.
1.625	72.802	4.7619E-04	1350.
1.662	72.870	4.7717E-04	1430.
1.701	72.916	4.7786E-04	1511.
1.741	72.973	4.7869E-04	1594.
1.782	73.017	4.7935E-04	1679.
1.823	73.042	4.7977E-04	1766.
1.866	73.040	4.7986E-04	1855.
1.910	73.020	4.7971E-04	1946.
1.954	73.016	4.7977E-04	2039.
2.000	72.988	4.7953E-04	2134.
2.047	72.933	4.7894E-04	2232.
2.095	72.859	4.7810E-04	2332.
2.144	72.756	4.7691E-04	2434.
2.194	72.679	4.7613E-04	2539.
2.245	72.624	4.7572E-04	2647.
2.297	72.574	4.7538E-04	2757.
2.351	72.495	4.7468E-04	2870.
2.406	72.386	4.7361E-04	2986.
2.462	72.250	4.7222E-04	3105.
2.520	72.079	4.7040E-04	3227.
2.579	71.876	4.6821E-04	3353.
2.639	71.636	4.6558E-04	3482.

Appendix C

BIGIF COMPUTER OUTPUT FOR J-GROOVE FLAW EVALUATION (DOWNHILL SIDE)

```
SONGS PZR HEATER SLEEVE REPAIR EVALUATION BOTTOM HEAD FLAW DOWNHILL SIDE

BIGIF:  BOUNDARY INTEGRAL EQUATION          IBM PC VERSION   REV. 0 - SEPTEMBER 23, 1985
        GENERATED INFLUENCE FUNCTIONS
        FOR USE IN FRACTURE MECHANICS
        PROBLEMS

          ANALYSIS SELECTION (IFAT)

                    1 FATIGUE ANALYSIS

          CRACK GEOMETRY MODEL INDEX NUMBER (IFI)

                  303 SURFACE 1/4 CIRCULAR CRACK

          VARIABLE THICKNESS SPECIFICATION (NTH)

                    0 CONSTANT BODY THICKNESS

          CRACK GROWTH RATE RULE (IDADN)

                    2 INPUT TABULAR DA/DN, DELTA-K DATA

          INTEGRATION INCREMENT SCHEME (INUM)

                    3 REFINED

          SINGLE OR MULT INTEGRATION SCHEMES (INCL)

                    0 SINGLE

          INCREMENTS USED TO DOUBLE CRACK SIZE (NDUB)

                      USER SPECIFIED NDUB =     30
```

```
        GEOMETRY AND MATERIAL                    SONGS PZR HEATER SLEEVE REPAIR EVALUATION BOTTOM HEAD FLAW DOWNHILL SIDE
CRACK GROWTH INPUT

NUMBER OF DEGREES OF FREEDOM =  1

            INITIAL A-VALUES FOR EACH DEGREE OF FREEDOM

                CRACK LENGTH AI(1) =   .87500


            GEOMETRY FACTORS

              G(1)    2.5000        BODY WIDTH
              G(2)    .00000
              G(3)    .00000
              G(4)    .00000
              G(5)    .00000
              G(6)    .00000        X-COORD. TO CRACK CENTER (XC)
              G(7)    .00000        Y-COORD. TO CRACK CENTER (YC)
              G(8)    .00000        CRACK ORIENTATION ANGLE (PHI, DEGREES)

            DA/DN OPTION SELECTED:  2

                KIC =  1000.0      FRACTURE TOUGHNESS

            THERE ARE SETS OF INPUT DATA FOR  1 R-RATIOS

            R-RATIO =   .25000          3 POINTS INPUT
                DELTA-K      DA/DN
              1.0000     1.02000E-12
              17.740     2.75000E-05
              100.00     8.02000E-04
```

LOAD TRANSIENTS: 8 TRANSIENT(S) IN PROBLEM SONGS PZR HEATER SLEEVE REPAIR EVALUATION BOTTOM HEAD FLAW DOWNHILL SIDE

NUMBER	NAME	NUMBER OF CYCLES PER BLOCK	SPECIFIER	AGLD	IPSRD	IPLD	KAME	IWO	NPX	NPY
1	STARTUP/SHUTDOWN	.00000	1	1.0000	2	5	0	0	6	5

BIVARIATE STRESS TABLE

X	Y	SIGMA(X,Y)
.00000	.00000	54.880
.00000	.26600	33.440
.00000	.56500	11.960
.00000	1.6600	.40000
.00000	2.7560	1.0200
.19400	.00000	44.840
.19400	.26600	47.130
.19400	.56500	42.840
.19400	1.6600	26.140
.19400	2.7560	18.990
.61900	.00000	25.870
.61900	.26600	30.820
.61900	.56500	23.880
.61900	1.6600	16.630
.61900	2.7560	12.210
1.3010	.00000	25.090
1.3010	.26600	22.240
1.3010	.56500	18.700
1.3010	1.6600	12.330
1.3010	2.7560	9.0600
1.9850	.00000	21.850
1.9850	.26600	19.810
1.9850	.56500	16.140
1.9850	1.6600	10.670
1.9850	2.7560	7.7000
2.4910	.00000	22.280
2.4910	.26600	19.060
2.4910	.56500	15.130
2.4910	1.6600	9.9300
2.4910	2.7560	7.1500

THE DATA FOR THE STRESS FIELD HAS BEEN READ CORRECTLY

			2	.00000	3	0	0	0	0	0
2	STARTUP/SHUTDOWN/FLOODING	1.0420	1	1.0000	2	5	0	0	6	5

BIVARIATE STRESS TABLE

X	Y	SIGMA(X,Y)
.00000	.00000	165.20
.00000	.26600	110.10
.00000	.56500	40.660
.00000	1.6600	4.6100
.00000	2.7560	.62000
.19400	.00000	121.80
.19400	.26600	106.20
.19400	.56500	97.720
.19400	1.6600	47.800
.19400	2.7560	18.520
.61900	.00000	85.150
.61900	.26600	79.360
.61900	.56500	55.310
.61900	1.6600	31.170
.61900	2.7560	10.920
1.3010	.00000	77.660
1.3010	.26600	59.240
1.3010	.56500	43.770
1.3010	1.6600	23.170
1.3010	2.7560	7.9400
1.9850	.00000	72.540
1.9850	.26600	54.000
1.9850	.56500	38.880
1.9850	1.6600	20.470

```
1.9850        2.7560        6.8000
2.4910        .00000        72.730
2.4910        .26600        52.300
2.4910        .56500        37.150
2.4910        1.6600        19.180
2.4910        2.7560        6.0200
THE DATA FOR THE STRESS FIELD HAS BEEN READ CORRECTLY

                                                2     .00000      3   0   0   0   0   0

        3     PLANT LOAD/STEP                 1042.0    1    1.0000      2   5   0   0   6   5

              BIVARIATE STRESS TABLE

  X           Y           SIGMA(X,Y)

.00000        .00000        8.4800
.00000        .26600        6.9400
.00000        .56500        3.1300
.00000        1.6600        .69000
.00000        2.7560        .19000
.19400        .00000        4.7200
.19400        .26600        3.3800
.19400        .56500        3.8600
.19400        1.6600        1.1500
.19400        2.7560        .77000
.61900        .00000        4.3500
.61900        .26600        3.5700
.61900        .56500        2.3200
.61900        1.6600        .74000
.61900        2.7560        .63000
1.3010        .00000        3.6300
1.3010        .26600        2.7500
1.3010        .56500        1.8300
1.3010        1.6600        .47000
1.3010        2.7560        .54000
1.9850        .00000        3.6500
1.9850        .26600        2.5600
1.9850        .56500        1.6600
1.9850        1.6600        .43000
1.9850        2.7560        .48000
2.4910        .00000        3.5800
2.4910        .26600        2.4800
2.4910        .56500        1.6100
2.4910        1.6600        .41000
2.4910        2.7560        .49000
THE DATA FOR THE STRESS FIELD HAS BEEN READ CORRECTLY

                                                2     .00000      3   0   0   0   0   0

        4     PLANT UNLOAD/STEP               1042.0    1    1.0000      2   5   0   0   6   5

              BIVARIATE STRESS TABLE

  X           Y           SIGMA(X,Y)

.00000        .00000        9.3900
.00000        .26600        7.7100
.00000        .56500        3.5300
.00000        1.6600        .71000
.00000        2.7560        .17000
.19400        .00000        5.1500
.19400        .26600        3.8800
.19400        .56500        4.4200
.19400        1.6600        1.5400
.23300        2.7560        .46000
.61900        .00000        4.7000
.61900        .26600        4.0200
.61900        .56500        2.6600
.61900        1.6600        .98000
.61900        2.7560        .44000
1.3010        .00000        3.9200
1.3010        .26600        3.0600
1.3010        .56500        2.0800
1.3010        1.6600        .63000
1.3010        2.7560        .41000
1.9850        .00000        3.9300
1.9850        .26600        2.8300
1.9850        .56500        1.8700
```

```
1.9850        1.6600        .57000
1.9850        2.7560        .37000
2.4910        .00000        3.8400
2.4910        .26600        2.7400
2.4910        .56500        1.8100
2.4910        1.6600        .53000
2.4910        2.7560        .39000
THE DATA FOR THE STRESS FIELD HAS BEEN READ CORRECTLY

                                                2     .00000     3   0   0   0   0   0

      5     REACTOR TRIP                  1.0000   1     1.0000     2   5   0   0   6   5

            BIVARIATE STRESS TABLE

  X           Y           SIGMA(X,Y)

.00000      .00000        29.440
.00000      .26560        31.620
.00000      .56510        18.160
.00000      1.6600        3.4000
.00000      2.7557        .66000
.19400      .00000        6.2100
.19400      .26560        4.9300
.19400      .56510        13.800
.19400      1.6600        9.5600
.19400      2.7557        4.0400
.61900      .00000        11.370
.61900      .26560        11.430
.61900      .56510        8.8500
.61900      1.6600        5.2400
.61900      2.7557        1.6300
1.3010      .00000        7.5700
1.3010      .26560        7.7700
1.3010      .56510        6.0100
1.3010      1.6600        2.9200
1.3010      2.7557        .41000
1.9850      .00000        8.6100
1.9850      .26560        6.8700
1.9850      .56510        5.1300
1.9850      1.6600        2.3500
1.9850      2.7557        .11000
2.4910      .00000        7.8900
2.4910      .26560        6.3100
2.4910      .56510        4.7400
2.4910      1.6600        2.0500
2.4910      2.7557        .20000
THE DATA FOR THE STRESS FIELD HAS BEEN READ CORRECTLY

                                                2     .00000     3   0   0   0   0   0

      6     LOSS OF SECONDARY PRESSURE    1.05000E-02   1     1.0000     2   5   0   0   6   5

            BIVARIATE STRESS TABLE

  X           Y           SIGMA(X,Y)

.00000      .00000        19.760
.00000      .26600        5.1700
.00000      .56500        1.8700
.00000      1.6600        1.6300
.00000      2.7560        1.0300
.19400      .00000        24.870
.19400      .26600        25.860
.19400      .56500        19.180
.19400      1.6600        11.630
.19400      2.7560        8.9500
.61900      .00000        10.850
.61900      .26600        13.060
.61900      .56500        10.140
.61900      1.6600        7.9200
.61900      2.7560        6.1900
1.3010      .00000        12.060
1.3010      .26600        9.6200
1.3010      .56500        8.4600
1.3010      1.6600        6.4900
1.3010      2.7560        5.0100
1.9850      .00000        9.6600
1.9850      .26600        8.5800
```

1.9850	.56500	7.4800
1.9850	1.6600	5.7300
1.9850	2.7560	4.4000
2.4910	.00000	10.240
2.4910	.26600	8.4000
2.4910	.56500	7.1200
2.4910	1.6600	5.4200
2.4910	2.7560	4.2300

THE DATA FOR THE STRESS FIELD HAS BEEN READ CORRECTLY

2 .00000 3 0 0 0 0 0

7 PLANT LEAK TEST .41700 1 1.0000 2 5 0 0 6 5

BIVARIATE STRESS TABLE

X	Y	SIGMA(X,Y)
.00000	.00000	28.610
.00000	.26600	12.370
.00000	.56500	1.8200
.00000	1.6600	1.5200
.00000	2.7560	1.1700
.19400	.00000	29.540
.19400	.26600	31.720
.19400	.56500	25.920
.19400	1.6600	17.420
.19400	2.7560	14.090
.61900	.00000	14.100
.61900	.26600	17.750
.61900	.56500	14.050
.61900	1.6600	11.380
.61900	2.7560	9.3800
1.3010	.00000	14.860
1.3010	.26600	12.700
1.3010	.56500	11.270
1.3010	1.6600	8.9000
1.3010	2.7560	7.2300
1.9850	.00000	12.150
1.9850	.26600	11.190
1.9850	.56500	9.8200
1.9850	1.6600	7.7300
1.9850	2.7560	6.2300
2.4910	.00000	12.670
2.4910	.26600	10.810
2.4910	.56500	9.2500
2.4910	1.6600	7.2400
2.4910	2.7560	5.9000

THE DATA FOR THE STRESS FIELD HAS BEEN READ CORRECTLY

2 .00000 3 0 0 0 0 0

8 HYDROTEST 2.10000E-02 1 1.0000 2 5 0 0 6 5

BIVARIATE STRESS TABLE

X	Y	SIGMA(X,Y)
.00000	.00000	32.100
.00000	.26600	11.290
.00000	.56500	.10000
.00000	1.6600	2.4600
.00000	2.7560	1.7200
.19400	.00000	36.390
.19400	.26600	39.770
.19400	.56500	31.390
.19400	1.6600	21.430
.19400	2.7560	18.100
.61900	.00000	16.010
.61900	.26600	21.020
.61900	.56500	16.830
.61900	1.6600	14.100
.61900	2.7560	12.190
1.3010	.00000	17.550
1.3010	.26600	15.010
1.3010	.56500	13.610
1.3010	1.6600	11.170
1.3010	2.7560	9.4900
1.9850	.00000	13.950

```
1.9850        .26600        13.190
1.9850        .56500        11.860
1.9850        1.6600        9.7200
1.9850        2.7560        8.2100
2.4910        .00000        14.710
2.4910        .26600        12.780
2.4910        .56500        11.180
2.4910        1.6600        9.1200
2.4910        2.7560        7.8100
THE DATA FOR THE STRESS FIELD HAS BEEN READ CORRECTLY

                                    2     .00000     3     0     0     0     0     0
```

DETAILED OUTPUT FOR ALL LOAD TRANSIENT(S) AND CRACK DEGREE(S) OF FREEDOM

INTEGRATION BREAKUP ********** * REFINED * **********

SONGS PZR HEATER SLEEVE REPAIR EVALUATION BOTTOM HEAD FLAW DOWNHILL SIDE

TRANSIENT NUMBER	DEGREE OF FREEDOM	CYCLES /BLOCK	KMAX	KMIN	KMEAN	DEL-K	R-RAT	TRANSIENT DA/DN (PER CYCLE)	DA/DN (PER BLOCK)	DOF CRACK SIZE	N
1	1	.0000	37.83	.00	18.91	37.83	.000	1.2043E-04	8.030E-04	.875	.0000
2	1	1.042	95.37	.00	47.69	95.37	.000	7.3118E-04			
3	1	1042.	4.15	.00	2.08	4.15	.000	4.8654E-09			
4	1	1042.	4.73	.00	2.37	4.73	.000	1.0580E-08			
5	1	1.000	13.68	.00	6.84	13.68	.000	5.8653E-06			
6	1	1.0500E-02	16.69	.00	8.34	16.69	.000	1.9116E-05			
7	1	.4170	22.18	.00	11.09	22.18	.000	4.2526E-05			
8	1	2.1000E-02	26.45	.00	13.22	26.45	.000	5.9931E-05			
1	1	.0000	37.92	.00	18.96	37.92	.000	1.2098E-04	8.038E-04	.895	25.46
2	1	1.042	95.41	.00	47.71	95.41	.000	7.3180E-04			
3	1	1042.	4.15	.00	2.07	4.15	.000	4.8391E-09			
4	1	1042.	4.73	.00	2.36	4.73	.000	1.0531E-08			
5	1	1.000	13.72	.00	6.86	13.72	.000	5.9620E-06			
6	1	1.0500E-02	16.72	.00	8.36	16.72	.000	1.9352E-05			
7	1	.4170	22.25	.00	11.12	22.25	.000	4.2774E-05			
8	1	2.1000E-02	26.53	.00	13.27	26.53	.000	6.0307E-05			
1	1	.0000	38.03	.00	19.01	38.03	.000	1.2167E-04	8.052E-04	.916	51.47
2	1	1.042	95.49	.00	47.74	95.49	.000	7.3296E-04			
3	1	1042.	4.14	.00	2.07	4.14	.000	4.8107E-09			
4	1	1042.	4.72	.00	2.36	4.72	.000	1.0480E-08			
5	1	1.000	13.75	.00	6.87	13.75	.000	6.0372E-06			
6	1	1.0500E-02	16.77	.00	8.39	16.77	.000	1.9704E-05			
7	1	.4170	22.33	.00	11.17	22.33	.000	4.3094E-05			
8	1	2.1000E-02	26.64	.00	13.32	26.64	.000	6.0797E-05			
1	1	.0000	38.16	.00	19.08	38.16	.000	1.2249E-04	8.069E-04	.938	78.05
2	1	1.042	95.59	.00	47.80	95.59	.000	7.3453E-04			
3	1	1042.	4.14	.00	2.07	4.14	.000	4.7766E-09			
4	1	1042.	4.72	.00	2.36	4.72	.000	1.0419E-08			
5	1	1.000	13.77	.00	6.88	13.77	.000	6.0872E-06			
6	1	1.0500E-02	16.84	.00	8.42	16.84	.000	2.0177E-05			
7	1	.4170	22.44	.00	11.22	22.44	.000	4.3485E-05			
8	1	2.1000E-02	26.78	.00	13.39	26.78	.000	6.1400E-05			
1	1	.0000	38.28	.00	19.14	38.28	.000	1.2328E-04	8.084E-04	.960	105.2
2	1	1.042	95.68	.00	47.84	95.68	.000	7.3586E-04			
3	1	1042.	4.13	.00	2.07	4.13	.000	4.7352E-09			
4	1	1042.	4.71	.00	2.36	4.71	.000	1.0341E-08			
5	1	1.000	13.78	.00	6.89	13.78	.000	6.1279E-06			
6	1	1.0500E-02	16.91	.00	8.45	16.91	.000	2.0648E-05			
7	1	.4170	22.54	.00	11.27	22.54	.000	4.3873E-05			
8	1	2.1000E-02	26.91	.00	13.46	26.91	.000	6.2003E-05			
1	1	.0000	38.41	.00	19.20	38.41	.000	1.2404E-04	8.096E-04	.982	132.9
2	1	1.042	95.75	.00	47.88	95.75	.000	7.3693E-04			
3	1	1042.	4.13	.00	2.06	4.13	.000	4.6828E-09			
4	1	1042.	4.71	.00	2.35	4.71	.000	1.0240E-08			
5	1	1.000	13.79	.00	6.90	13.79	.000	6.1505E-06			
6	1	1.0500E-02	16.97	.00	8.49	16.97	.000	2.1126E-05			
7	1	.4170	22.64	.00	11.32	22.64	.000	4.4262E-05			
8	1	2.1000E-02	27.05	.00	13.52	27.05	.000	6.2610E-05			
1	1	.0000	38.38	.00	19.19	38.38	.000	1.2388E-04	8.067E-04	1.01	161.3
2	1	1.042	95.58	.00	47.79	95.58	.000	7.3426E-04			
3	1	1042.	4.12	.00	2.06	4.12	.000	4.6282E-09			
4	1	1042.	4.70	.00	2.35	4.70	.000	1.0116E-08			
5	1	1.000	13.84	.00	6.92	13.84	.000	6.2704E-06			
6	1	1.0500E-02	16.94	.00	8.47	16.94	.000	2.0904E-05			
7	1	.4170	22.63	.00	11.31	22.63	.000	4.4199E-05			
8	1	2.1000E-02	27.03	.00	13.51	27.03	.000	6.2514E-05			
1	1	.0000	38.34	.00	19.17	38.34	.000	1.2363E-04	8.033E-04	1.03	190.5
2	1	1.042	95.37	.00	47.68	95.37	.000	7.3113E-04			
3	1	1042.	4.11	.00	2.05	4.11	.000	4.5651E-09			
4	1	1042.	4.68	.00	2.34	4.68	.000	9.9747E-09			
5	1	1.000	13.88	.00	6.94	13.88	.000	6.3785E-06			
6	1	1.0500E-02	16.90	.00	8.45	16.90	.000	2.0641E-05			
7	1	.4170	22.60	.00	11.30	22.60	.000	4.4109E-05			

8	1	2.1000E-02	27.00	.00	13.50	27.00	.000	6.2380E-05			
1	1	.0000	38.28	.00	19.14	38.28	.000	1.2328E-04	7.992E-04	1.05	220.5
2	1	1.042	95.12	.00	47.56	95.12	.000	7.2739E-04			
3	1	1042.	4.10	.00	2.05	4.10	.000	4.4892E-09			
4	1	1042.	4.67	.00	2.34	4.67	.000	9.8099E-09			
5	1	1.000	13.91	.00	6.95	13.91	.000	6.4682E-06			
6	1	1.0500E-02	16.86	.00	8.43	16.86	.000	2.0338E-05			
7	1	.4170	22.57	.00	11.29	22.57	.000	4.3987E-05			
8	1	2.1000E-02	26.96	.00	13.48	26.96	.000	6.2202E-05			
1	1	.0000	38.26	.00	19.13	38.26	.000	1.2310E-04	7.958E-04	1.08	251.4
2	1	1.042	94.91	.00	47.46	94.91	.000	7.2437E-04			
3	1	1042.	4.08	.00	2.04	4.08	.000	4.4143E-09			
4	1	1042.	4.66	.00	2.33	4.66	.000	9.6545E-09			
5	1	1.000	13.93	.00	6.97	13.93	.000	6.5362E-06			
6	1	1.0500E-02	16.84	.00	8.42	16.84	.000	2.0186E-05			
7	1	.4170	22.56	.00	11.28	22.56	.000	4.3954E-05			
8	1	2.1000E-02	26.95	.00	13.48	26.95	.000	6.2165E-05			
1	1	.0000	38.24	.00	19.12	38.24	.000	1.2303E-04	7.929E-04	1.10	283.1
2	1	1.042	94.74	.00	47.37	94.74	.000	7.2171E-04			
3	1	1042.	4.07	.00	2.04	4.07	.000	4.3372E-09			
4	1	1042.	4.65	.00	2.32	4.65	.000	9.5005E-09			
5	1	1.000	13.95	.00	6.98	13.95	.000	6.5837E-06			
6	1	1.0500E-02	16.83	.00	8.42	16.83	.000	2.0127E-05			
7	1	.4170	22.57	.00	11.28	22.57	.000	4.3978E-05			
8	1	2.1000E-02	26.96	.00	13.48	26.96	.000	6.2218E-05			
1	1	.0000	38.22	.00	19.11	38.22	.000	1.2286E-04	7.893E-04	1.13	315.6
2	1	1.042	94.52	.00	47.26	94.52	.000	7.1853E-04			
3	1	1042.	4.06	.00	2.03	4.06	.000	4.2496E-09			
4	1	1042.	4.63	.00	2.32	4.63	.000	9.3271E-09			
5	1	1.000	13.96	.00	6.98	13.96	.000	6.6121E-06			
6	1	1.0500E-02	16.82	.00	8.41	16.82	.000	2.0036E-05			
7	1	.4170	22.57	.00	11.28	22.57	.000	4.3978E-05			
8	1	2.1000E-02	26.97	.00	13.48	26.97	.000	6.2240E-05			
1	1	.0000	38.18	.00	19.09	38.18	.000	1.2262E-04	7.852E-04	1.15	349.1
2	1	1.042	94.27	.00	47.14	94.27	.000	7.1483E-04			
3	1	1042.	4.04	.00	2.02	4.04	.000	4.1518E-09			
4	1	1042.	4.62	.00	2.31	4.62	.000	9.1338E-09			
5	1	1.000	13.96	.00	6.98	13.96	.000	6.6219E-06			
6	1	1.0500E-02	16.80	.00	8.40	16.80	.000	1.9914E-05			
7	1	.4170	22.56	.00	11.28	22.56	.000	4.3953E-05			
8	1	2.1000E-02	26.96	.00	13.48	26.96	.000	6.2229E-05			
1	1	.0000	38.13	.00	19.06	38.13	.000	1.2231E-04	7.806E-04	1.18	383.6
2	1	1.042	93.99	.00	47.00	93.99	.000	7.1074E-04			
3	1	1042.	4.03	.00	2.01	4.03	.000	4.0474E-09			
4	1	1042.	4.60	.00	2.30	4.60	.000	8.9278E-09			
5	1	1.000	13.96	.00	6.98	13.96	.000	6.6159E-06			
6	1	1.0500E-02	16.78	.00	8.39	16.78	.000	1.9764E-05			
7	1	.4170	22.55	.00	11.28	22.55	.000	4.3910E-05			
8	1	2.1000E-02	26.96	.00	13.48	26.96	.000	6.2194E-05			
1	1	.0000	38.06	.00	19.03	38.06	.000	1.2191E-04	7.752E-04	1.21	419.1
2	1	1.042	93.68	.00	46.84	93.68	.000	7.0607E-04			
3	1	1042.	4.01	.00	2.00	4.01	.000	3.9315E-09			
4	1	1042.	4.58	.00	2.29	4.58	.000	8.6843E-09			
5	1	1.000	13.95	.00	6.98	13.95	.000	6.5837E-06			
6	1	1.0500E-02	16.76	.00	8.38	16.76	.000	1.9589E-05			
7	1	.4170	22.53	.00	11.27	22.53	.000	4.3845E-05			
8	1	2.1000E-02	26.94	.00	13.47	26.94	.000	6.2132E-05			
1	1	.0000	37.99	.00	18.99	37.99	.000	1.2141E-04	7.693E-04	1.24	455.7
2	1	1.042	93.32	.00	46.66	93.32	.000	7.0086E-04			
3	1	1042.	3.98	.00	1.99	3.98	.000	3.8076E-09			
4	1	1042.	4.55	.00	2.28	4.55	.000	8.4221E-09			
5	1	1.000	13.93	.00	6.97	13.93	.000	6.5328E-06			
6	1	1.0500E-02	16.73	.00	8.36	16.73	.000	1.9381E-05			
7	1	.4170	22.51	.00	11.25	22.51	.000	4.3751E-05			
8	1	2.1000E-02	26.92	.00	13.46	26.92	.000	6.2031E-05			
1	1	.0000	37.89	.00	18.95	37.89	.000	1.2083E-04	7.628E-04	1.27	493.5
2	1	1.042	92.93	.00	46.46	92.93	.000	6.9512E-04			
3	1	1042.	3.96	.00	1.98	3.96	.000	3.6766E-09			
4	1	1042.	4.53	.00	2.26	4.53	.000	8.1433E-09			
5	1	1.000	13.91	.00	6.95	13.91	.000	6.4634E-06			
6	1	1.0500E-02	16.69	.00	8.35	16.69	.000	1.9138E-05			
7	1	.4170	22.48	.00	11.24	22.48	.000	4.3631E-05			
8	1	2.1000E-02	26.89	.00	13.45	26.89	.000	6.1894E-05			

1	1	.0000	37.78	.00	18.89	37.78	.000	1.2016E-04	7.557E-04	1.30	532.4
2	1	1.042	92.50	.00	46.25	92.50	.000	6.8891E-04			
3	1	1042.	3.94	.00	1.97	3.94	.000	3.5400E-09			
4	1	1042.	4.50	.00	2.25	4.50	.000	7.8513E-09			
5	1	1.000	13.88	.00	6.94	13.88	.000	6.3765E-06			
6	1	1.0500E-02	16.65	.00	8.33	16.65	.000	1.8863E-05			
7	1	.4170	22.44	.00	11.22	22.44	.000	4.3486E-05			
8	1	2.1000E-02	26.85	.00	13.43	26.85	.000	6.1724E-05			
1	1	.0000	37.67	.00	18.84	37.67	.000	1.1947E-04	7.484E-04	1.33	572.7
2	1	1.042	92.06	.00	46.03	92.06	.000	6.8251E-04			
3	1	1042.	3.91	.00	1.95	3.91	.000	3.4004E-09			
4	1	1042.	4.47	.00	2.24	4.47	.000	7.5525E-09			
5	1	1.000	13.84	.00	6.92	13.84	.000	6.2722E-06			
6	1	1.0500E-02	16.61	.00	8.31	16.61	.000	1.8601E-05			
7	1	.4170	22.40	.00	11.20	22.40	.000	4.3344E-05			
8	1	2.1000E-02	26.82	.00	13.41	26.82	.000	6.1563E-05			
1	1	.0000	37.62	.00	18.81	37.62	.000	1.1915E-04	7.430E-04	1.36	614.3
2	1	1.042	91.74	.00	45.87	91.74	.000	6.7780E-04			
3	1	1042.	3.89	.00	1.94	3.89	.000	3.2760E-09			
4	1	1042.	4.44	.00	2.22	4.44	.000	7.2929E-09			
5	1	1.000	13.80	.00	6.90	13.80	.000	6.1667E-06			
6	1	1.0500E-02	16.61	.00	8.30	16.61	.000	1.8581E-05			
7	1	.4170	22.41	.00	11.20	22.41	.000	4.3367E-05			
8	1	2.1000E-02	26.84	.00	13.42	26.84	.000	6.1655E-05			
1	1	.0000	37.56	.00	18.78	37.56	.000	1.1876E-04	7.372E-04	1.39	657.2
2	1	1.042	91.38	.00	45.69	91.38	.000	6.7273E-04			
3	1	1042.	3.86	.00	1.93	3.86	.000	3.1488E-09			
4	1	1042.	4.42	.00	2.21	4.42	.000	7.0257E-09			
5	1	1.000	13.76	.00	6.88	13.76	.000	6.0530E-06			
6	1	1.0500E-02	16.60	.00	8.30	16.60	.000	1.8535E-05			
7	1	.4170	22.41	.00	11.20	22.41	.000	4.3371E-05			
8	1	2.1000E-02	26.85	.00	13.43	26.85	.000	6.1720E-05			
1	1	.0000	37.49	.00	18.74	37.49	.000	1.1833E-04	7.312E-04	1.42	701.4
2	1	1.042	91.01	.00	45.51	91.01	.000	6.6745E-04			
3	1	1042.	3.83	.00	1.92	3.83	.000	3.0212E-09			
4	1	1042.	4.39	.00	2.19	4.39	.000	6.7572E-09			
5	1	1.000	13.71	.00	6.85	13.71	.000	5.9344E-06			
6	1	1.0500E-02	16.59	.00	8.30	16.59	.000	1.8471E-05			
7	1	.4170	22.41	.00	11.20	22.41	.000	4.3367E-05			
8	1	2.1000E-02	26.86	.00	13.43	26.86	.000	6.1775E-05			
1	1	.0000	37.41	.00	18.70	37.41	.000	1.1785E-04	7.248E-04	1.45	747.0
2	1	1.042	90.62	.00	45.31	90.62	.000	6.6187E-04			
3	1	1042.	3.80	.00	1.90	3.80	.000	2.8909E-09			
4	1	1042.	4.36	.00	2.18	4.36	.000	6.4816E-09			
5	1	1.000	13.66	.00	6.83	13.66	.000	5.8030E-06			
6	1	1.0500E-02	16.58	.00	8.29	16.58	.000	1.8396E-05			
7	1	.4170	22.40	.00	11.20	22.40	.000	4.3353E-05			
8	1	2.1000E-02	26.87	.00	13.44	26.87	.000	6.1819E-05			
1	1	.0000	37.32	.00	18.66	37.32	.000	1.1732E-04	7.181E-04	1.49	794.1
2	1	1.042	90.21	.00	45.11	90.21	.000	6.5601E-04			
3	1	1042.	3.77	.00	1.89	3.77	.000	2.7603E-09			
4	1	1042.	4.33	.00	2.16	4.33	.000	6.2041E-09			
5	1	1.000	13.60	.00	6.80	13.60	.000	5.6689E-06			
6	1	1.0500E-02	16.57	.00	8.28	16.57	.000	1.8300E-05			
7	1	.4170	22.40	.00	11.20	22.40	.000	4.3326E-05			
8	1	2.1000E-02	26.88	.00	13.44	26.88	.000	6.1845E-05			
1	1	.0000	37.22	.00	18.61	37.22	.000	1.1671E-04	7.109E-04	1.52	842.8
2	1	1.042	89.76	.00	44.88	89.76	.000	6.4962E-04			
3	1	1042.	3.74	.00	1.87	3.74	.000	2.6253E-09			
4	1	1042.	4.29	.00	2.15	4.29	.000	5.9158E-09			
5	1	1.000	13.54	.00	6.77	13.54	.000	5.5180E-06			
6	1	1.0500E-02	16.55	.00	8.27	16.55	.000	1.8175E-05			
7	1	.4170	22.38	.00	11.19	22.38	.000	4.3275E-05			
8	1	2.1000E-02	26.88	.00	13.44	26.88	.000	6.1840E-05			
1	1	.0000	37.11	.00	18.56	37.11	.000	1.1604E-04	7.032E-04	1.56	893.2
2	1	1.042	89.28	.00	44.64	89.28	.000	6.4288E-04			
3	1	1042.	3.71	.00	1.85	3.71	.000	2.4896E-09			
4	1	1042.	4.25	.00	2.13	4.25	.000	5.6248E-09			
5	1	1.000	13.48	.00	6.74	13.48	.000	5.3617E-06			
6	1	1.0500E-02	16.52	.00	8.26	16.52	.000	1.8029E-05			
7	1	.4170	22.36	.00	11.18	22.36	.000	4.3208E-05			
8	1	2.1000E-02	26.87	.00	13.44	26.87	.000	6.1814E-05			

1	1	.0000	37.00	.00	18.50	37.00	.000	1.1534E-04	6.955E-04	1.60	945.3
2	1	1.042	88.79	.00	44.40	88.79	.000	6.3606E-04			
3	1	1042.	3.68	.00	1.84	3.68	.000	2.3576E-09			
4	1	1042.	4.22	.00	2.11	4.22	.000	5.3413E-09			
5	1	1.000	13.41	.00	6.71	13.41	.000	5.2071E-06			
6	1	1.0500E-02	16.50	.00	8.25	16.50	.000	1.7872E-05			
7	1	.4170	22.35	.00	11.17	22.35	.000	4.3136E-05			
8	1	2.1000E-02	26.87	.00	13.43	26.87	.000	6.1782E-05			
1	1	.0000	36.87	.00	18.44	36.87	.000	1.1456E-04	6.872E-04	1.63	999.3
2	1	1.042	88.27	.00	44.13	88.27	.000	6.2872E-04			
3	1	1042.	3.64	.00	1.82	3.64	.000	2.2230E-09			
4	1	1042.	4.18	.00	2.09	4.18	.000	5.0504E-09			
5	1	1.000	13.34	.00	6.67	13.34	.000	5.0348E-06			
6	1	1.0500E-02	16.47	.00	8.24	16.47	.000	1.7690E-05			
7	1	.4170	22.32	.00	11.16	22.32	.000	4.3041E-05			
8	1	2.1000E-02	26.85	.00	13.43	26.85	.000	6.1721E-05			
1	1	.0000	36.72	.00	18.36	36.72	.000	1.1367E-04	6.782E-04	1.67	1055.
2	1	1.042	87.70	.00	43.85	87.70	.000	6.2081E-04			
3	1	1042.	3.60	.00	1.80	3.60	.000	2.0866E-09			
4	1	1042.	4.14	.00	2.07	4.14	.000	4.7542E-09			
5	1	1.000	13.25	.00	6.63	13.25	.000	4.8491E-06			
6	1	1.0500E-02	16.44	.00	8.22	16.44	.000	1.7474E-05			
7	1	.4170	22.29	.00	11.14	22.29	.000	4.2916E-05			
8	1	2.1000E-02	26.83	.00	13.41	26.83	.000	6.1619E-05			
1	1	.0000	36.58	.00	18.29	36.58	.000	1.1280E-04	6.694E-04	1.71	1113.
2	1	1.042	87.13	.00	43.56	87.13	.000	6.1299E-04			
3	1	1042.	3.56	.00	1.78	3.56	.000	1.9596E-09			
4	1	1042.	4.09	.00	2.05	4.09	.000	4.4763E-09			
5	1	1.000	13.17	.00	6.59	13.17	.000	4.6764E-06			
6	1	1.0500E-02	16.40	.00	8.20	16.40	.000	1.7252E-05			
7	1	.4170	22.25	.00	11.13	22.25	.000	4.2787E-05			
8	1	2.1000E-02	26.80	.00	13.40	26.80	.000	6.1507E-05			
1	1	.0000	36.44	.00	18.22	36.44	.000	1.1196E-04	6.608E-04	1.75	1173.
2	1	1.042	86.56	.00	43.28	86.56	.000	6.0525E-04			
3	1	1042.	3.53	.00	1.76	3.53	.000	1.8435E-09			
4	1	1042.	4.05	.00	2.03	4.05	.000	4.2175E-09			
5	1	1.000	13.09	.00	6.55	13.09	.000	4.5088E-06			
6	1	1.0500E-02	16.37	.00	8.18	16.37	.000	1.7035E-05			
7	1	.4170	22.22	.00	11.11	22.22	.000	4.2660E-05			
8	1	2.1000E-02	26.78	.00	13.39	26.78	.000	6.1396E-05			
1	1	.0000	36.29	.00	18.15	36.29	.000	1.1107E-04	6.518E-04	1.79	1236.
2	1	1.042	85.97	.00	42.99	85.97	.000	5.9726E-04			
3	1	1042.	3.49	.00	1.75	3.49	.000	1.7332E-09			
4	1	1042.	4.01	.00	2.01	4.01	.000	3.9678E-09			
5	1	1.000	13.00	.00	6.50	13.00	.000	4.3329E-06			
6	1	1.0500E-02	16.33	.00	8.17	16.33	.000	1.6804E-05			
7	1	.4170	22.18	.00	11.09	22.18	.000	4.2518E-05			
8	1	2.1000E-02	26.75	.00	13.37	26.75	.000	6.1263E-05			
1	1	.0000	36.16	.00	18.08	36.16	.000	1.1031E-04	6.434E-04	1.83	1300.
2	1	1.042	85.42	.00	42.71	85.42	.000	5.8972E-04			
3	1	1042.	3.46	.00	1.73	3.46	.000	1.6327E-09			
4	1	1042.	3.97	.00	1.99	3.97	.000	3.7376E-09			
5	1	1.000	12.91	.00	6.46	12.91	.000	4.1531E-06			
6	1	1.0500E-02	16.31	.00	8.15	16.31	.000	1.6650E-05			
7	1	.4170	22.16	.00	11.08	22.16	.000	4.2430E-05			
8	1	2.1000E-02	26.74	.00	13.37	26.74	.000	6.1218E-05			
1	1	.0000	36.09	.00	18.05	36.09	.000	1.0988E-04	6.364E-04	1.88	1367.
2	1	1.042	84.95	.00	42.48	84.95	.000	5.8347E-04			
3	1	1042.	3.42	.00	1.71	3.42	.000	1.5423E-09			
4	1	1042.	3.93	.00	1.97	3.93	.000	3.5313E-09			
5	1	1.000	12.82	.00	6.41	12.82	.000	3.9744E-06			
6	1	1.0500E-02	16.31	.00	8.16	16.31	.000	1.6704E-05			
7	1	.4170	22.18	.00	11.09	22.18	.000	4.2501E-05			
8	1	2.1000E-02	26.78	.00	13.39	26.78	.000	6.1416E-05			
1	1	.0000	36.02	.00	18.01	36.02	.000	1.0945E-04	6.294E-04	1.92	1436.
2	1	1.042	84.48	.00	42.24	84.48	.000	5.7715E-04			
3	1	1042.	3.39	.00	1.70	3.39	.000	1.4589E-09			
4	1	1042.	3.90	.00	1.95	3.90	.000	3.3374E-09			
5	1	1.000	12.72	.00	6.36	12.72	.000	3.8000E-06			
6	1	1.0500E-02	16.32	.00	8.16	16.32	.000	1.6753E-05			
7	1	.4170	22.19	.00	11.10	22.19	.000	4.2569E-05			
8	1	2.1000E-02	26.83	.00	13.41	26.83	.000	6.1612E-05			

1	1	.0000	35.95	.00	17.98	35.95	.000	1.0905E-04	6.225E-04	1.96	1508.
2	1	1.042	84.01	.00	42.00	84.01	.000	5.7093E-04			
3	1	1042.	3.36	.00	1.68	3.36	.000	1.3836E-09			
4	1	1042.	3.86	.00	1.93	3.86	.000	3.1589E-09			
5	1	1.000	12.63	.00	6.31	12.63	.000	3.6376E-06			
6	1	1.0500E-02	16.33	.00	8.17	16.33	.000	1.6804E-05			
7	1	.4170	22.21	.00	11.11	22.21	.000	4.2645E-05			
8	1	2.1000E-02	26.87	.00	13.44	26.87	.000	6.1818E-05			
1	1	.0000	35.88	.00	17.94	35.88	.000	1.0862E-04	6.153E-04	2.01	1582.
2	1	1.042	83.51	.00	41.76	83.51	.000	5.6434E-04			
3	1	1042.	3.33	.00	1.67	3.33	.000	1.3106E-09			
4	1	1042.	3.82	.00	1.91	3.82	.000	2.9835E-09			
5	1	1.000	12.53	.00	6.26	12.53	.000	3.4683E-06			
6	1	1.0500E-02	16.34	.00	8.17	16.34	.000	1.6841E-05			
7	1	.4170	22.23	.00	11.12	22.23	.000	4.2707E-05			
8	1	2.1000E-02	26.92	.00	13.46	26.92	.000	6.2008E-05			
1	1	.0000	35.80	.00	17.90	35.80	.000	1.0816E-04	6.078E-04	2.06	1659.
2	1	1.042	82.99	.00	41.50	82.99	.000	5.5750E-04			
3	1	1042.	3.30	.00	1.65	3.30	.000	1.2401E-09			
4	1	1042.	3.79	.00	1.89	3.79	.000	2.8121E-09			
5	1	1.000	12.42	.00	6.21	12.42	.000	3.2921E-06			
6	1	1.0500E-02	16.34	.00	8.17	16.34	.000	1.6884E-05			
7	1	.4170	22.25	.00	11.12	22.25	.000	4.2771E-05			
8	1	2.1000E-02	26.96	.00	13.48	26.96	.000	6.2206E-05			
1	1	.0000	35.72	.00	17.86	35.72	.000	1.0769E-04	6.000E-04	2.11	1739.
2	1	1.042	82.45	.00	41.22	82.45	.000	5.5040E-04			
3	1	1042.	3.27	.00	1.63	3.27	.000	1.1738E-09			
4	1	1042.	3.75	.00	1.87	3.75	.000	2.6481E-09			
5	1	1.000	12.30	.00	6.15	12.30	.000	3.1123E-06			
6	1	1.0500E-02	16.35	.00	8.17	16.35	.000	1.6923E-05			
7	1	.4170	22.26	.00	11.13	22.26	.000	4.2829E-05			
8	1	2.1000E-02	27.00	.00	13.50	27.00	.000	6.2400E-05			
1	1	.0000	35.64	.00	17.82	35.64	.000	1.0721E-04	5.920E-04	2.15	1821.
2	1	1.042	81.89	.00	40.94	81.89	.000	5.4313E-04			
3	1	1042.	3.24	.00	1.62	3.24	.000	1.1110E-09			
4	1	1042.	3.71	.00	1.86	3.71	.000	2.4910E-09			
5	1	1.000	12.17	.00	6.09	12.17	.000	2.9283E-06			
6	1	1.0500E-02	16.36	.00	8.18	16.36	.000	1.6971E-05			
7	1	.4170	22.28	.00	11.14	22.28	.000	4.2893E-05			
8	1	2.1000E-02	27.05	.00	13.52	27.05	.000	6.2608E-05			
1	1	.0000	35.55	.00	17.77	35.55	.000	1.0669E-04	5.837E-04	2.20	1907.
2	1	1.042	81.30	.00	40.65	81.30	.000	5.3551E-04			
3	1	1042.	3.21	.00	1.60	3.21	.000	1.0505E-09			
4	1	1042.	3.67	.00	1.84	3.67	.000	2.3380E-09			
5	1	1.000	12.04	.00	6.02	12.04	.000	2.7413E-06			
6	1	1.0500E-02	16.36	.00	8.18	16.36	.000	1.7005E-05			
7	1	.4170	22.29	.00	11.15	22.29	.000	4.2944E-05			
8	1	2.1000E-02	27.09	.00	13.55	27.09	.000	6.2799E-05			
1	1	.0000	35.47	.00	17.74	35.47	.000	1.0622E-04	5.756E-04	2.26	1996.
2	1	1.042	80.71	.00	40.36	80.71	.000	5.2807E-04			
3	1	1042.	3.18	.00	1.59	3.18	.000	9.9588E-10			
4	1	1042.	3.63	.00	1.82	3.63	.000	2.1975E-09			
5	1	1.000	11.91	.00	5.95	11.91	.000	2.5663E-06			
6	1	1.0500E-02	16.37	.00	8.19	16.37	.000	1.7063E-05			
7	1	.4170	22.31	.00	11.16	22.31	.000	4.3015E-05			
8	1	2.1000E-02	27.14	.00	13.57	27.14	.000	6.3024E-05			
1	1	.0000	35.39	.00	17.70	35.39	.000	1.0577E-04	5.675E-04	2.31	2088.
2	1	1.042	80.13	.00	40.06	80.13	.000	5.2059E-04			
3	1	1042.	3.15	.00	1.58	3.15	.000	9.4650E-10			
4	1	1042.	3.60	.00	1.80	3.60	.000	2.0680E-09			
5	1	1.000	11.78	.00	5.89	11.78	.000	2.4037E-06			
6	1	1.0500E-02	16.38	.00	8.19	16.38	.000	1.7110E-05			
7	1	.4170	22.33	.00	11.17	22.33	.000	4.3085E-05			
8	1	2.1000E-02	27.19	.00	13.59	27.19	.000	6.3246E-05			
1	1	.0000	35.31	.00	17.65	35.31	.000	1.0527E-04	5.589E-04	2.36	2184.
2	1	1.042	79.50	.00	39.75	79.50	.000	5.1271E-04			
3	1	1042.	3.13	.00	1.56	3.13	.000	8.9954E-10			
4	1	1042.	3.56	.00	1.78	3.56	.000	1.9430E-09			
5	1	1.000	11.64	.00	5.82	11.64	.000	2.2404E-06			
6	1	1.0500E-02	16.38	.00	8.19	16.38	.000	1.7135E-05			
7	1	.4170	22.35	.00	11.17	22.35	.000	4.3137E-05			
8	1	2.1000E-02	27.23	.00	13.62	27.23	.000	6.3446E-05			

1	1	.0000	35.22	.00	17.61	35.22	.000	1.0475E-04	5.502E-04	2.42	2284.
2	1	1.042	78.86	.00	39.43	78.86	.000	5.0462E-04			
3	1	1042.	3.10	.00	1.55	3.10	.000	8.5499E-10			
4	1	1042.	3.52	.00	1.76	3.52	.000	1.8232E-09			
5	1	1.000	11.49	.00	5.75	11.49	.000	2.0788E-06			
6	1	1.0500E-02	16.39	.00	8.19	16.39	.000	1.7163E-05			
7	1	.4170	22.36	.00	11.18	22.36	.000	4.3189E-05			
8	1	2.1000E-02	27.28	.00	13.64	27.28	.000	6.3650E-05			
1	1	.0000	35.12	.00	17.56	35.12	.000	1.0418E-04	5.410E-04	2.47	2387.
2	1	1.042	78.17	.00	39.09	78.17	.000	4.9609E-04			
3	1	1042.	3.07	.00	1.54	3.07	.000	8.1235E-10			
4	1	1042.	3.48	.00	1.74	3.48	.000	1.7074E-09			
5	1	1.000	11.34	.00	5.67	11.34	.000	1.9182E-06			
6	1	1.0500E-02	16.39	.00	8.19	16.39	.000	1.7165E-05			
7	1	.4170	22.37	.00	11.18	22.37	.000	4.3220E-05			
8	1	2.1000E-02	27.32	.00	13.66	27.32	.000	6.3828E-05			

NOTE: CRACK SIZE OF 1ST DOF WILL EXCEED BODY WIDTH, G(1), ON NEXT ITERATION. PROCESSING TERMINATED.

REFINED BREAKUP SONGS PZR HEATER SLEEVE REPAIR EVALUATION BOTTOM HEAD FLAW DOWNHILL SIDE

FATIGUE CRACK GROWTH ANALYSIS SUMMARY

CRACK DIMENSION(S) A(I)	MAXIMUM STRESS INTENSITY FACTOR(S) FOR WORST INPUT LOAD TRANSIENT KMAX	TOTAL CRACK GROWTH RATE(S) DADN(I)	NUMBER OF CYCLES OR BLOCKS TO GROW CRACK FROM INITIAL SIZE N
A1	K1	DADN1	N
.875	95.371	8.0304E-04	.0000
.895	95.412	8.0382E-04	25.46
.916	95.489	8.0517E-04	51.47
.938	95.595	8.0694E-04	78.05
.960	95.684	8.0844E-04	105.2
.982	95.754	8.0957E-04	132.9
1.005	95.576	8.0669E-04	161.3
1.029	95.367	8.0329E-04	190.5
1.053	95.117	7.9917E-04	220.5
1.077	94.914	7.9583E-04	251.4
1.102	94.735	7.9288E-04	283.1
1.128	94.521	7.8933E-04	315.6
1.155	94.271	7.8516E-04	349.1
1.182	93.994	7.8055E-04	383.6
1.209	93.677	7.7524E-04	419.1
1.237	93.322	7.6932E-04	455.7
1.266	92.930	7.6279E-04	493.5
1.296	92.503	7.5572E-04	532.4
1.326	92.061	7.4842E-04	572.7
1.357	91.735	7.4302E-04	614.3
1.389	91.383	7.3722E-04	657.2
1.421	91.014	7.3119E-04	701.4
1.455	90.623	7.2481E-04	747.0
1.489	90.211	7.1813E-04	794.1
1.523	89.759	7.1086E-04	842.8
1.559	89.280	7.0320E-04	893.2
1.596	88.793	6.9547E-04	945.3
1.633	88.267	6.8717E-04	999.3
1.671	87.695	6.7823E-04	1055.
1.710	87.128	6.6943E-04	1113.
1.750	86.562	6.6076E-04	1173.
1.791	85.974	6.5181E-04	1236.
1.833	85.415	6.4339E-04	1300.
1.876	84.950	6.3643E-04	1367.
1.919	84.477	6.2941E-04	1436.
1.964	84.009	6.2254E-04	1508.
2.010	83.511	6.1527E-04	1582.
2.057	82.990	6.0775E-04	1659.
2.105	82.447	5.9996E-04	1739.
2.154	81.887	5.9201E-04	1821.
2.205	81.295	5.8368E-04	1907.
2.256	80.714	5.7558E-04	1996.
2.309	80.126	5.6747E-04	2088.
2.363	79.502	5.5894E-04	2184.
2.418	78.856	5.5021E-04	2284.
2.475	78.170	5.4102E-04	2387.